Age determination in detached eclipsing binary systems

Scilla Degl'Innocenti
(Physics Department Pisa University, INFN Pisa)

The described works of the "Pisa group" have been performed in collaboration with:

P. G. Prada Moroni, G. Valle, M. Dell'Omodarme, E. Tognelli (Physics Department, Pisa University, INFN Pisa)

Detached eclipsing binary systems are fundamental to test stellar models

(see e.g. Popper 1980, Andersen 1991, Lastennet & Valls-Gabaud 2002, Ribas 2006,Torres et al. 2010, Fernandez et al. 2012, Southworth 2012, 2014, etc..)

- Stars evolve as single stars
- Masses and radii determined with great precision
- Same initial chemical composition for the two stars
- Stars are assumed coeval
- Distance can be estimated

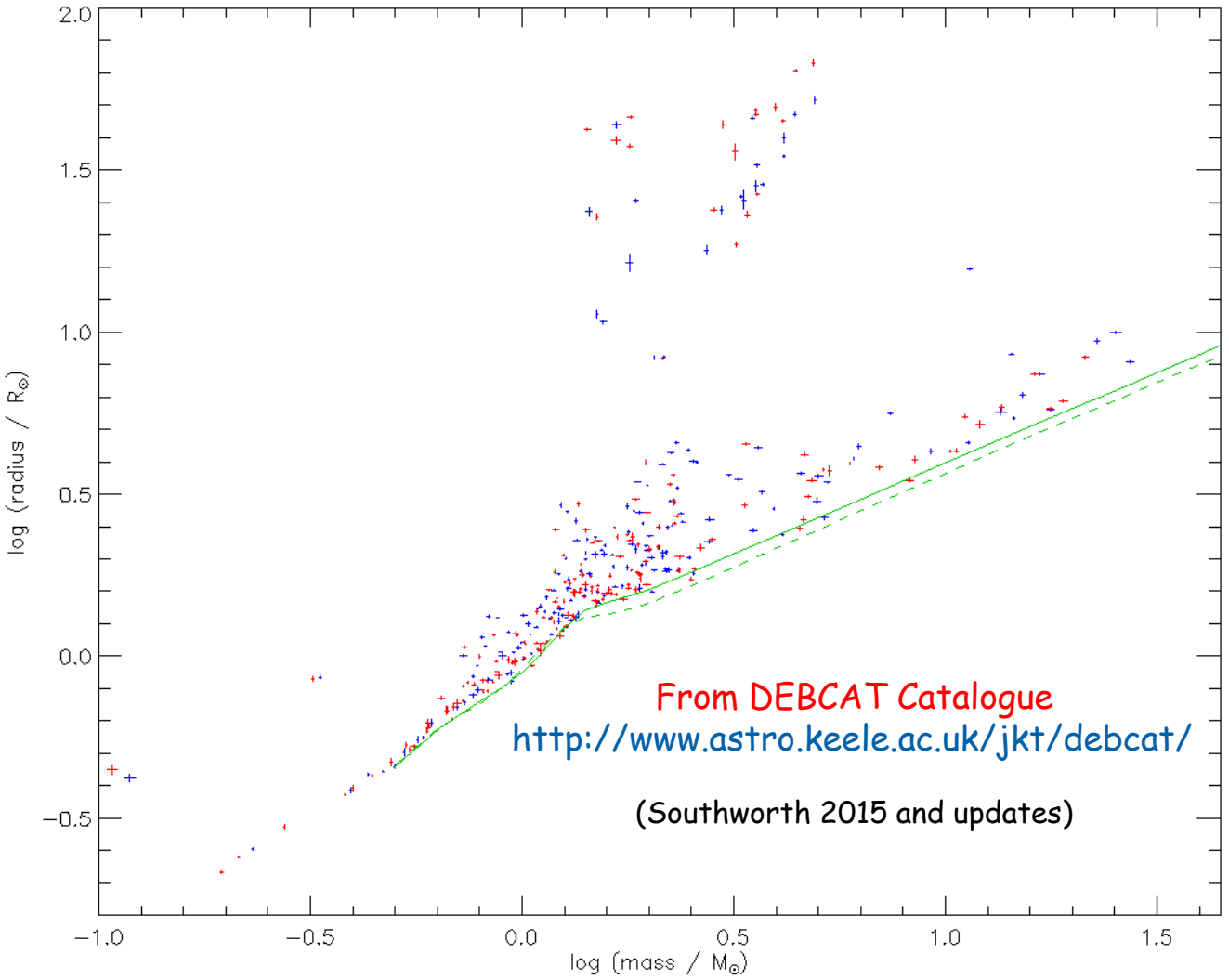

(The primary components are in blue and the secondary components in red)

About 200 detached binary systems with mass and radius measurements accurate to at least 2%

Some systems have a mass error of few parts per thousand (see e.g. Gallenne et al. 2016, Kirby-Kent et al. 2016, Torres et al. 2015, Lacy et al. 2012, Sandberg Lacy & Fekel 2011, Torres et al. 2010…)

- Both stars with measured temperatures
- For a fraction of them spectroscopic metallicity determination is available

"DEB systems are especially helpful in calibrating and checking age relations"
(Soderblom 2010)

However….

A rigorous analysis of the uncertainties in theoretical models and observational data and of their influence on the recovered system age is mandatory

Determining the physical characteristics (e.g. age) of a binary system is an inverse problem consisting of estimating the parameters of stellar models through the comparison with some observable quantities

Extensive grids of stellar models are available

see e.g. SEEK package, Aarhus Stellar Evolution Code Code (e.g. Quirion et al. 2010, Christensen-Dalsgaard 2008), BASTI, Teramo version of the FRANEC code (see e.g. Hidalgo et al. 2018, Pietrinferni et al. 2004), PARSEC, Padova code (see e.g. Bressan et al. 2012, Chen et al. 2014), MIST, MESA Code (see e.g. Paxton et al. 2011, 2013, 2015, Choi et al. 2016, Dotter et al. 2016), Lyon, Pre-MS models (see e.g. Baraffe et al. 2015, BAHC15), CESAM 2k code (see e.g. Morel & Lebreton 2010), Y2 (Demarque et al. 2004), DSEP (Dotter et al. 2008), Geneva models (see e.g. Schaller et al. 1992, Mowlawi et al. 2012, Georgy et al. 2012, 2013), Granada models (see e.g. Claret & Giménez 1992, Claret 2004), Bonn stellar models (Brott et al. 2011, Köhler et al. 2014), Pisa evolutionary library, Pisa version of the FRANEC code (see e.g. Tognelli et al. 2011, Dell'Omodarme et al. 2012, Tognelli et al. 2015), etc..

The adopted fitting algorithms are many:

isochrones χ^2 fitting for binary age estimations, Bayesian techniques, maximum likelihood techniques on model grids, Bayesian statistic with Markov chain Monte Carlo algorithms…

(see e.g. Pols et al. 1997, Roczycka et al. 2001, Lastennet & valls Gabaud 2002, da Silva et al. 2006; Takeda et al. 2007, SandBerg Lacy et al. 2010, Clausen et al. 2010, Gennaro et al. 2012, Welsh et al. 2012, Vos et al. 2012, Schneider et al. 2014, 2017, Valle et al. 2015, Bazot et al. 2008, 2012, 2016, White et al. 2017, Claret & Torres 2016, 2017, 2018 etc..)

The calibration of parameters from binary systems is a delicate task, affected by many decisions in the fitting stage in addition to the choice of the stellar models grid: e.g. mass fixed to the central value, age estimates for a set of different metallicities compatible with the errors on [Fe/H], two steps fitting procedure, differences in the explored evolutionary phases etc..

Different fitting algorithms and different stellar models, computed with different chemical compositions and input physics → age estimates sometimes very different

Lack of homogeneity in the treatment of statistical errors due to the observational uncertainties

Sometimes reliable error on age estimates is not provided.

↓

It's difficult to compare the results of different authors

Cumulative uncertainty affecting the current generation of stellar models is still not negligible

(see e.g. Krauss & Chaboyer 2003, Imbriani et al. 2004, Weiss et al. 2005, Bjork & Chaboyer 2006, Prada Moroni & Straniero 2007, Cassisi et al. 2007, Valle et al. 2009, 2013, Cassisi 2014, Lebreton et al. 2014, Salaris & Cassisi 2017, Dotter et al. 2017, Vinyoles et al. 2017, Tognelli et al. 2011, 2018, etc…)

To estimate stellar parameters it's a quite common procedure to adopt independent sets of stellar models to have a rough idea of the uncertainty on the results

(see e.g. Lastennet and Valls-Gabaud 2002, Gai et al. 2011, Basu et al. 2012, Stancliffe et al. 2015, 2016, Claret & Torres 2016, 2017, White et al. 2017, etc..)

Comparison of isochrones from different model sets

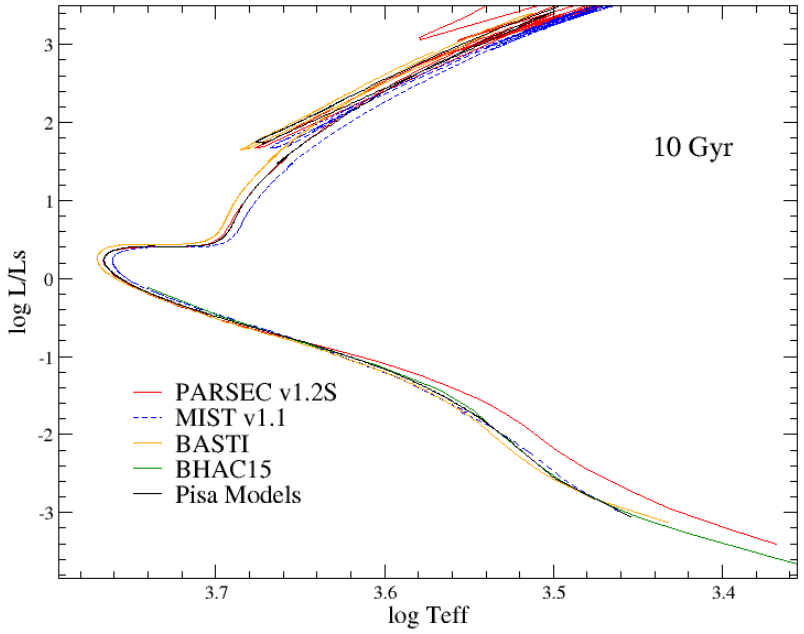

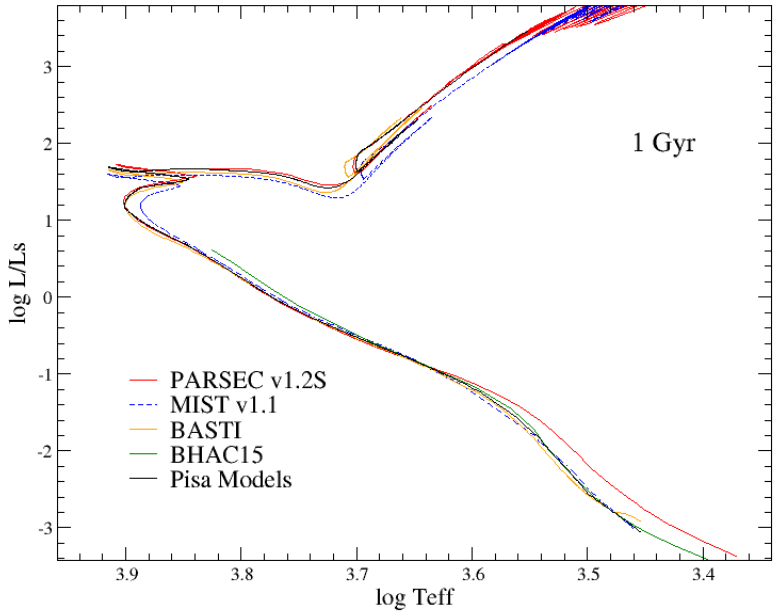

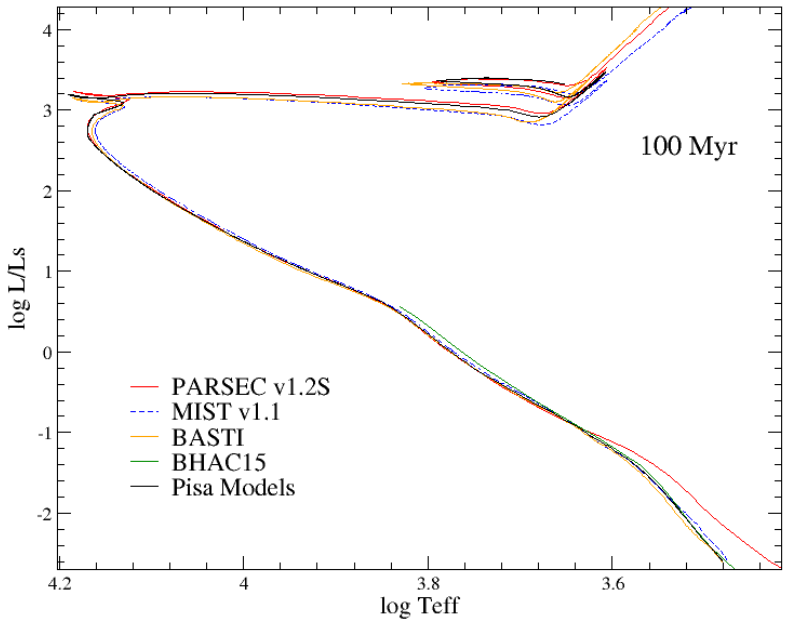

(See also for models comparison e.g. Hidalgo et al. 2018, Stancliffe et al. 2015, 2016, Choi et al. 2016, Jones et al. 2015, Martins & Palacios 2013, Tognelli et al. 2011, Gallart et al. 2005 and many others…)

The bias in statistically age estimates due to the adopted set of stellar models strongly depends on the assumed observational constraints and it should be evaluated case by case

The effect on age determination of a given error source could be different for different masses and evolutionary phases

Low and intermediate mass stars ($M < 2\,M_{\odot}$) from the Main Sequence to the Red Giant Branch phase

Errors in DEB system age determination

Bias in the age estimates

- Systematic observational errors
- Choice of the stellar model grid

  (different input physics, chemical compositions, efficiency of physical mechanisms)
- Intrinsic: due to the morphology of the stellar tracks

Statistical errors in age determination → Uncertainty on the observed quantities

↓

Synthetic binary systems

(see e.g. Gennaro et al. 2012, Schneider et al. 2014, Valle et al. 2015, 2016)

(For the analysis of statistical errors due to observational uncertainties in single stars with different observed quantities see e.g. Gai et al. 2011, Basu et al. 2012, Maxted et al. 2015, Valle et al. 2014, 2015, Schneider et al. 2014, 2017, etc.)

Evaluation of statistical error on age estimation with mock binary systems

(Valle et al. 2015)

Grid of precomputed stellar models with mass in the range [0.8; 1.6] $M_{\odot}$, $-0.55 \leq [Fe/H] \leq 0.55$ and evolutionary stages from the zero-age main sequence to the central H depletion

Synthetic dataset obtained by sampling N = 50000 artificial binary systems from the same grid of stellar models used in the recovery procedure ⟹ **ideal case in which stellar models are in perfect agreement with observed stars**

Observables: M, R, T_{eff} and [Fe/H] of the two stars with their uncertainty σ

Typical errors of: 1% in mass, 0.5% in radius, 0.1 dex in [Fe/H] and 100 K in T_{eff} (see e.g. Casagrande et al. 2010, Metcalfe et al. 2010, Pinsonneault et al. 2012, Schmidt et al. 2016)

To simulate the effect of observational uncertainties, we added a Gaussian noise in all the synthetic systems.

The age is estimated through a maximum likelihood technique relying on the same grid of stellar models (following the procedure described in Basu et al. 2012 for single stars) assuming coevality (within 10 Myr)

The method allows to define a confidence interval for age estimates

Monte Carlo median bias in estimated age and position of the 1σ envelope of relative error in age

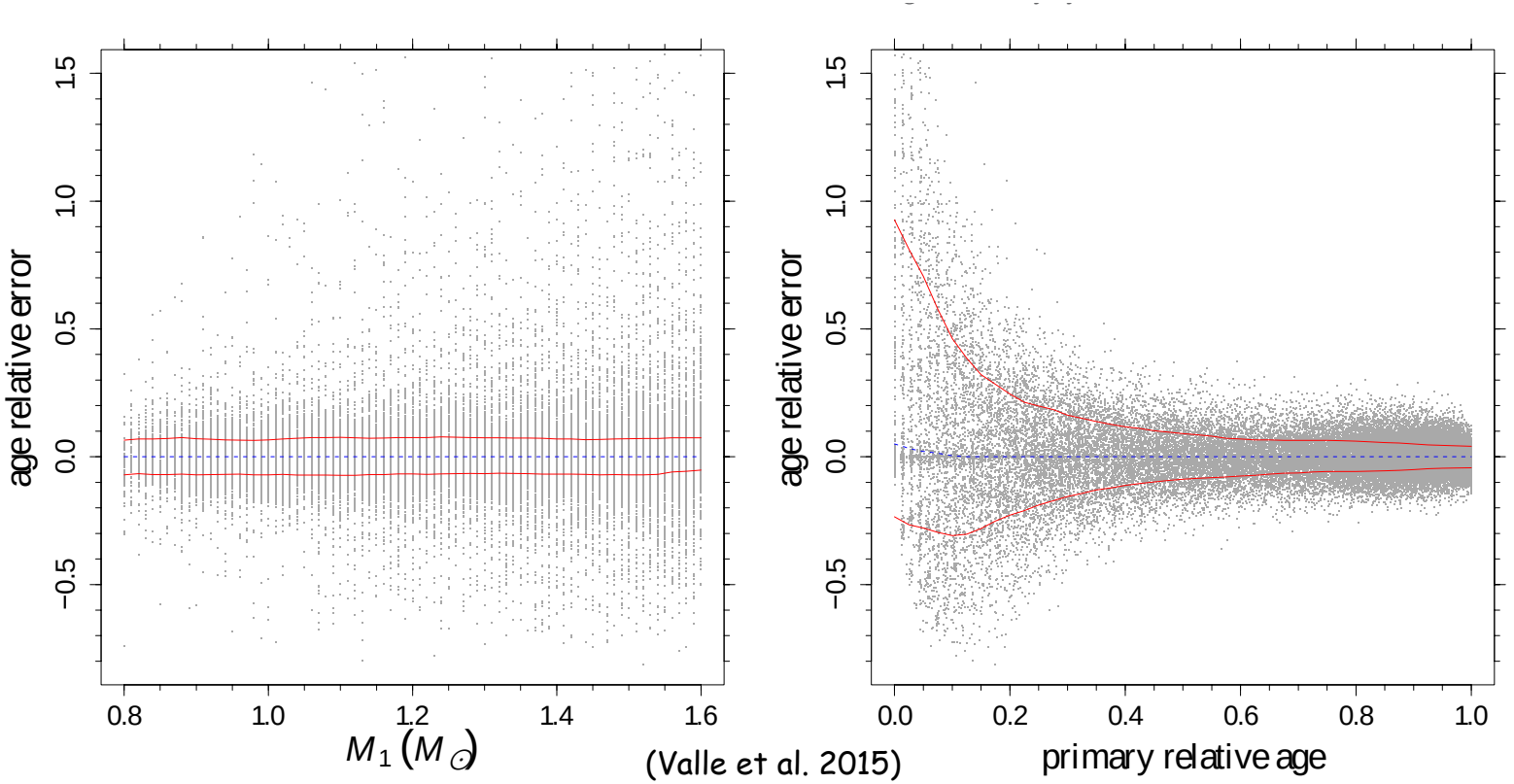

relative age: ratio between the age of the star and the age of the same star at central hydrogen exhaustion

A positive value of the relative error corresponds to an overestimated age

Typical relative age error as a function of the primary star mass is about 7%

The 1σ envelope is larger for models near the ZAMS, where the envelope is highly asymmetric

For relative ages of the primary star larger than 0.4 the precision is always better than 12%

Fig. 1. *Left*: age relative error in dependence on the mass of the primary star with its 1σ envelope (red solid line). The blue long dashed line marks the relative errors median. *Right*: same as the left panel, but in dependence on the relative age of the primary star.

- **The estimated age is unbiased**
- **Mean 1σ relative error in age of the order of 10% except for models near the ZAMS**

A quite good result but…

A statistical approach to the coevality problem

(Valle et al. 2015, 2016)

Several real eclipsing binary systems whose components are estimated to be non-coeval
(see e.g. Clausen et al. 2009, Vos et al. 2012, Sandquist et al. 2013, 2016 Schneider et al. 2014, etc..)

→ Some weaknesses of current generation of stellar models?

Some estimates of non-coevality of real binary could be a fluctuation arising from observational errors?

↓

Quantification of the expected difference in the estimated ages of two genuine coeval stars caused simply by the observational uncertainties

↓

binary systems generated coeval + random perturbations to account for the observational errors → the age of the single stellar members is recovered

How large the relative age difference, $W = (age_1 - age_2)/age_1$, can become only because of the random fluctuations in age estimates?

Distribution of W estimated by means of a Monte Carlo simulation

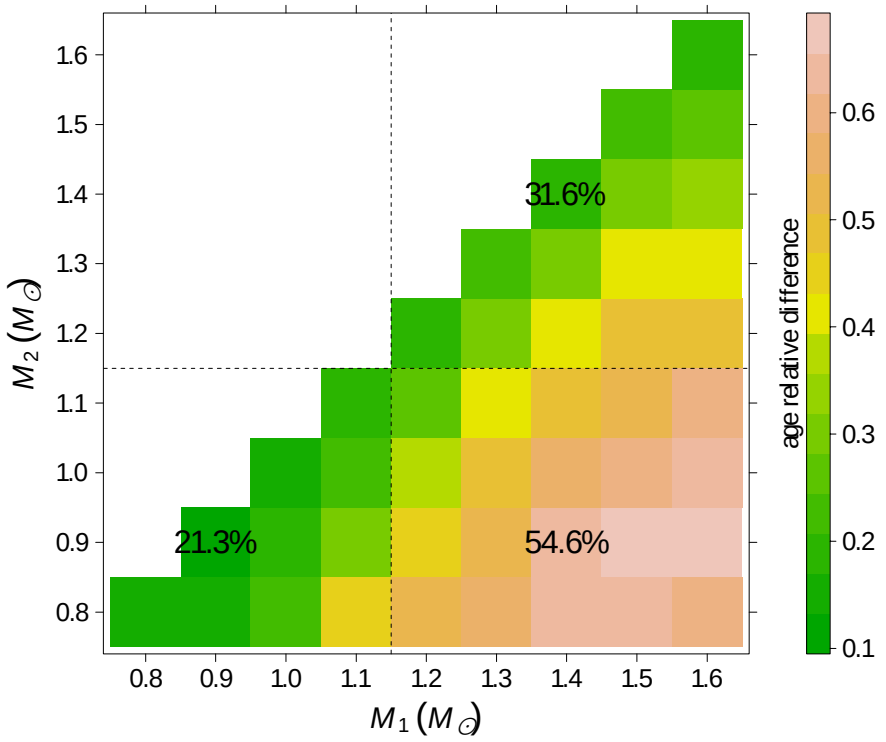

Fig. 11. Critical values $W_{0.95}$ of the statistic W for the expected differences in the ages of the two stars, only due to the observational uncertainties (see text).

critical W value ($W_{0.95}$) to identify systems that are too extreme to be compatible with the coevality hypothesis[1]

Genuine coeval stars can be reconstructed as non coeval with a sizeable relative age difference only because of the current uncertainty in the observational constraints

If $W > W_{0.95}$, the possibility that non-coevality is the result of observational uncertainties should be considered as negligible
(see e.g. V636 Cent and EF Aqr, Clausen et al. 2009, Vos et al. 2012, …)

The critical W value directly depends on the assumed magnitude of the observational uncertainties.

The critical W value also depends on the relative age while the dependence on the original [Fe/H] is very weak

The critical W value should be evaluated case by case

[1] the critical value is chosen as the 95th quantile of the W distribution

Grid of stellar models of the "Pisa Evolutionary Library"

http://astro.df.unipi.it/stellar- models/

SCEPtER (Stellar CharactEristics Pisa Estimation gRid) tool for age estimates for single stars and binary systems

http://CRAN.R- project.org/package=SCEPtER
http://CRAN.R- project.org/package=SCEPtERbinary

On line calculator to estimate the critical value for coevality in binary systems

http://astro.df.unipi.it/stellar-models/W/

(Dell'Omodarme et al. 2012, Tognelli et al. 2011, Valle et al. 2014, 2015 a,b, 2016)

Main sources of model uncertainty

- Chemical composition determination
- Adopted input physics
  (nuclear reaction rates, opacity, EOS..)
- Efficiency of macroscopic mechanisms
  (diffusion, overshooting, external convection efficiency..)

Uncertainty on the original He abundance

For the original helium abundance a linear relation is generally adopted :

$$Y = Y_p + \frac{\Delta Y}{\Delta Z} Z$$

Where Y_P is the cosmological helium abundance: $Y_P = 0.2446 \pm 0.0029$ (Peimbert et al. 2016), $Y_P = 0.2551 \pm 0.0022$ (Izotov et al. 2014), $Y_P = 0.2470 \pm 0.0003$ (Cyburt et al. 2016, Planck satellite data), see also Coc et al. (2013), Izotov et al. (2013,2014), Aver et al. (2015), etc..

$\frac{\Delta Y}{\Delta Z}$ could vary from 0.5 to 5 (at least), currently preferred values are $\frac{\Delta Y}{\Delta Z} = 2 \pm 1$

(see e.g. Pagel & Portinari 1998, Lebreton et al. 1999, Jimenez et al. 2003, Balser 2006, Casagrande et al. 2007, Bertelli et al. 2008, Portinari et al. 2010, Gennaro et al. 2010, Serenelli & Basu 2010, Lebreton et al. 2014, etc..)

The effects of He abundance variations on stellar models are well known
(see e.g. discussions in Buzzoni et al. 1983, Sweigart & Gross 1976, 1978)

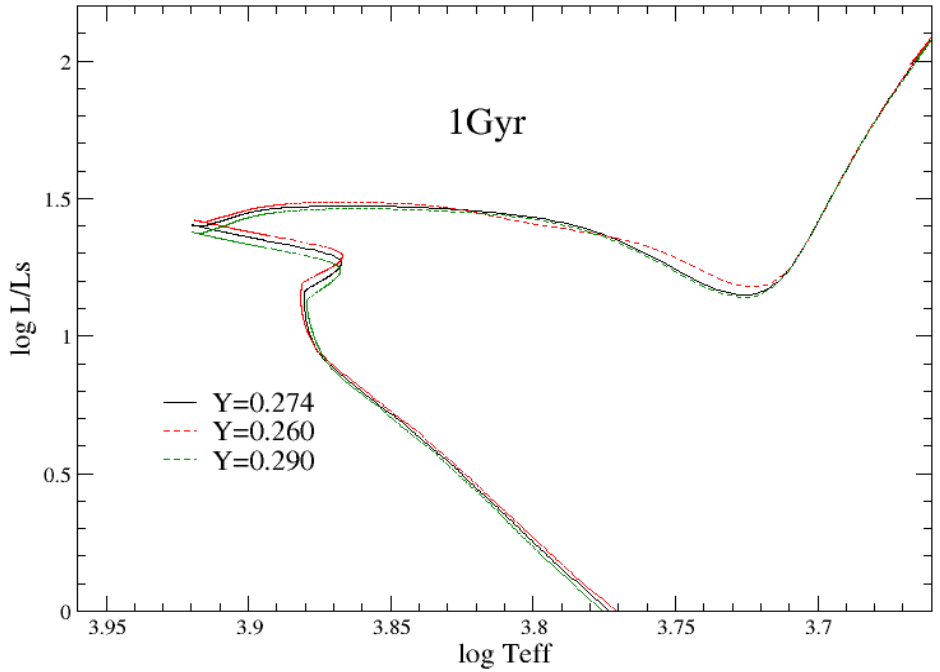

Effect of the original He abundance uncertainty on the recovered age of binary systems

- Mass in the range [0.8; 1.6] $M_\odot$ and evolutionary stages from the ZAMS to the central H depletion
- two non-standard grids of perturbed stellar models with $\frac{\Delta Y}{\Delta Z}$ = 1,3
- Artificial binary systems are sampled from these grids, and their ages are estimated on the reference one (with $\frac{\Delta Y}{\Delta Z}$ = 2)

$-0.55 \leq [Fe/H] \leq 0.55$

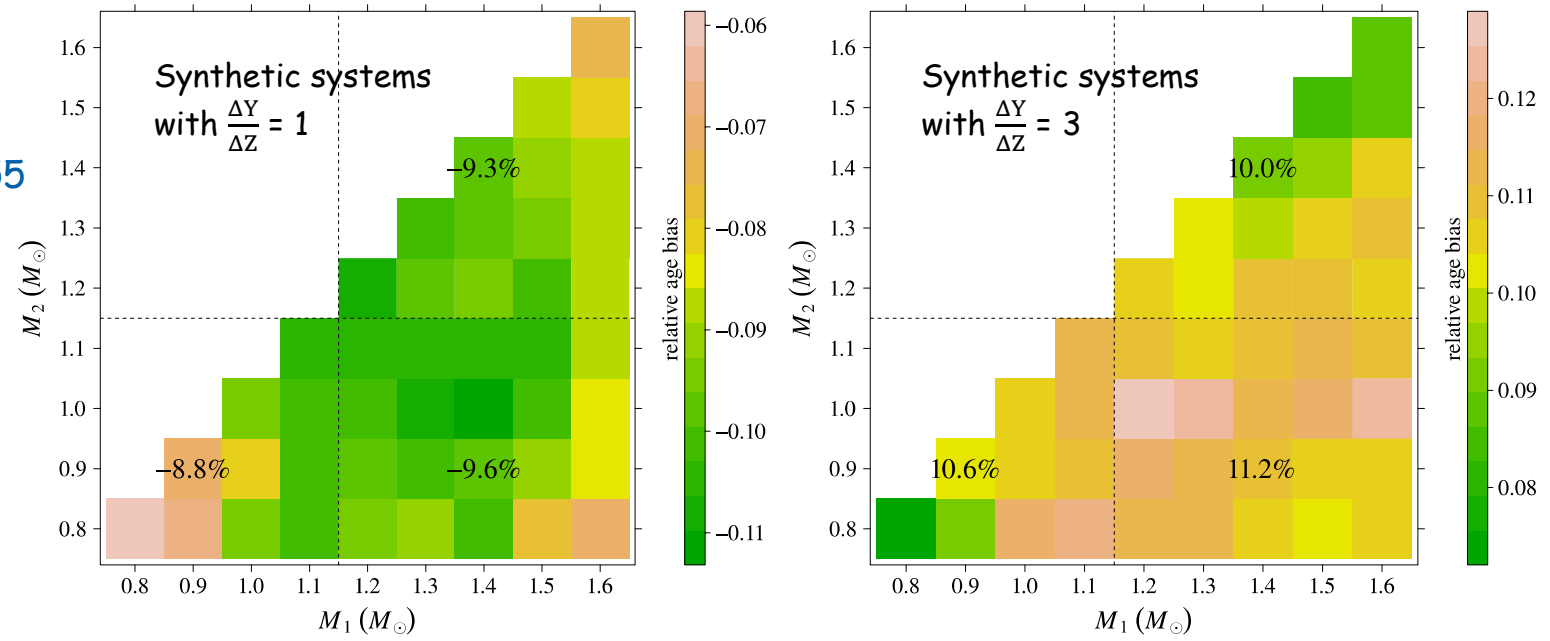

(Valle et al. 2015)

Fig. 8. *Left*: relative-age bias due to adopting a low initial helium abundance as a function of the masses of the binary system. Artificial stars are sampled from the grid with $\Delta Y/\Delta Z = 1$, and their age is estimated on the standard grid ($\Delta Y/\Delta Z = 2$). *Right*: same as the left panel, but sampling from a grid with $\Delta Y/\Delta Z = 3$.

In the considered mass range the initial helium abundance induced bias is almost constant at about ±10% for a change in ΔY/ΔZ by ±1

Effects of input physics uncertainties on the recovered age of artificial binary systems

Mass in the range [0.8; 1.1] $M_{\odot}$, $-0.55 \leq [Fe/H] \leq 0.55$ and evolutionary stages from the ZAMS to the central H depletion

The error on radiative opacity and $^{14}N+p$ cross section are the most relevant in the evolutionary stage and mass range studied here (Valle et al. 2013a,b)

See also for the analysis of selected inputs physics in different evolutionary phases and mass ranges: Chaboyer et al. 1995, 1996, 1998, Brocato et al. 1998, Castellani & Degl'Innocenti 1999, Imbriani et al. 2001, Salaris et al. 2002, Chaboyer & Krauss 2002, Straniero et al. 2002, Krauss & Chaboyer 2003, Imbriani et al. 2004, Degl'Innocenti et al. 2004, Weiss et al. 2005, Bjork & Chaboyer 2006, Cassisi et al. 2007, Prada Moroni & Straniero 2007; Valle et al. 2009,Cassisi 2014, Cassisi et al. 2016, Lebreton et al. 2014, Tognelli et al. 2015, etc..

- **Assumed error on $^{14}N+p$ cross section: 10%** (see e.g. Marta et al. 2011, Imbriani et al. 2005)

(See also Straniero et al. 2002, Imbriani et al. 2004, Degl'Innocenti et al. 2004, Weiss et al. 2005, Pietrinferni et al. 2010 for the effects of $^{14}N+p$ cross section on stellar models)

- **Assumed mean error on radiative opacity: 5%** (see e.g. Rose 2001, Seaton & Badnell 2004, Badnell et al. 2005, Blancard et al. 2012, Mondet et al. 2015, Valle et al. 2013, Vinyoles et al. 2017)

two non-standard grids of perturbed stellar models by varying the chosen individual input to its extreme values, while keeping all the others fixed to their reference values.

Artificial binary systems are sampled from these grids, and their ages are estimated on the reference one.

- The effect of the error on $^{14}N+p$ cross section is negligible for binary system age determination
- The assumed error on radiative opacity leads to a mean bias on age determination of about 8%

Relative age bias due to the adoption for the mock systems of a radiative opacity lowered by 5% (left panel) and increased by 5% (right panel). Systems are recovered with the grid of models with reference opacity values.

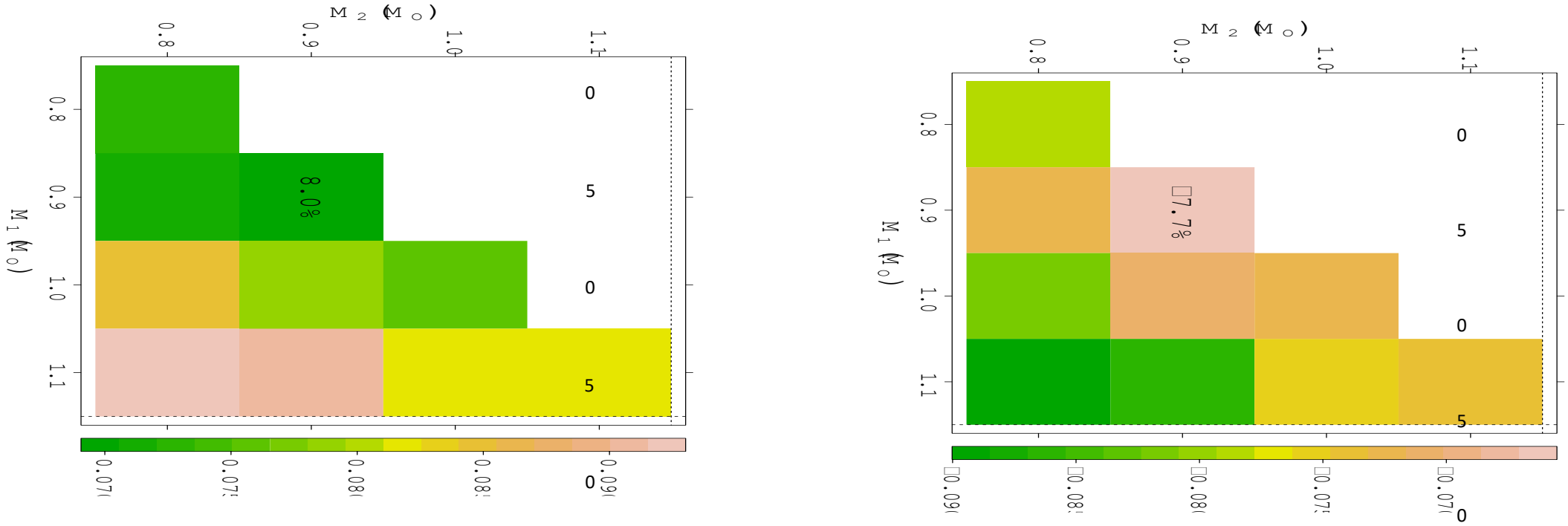

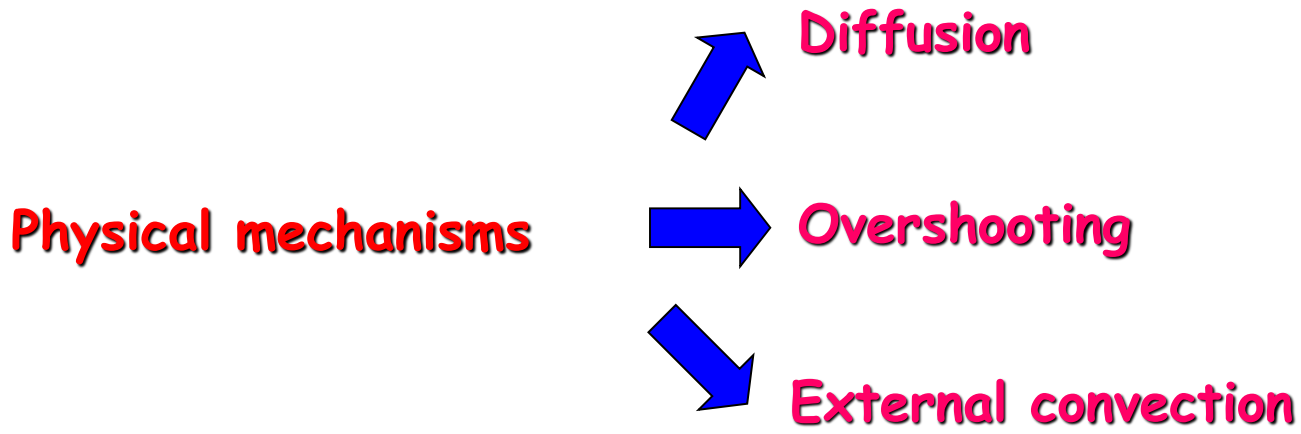
Physical mechanisms
Diffusion
Overshooting
External convection

Uncertainty on diffusion efficiency

Element diffusion in stars (Eddington 1926, Aller & Chapman, 1960) includes different processes:
• gravitational settling • thermal diffusion • diffusion driven by composition gradients • radiative acceleration of individual ions (Michaud 1970) . Often a turbulent diffusion term (Schatzman 1969) is included

- He and Z settling is a long term process (~ Gyr) → influences on the internal structure of low mass stars only ($M \leq 1.2\ M_{\odot}$)

- Diffusion is certainly active in the Sun

(see e.g. Demarque & Guenter 1988, Cox et al. 1989, Bahcall & Pinsonneault 1992, 1995, Guzik & Cox 1992,1993, Gough et al. 1996, Christensen-Dalsgaard et al. 1993, Lydon et al. 1993, Basu et al. 2000…)

- Estimated uncertainty of diffusion (for the Sun) ~ 10%-15%

(Thoul et al. 1994, see also discussions in e.g. Bahcall & Pinsonneault 1995, Vinyoles et al. 2017, etc.. but also discussions in Roussel-Dupré 1982, Turcotte et al. 1998, Schlattl 2002, Schlattl & Salaris 2003, Montalbán et al. 2006, Thoul & Montalbán 2007, etc..)

- For the Sun an extra-mixing at the bottom of the convective envelope seems to be present (see e.g. Richard et al. 1996, Brun et al. 1999, 2011, Basu 2009, Christensen-Dalsgaard et al. 2011, 2018, etc..)

The situation for other stars is less clear…

- Abundance observations in globular clusters (and in some open cluster) indicate a reduction of the diffusion effects at least on the surface abundances

(see e.g. Castilho et al. 2000, Gratton et al. 2001, 2011, Thevenin et al. 2001, Ramirez & Cohen 2001, 2003, Bonifacio et al. 2002, James et al. 2004, Carretta et al. 2004, Korn et al. 2006, 2007, Lind et al. 2008, 2016, Gebran et al. 2010, Mucciarelli et al. 2011, Nordlander et al. 2012, Gruyters et al. 20213, 2014, Önehag et al. 2014, etc..)

→ **existence of some competing mechanism that inhibits diffusion:** turbulent diffusion, rotational instabilities of various kinds, radiative levitation, etc..

(see e.g. Richard et al. 1996, 2000, 2001, 2002, 2005, Turcotte et al. 1998, Brun et al. 1999, Richer et al. 2000, Maeder & Meynet 2000, VandenBerg et al. 2002, Alecian & Leblanc 2004 , LeBlanc & Alecian 2004, Vauclair 2004, Tassoul 2007, Hui-Bon-Hoa 2008 , Michaud & Richer 2008, Maeder 2009, Garaud 2011, Michaud et al. 2010, 2011, Théado et al. 2012, Lebreton & Goupil 2012, Palacios, 2013, Maeder et al. 2013; Meynet et al. 2013; Mathis 2013, Goupil et al. 2014, Deal et al. 2013, 2016, 2017, etc..)

Obviously spectroscopy cannot tell us anything about the efficiency of diffusion in the interiors

The influence of Y and Z settling on evolutionary characteristics is well studied

(See e.g. Proffitt & Michaud 1991, Delyannis et al. 1990, Proffitt & VandenBerg 1991, Chaboyer et al. 1992, Chaboyer 1995, Canuto et al. 1996, VandenBerg et al. 1996, Castellani et al. 1997, Straniero et al. 1997, D'Antona et al. 1997, Caloi et al. 1997, Weiss & Schlattl 1999, Salaris et al. 2000, Valle et al. etc…)

Effect on binary system age estimates of neglecting microscopic diffusion

- Mass in the range [0.8; 1.6] $M_{\odot}$ and evolutionary stages from the ZAMS to the central H depletion

- Synthetic data set obtained by sampling artificial binary systems from stellar models with diffusion (no radiative acceleration, no extra-mixings) + Gaussian noise

- Age estimated adopting the grid of models without diffusion

The bias due to the neglect of microscopic diffusion has a mean value of 3.6% (it ranges from about one-half to one-third of the bias due to initial He change)

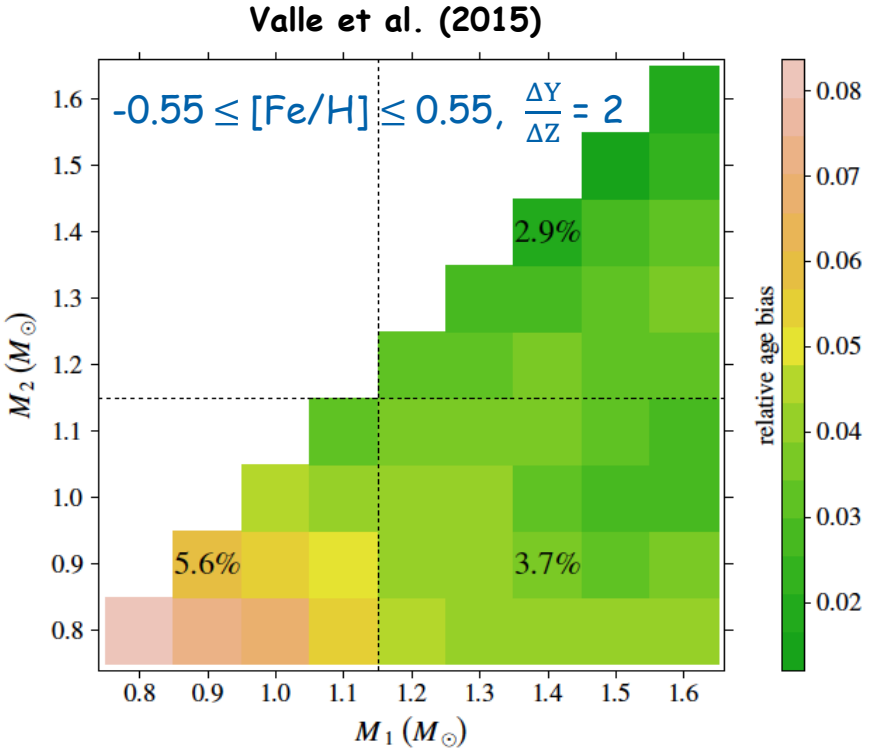

Fig. 10. Relative-age bias due to neglecting elements diffusion as a function of the masses of the binary system. Artificial stars are sampled from the standard grid, and their ages are estimated on a grid computed without microscopic diffusion.

Uncertainty on the external convection efficiency

- **In 1D models convection is typically treated using the parametric description of the mixing length theory** (Bohm-Vitense 1958) **which relies on rather crude assumptions. The free parameter α is usually calibrated to reproduce the solar radius at the solar age**

- **3D hydrodynamics convection simulations indicate that α should depend on parameters like luminosity, gravity and metallicity**
(see e.g. Ludwig et al. 1995, 1998, 1999, 2009, Freytag et al. 1999, Trampedach 2007, Trampedach & Stein 2011, Collet et al. 2011, Trampedach et al. 2013, 2014, 2015, Tanner et al. 2013, Magic et al. 2013, 2014, 2015, Arnett et al. 2015, Pratt et al. 2016, Musumgaard et al. 2017 and references therein)

- **Comparisons with stellar data for clusters, field stars and binary systems seems to indicate that a solar calibrated α is not able to reproduce all the observations** (see e.g. Guenther & Demarque 2000, Eggenberger et al. 2004, Miglio & Montalbán 2005, Straka et al. (2005), Clausen et al. 2008, 2009, Morales et al. 2009, 2010, Gennaro et al. 2010, Bonaca et al. 2012, Fernandes et al. 2012, Mathur et al. 2012, Metcalfe et al. 2012, 2014, Tanner et al. 2014, Mann et al. 2015, Saio et al. 2015, Wu et al. 2015, Joyce & Chaboyer 2017, Silva Aguirre et al. 2017) **and in some cases relations between α and metallicity** (see e.g. Tanner et al. 2014, Chun et al. 2018, Creevey et al. 2017, Tayar et al. 2017, Basu & Bonaca 2018) **or between α and the stellar mass have been found** (Ludwig & Salaris 1999, Morel et al. 2000, Lebreton et al. 2001, Lastennet et al. 2003, Yildiz et al. 2006, etc..) but see also e.g. Salaris & Cassisi 2015, 2018 for a different point of view..

Effect of α uncertainty on binary system age determination

(Valle et al. 2015)

- Mass in the range [0.8; 1.6] $M_{\odot}$, $-0.55 \leq [Fe/H] \leq 0.55$ and evolutionary stages from the ZAMS to the central H depletion

- Artificial binary systems are sampled from stellar model grids with $\alpha \pm 0.24$ with respect to our solar calibrated value (α = 1.74) + Gaussian noise

- Ages estimated adopting the model grid with solar calibrated α

However this approach could be not appropriate…

- Age bias ranging from $\pm$ 4% to $\pm$6%
- The bias on the age recovery due to the different choices of α is certainly important but not dominant
- For a more rigorous investigation, better knowledge of the dependence of the external convection efficiency on stellar parameters, such as mass, chemical composition, evolutionary phase, and stellar activity, is mandatory

(See also e.g. Basu et al. 2012, Stancliffe et al. 2015, Maxted et al. 2015, etc.. for the effect of α uncertainty on the recovery of single stars characteristics)

Uncertainty on overshooting value

- The extension of the extra-mixing region beyond the canonical border of a convective core, as defined by the Schwarzschild criterion (Saslaw & Schwarzschild 1965; Shaviv & Salpeter 1973, Maeder & Meynet 1991), is usually parametrized in terms of the pressure scale height H_P ($l_{ov} = \beta H_P$) where β is a free parameter
  (this could also be due to rotationally induced mixings, see e.g. Talon et al. 1997, Goupil & Talon 2002, Maeder 2009, Eggenberger et al. 2010, Marques et al. 2013, Lebreton et al. 2014 and references therein)

- Progresses are expected to come from prescription and/or calibration with 3D simulations
  (see e.g. Meakin & Arnett 2007, Gilet et al. 2013, Staritsin 2013, Gabriel et al. 2014, Viallet et al. 2013, 2015, Pratt et al. 2017, etc..)

- Several calibration methods: isochrone fitting of stellar cluster colour-magnitude diagrams (see e.g. Bertelli et al. 1992; Prada Moroni et al. 2001; Barmina et al. 2002; Brocato et al. 2003; VandenBerg et al. 2006; Bressan et al. 2012, etc..) comparison with asteroseismic constraints for single stars (see e.g Goupil et al. 2011, Lebreton & Goupil 2012, Neiner et al. 2012, Montalbán et al. 2013, Silva Aguirre et al. 2013, Guenther et al. 2014, Tkachenko et al. 2014, Aerts 2015, Deheuvels et al. 2010, 2016…) comparison with double-line eclipsing binary observations (see e.g Andersen et al. 1990, Ribas et al. 2000, Claret 2007, Meng & Zhang 2014, Stancliffe et al. 2015, Claret & Torres 2016, 2017, 2018…)

- Need for convective core extended beyond the Schwarzschild border

- A low β value (i.e. 0.2) is typically considered enough to match the observational data

Effect of the overshooting uncertainty on binary system age estimates

- Two additional model grids with β =0.2 and $\beta = 0.4$ for stars more massive than 1.1 $M_{\odot}$ extended with the standard grid at lower masses

- Synthetic data set obtained by sampling artificial binary systems from the β =0.2 and $\beta = 0.4$ grids + Gaussian noise

- Age estimated adopting the grid of models without overshooting

$-0.55 \leq [Fe/H] \leq 0.55$, $\frac{\Delta Y}{\Delta Z} = 2$

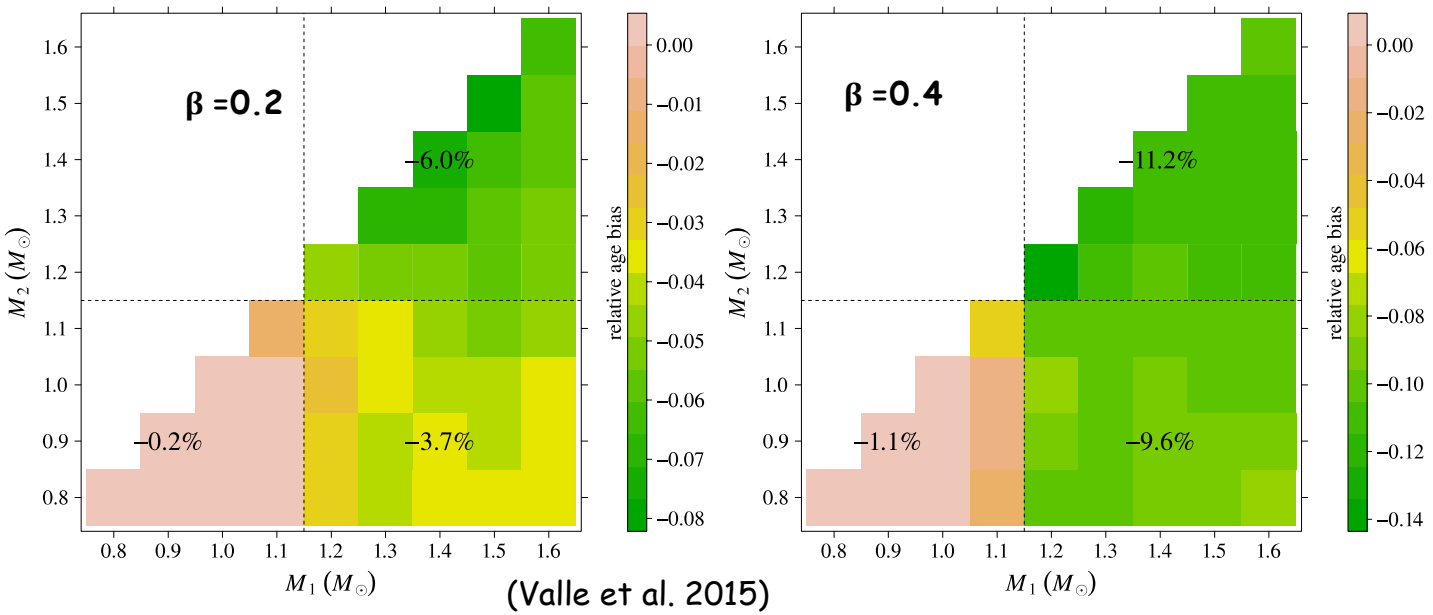

The bias induced by a mild convective core overshooting scenario (β =0.2) on age estimate is about one-half of the 1σ error due to observational uncertainties

Fig. 6. *Left*: relative age bias due to the mild core overshooting as a function of the masses of the binary system. Artificial stars are sampled from the grid with mild core overshooting ($\beta = 0.2$) and their age is estimated on the standard grid. *Right*: same as the left panel, but for the strong overshooting scenario ($\beta = 0.4$).

Investigations which tried to explore the dependence of β on stellar mass, performed on binary systems, reached somewhat different conclusions

(see e.g. Ribas et al. 2000, Claret 2007, Meng & Zhang 2014, Stancliffe et al. 2015, Claret & Torres 2016, 2017, 2018)

(Claret & Torres 2017, see also Claret & Torres 2016, 2018)

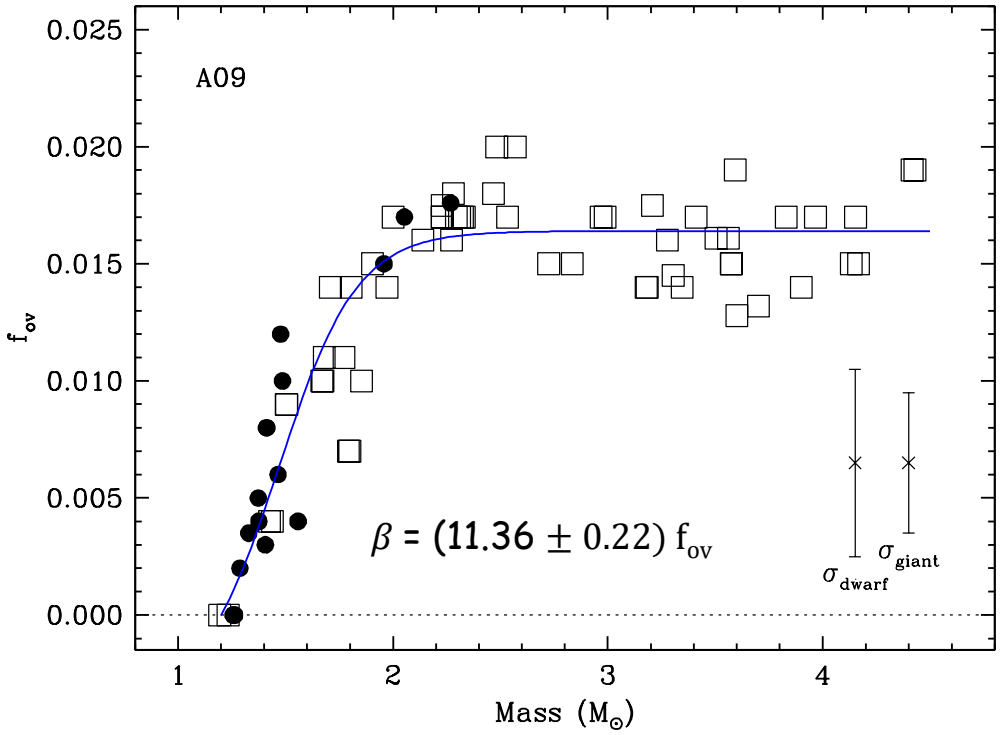

Figure 2. Inferred f_{ov} values from MESA models using the A09 mixture (Table 2) as a function of stellar mass. Filled circles represent the stars in the present sample (including YZ Cas and TZ For), and open squares are values taken for the 29 dwarf and giant DLEBs from Table 3 of Claret & Torres (2017), determined in the same way with the same element mixture and helium content. Typical error bars for dwarfs and giants are indicated on the lower right.

Some words of warning are needed….

How reliable is the overshooting calibration in binary system?

Uncertainty on overshooting calibration in Main Sequence binary systems

- Mass in the range [0.8; 1.6] $M_{\odot}$, -0.55 ≤ [Fe/H] ≤ 0.55 and evolutionary stages from the ZAMS to the central H depletion
- Typical errors of: 1% in mass, 0.5% in radius, 0.1 dex in [Fe/H] and 100 K in T_{eff}
- Artificial binary systems sampled from stellar model grid with $\beta = 0.2$ + Gaussian noise
- Age and β estimated adopting a full grid of stellar models with seventeen β values in the range [0.0; 0.4]

(Valle et al. 2016)

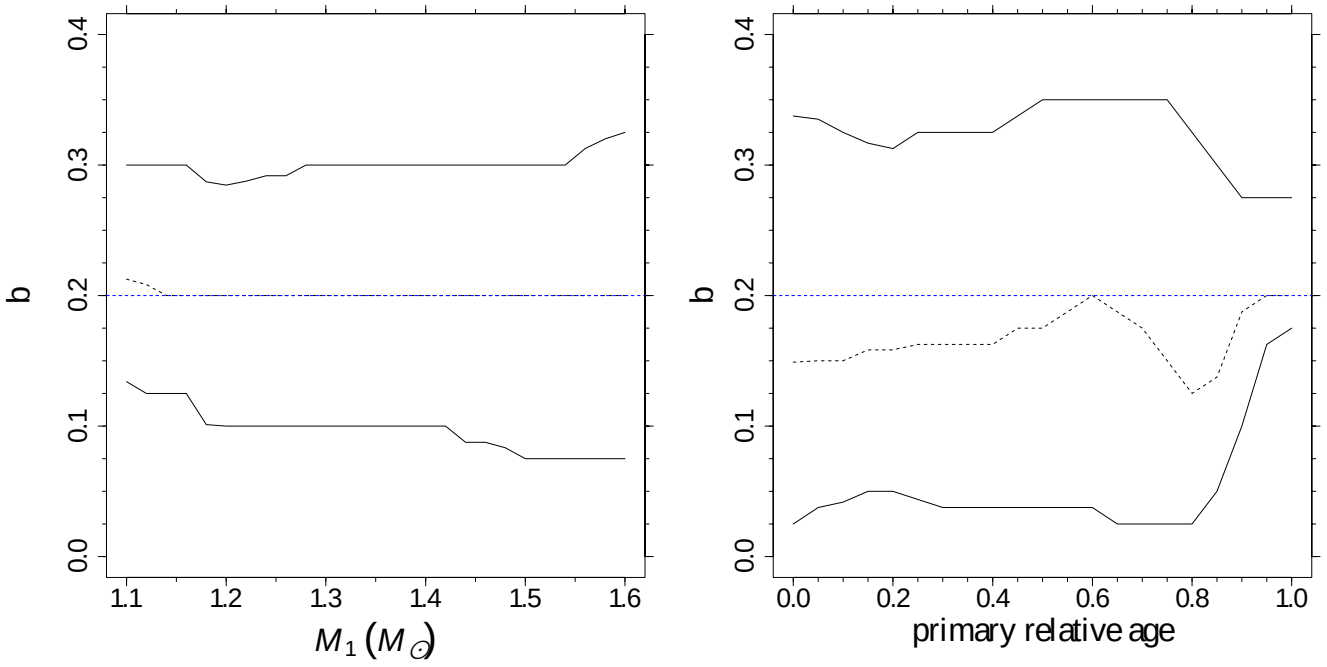

Fig. 2. *Left*: 1σ envelope of β estimates that are due to the observational errors (solid line) as a function of the mass of the primary star. The dashed line marks the position of the median. *Right*: same as in the *left panel*, but as a function of the relative age of the primary star.

- **Both large statistical uncertainties and biases on the estimated β values only due to observational errors**
- **The results are also affected by the indeterminations on the initial helium content and on the efficiencies of the superadiabatic convection and microscopic diffusion which lead to significant biases**

The large random errors and biases undermines the possibility of obtaining a β estimate from a single (or few) binary system with MS stars in the considered mass range

Uncertainty on overshooting calibration in evolved binary systems

- Synthetic binary systems generated from a 2.50 $M_{\odot}$ star coupled with a 2.38 $M_{\odot}$ (M_1/M_2=1.05) + Gaussian noise ([Fe/ H] = 0.0, Y = 0.275 , $\frac{\Delta Y}{\Delta Z}$ = 2, β =0.16, 250000 synthetic systems for each configuration)

- **Error of: 1% and 0.1% in mass, 0.5% in radius, 0.1 dex in [Fe/H] and 100 K in T_{eff}**

- Two configurations: 1) Primary at the RGB bottom + the secondary in MS phase 2) primary at the He core burning + the secondary in Subgiant Branch

- Stellar parameters (age, Y, Z and β) are recovered **adopting a model grid (2.26 $M_{\odot} \leq M \leq 2.62\ M_{\odot}$, $-0.4 \leq$ [Fe/H] ≤ 0.4, $\frac{\Delta Y}{\Delta Z}$ from 1 to 3, 18 β values in the range [0.00; 0.30])**

- **Parameters can be estimated both for the individual components and for the whole system.**

- Stellar models and artificial observations perfectly agree with respect to the adopted input physics

- Very precise mass determinations with uncertainty of few parts per thousand are required to obtain reliable determinations of overshooting efficiency, as mass errors of the order of 1% lead to a large variability of β estimates

- Even in the case of a very accurate mass determination the obtained β calibration for a primary star already evolved past the MS is biased toward lower values (by about 15-20%) and it's affected in general by a random 1σ error of about ±15%

- The bias in age ranges from 4 to 8% toward lower values with a random 1σ error of about ±15%

- For a calibration against a real binary system, the expected situation is even worse, because one cannot be confident that the adopted stellar models perfectly describe the reality

- Allowing the stars to have independent overshooting efficiency in the recovery of synthetic systems does not lead to additional bias but the precision of the result is reduced. For real systems this would lead to an additional free parameter, which could mask the possible difficulty of stellar tracks to fit the system

- The initial helium abundance is recovered with large variance and non-negligible bias

The distinction between models at β = 0.0 and β = 0.16 seems to be quite reliable for the case of 0.1% mass error when no systematic discrepancies between models and synthetic stars exist

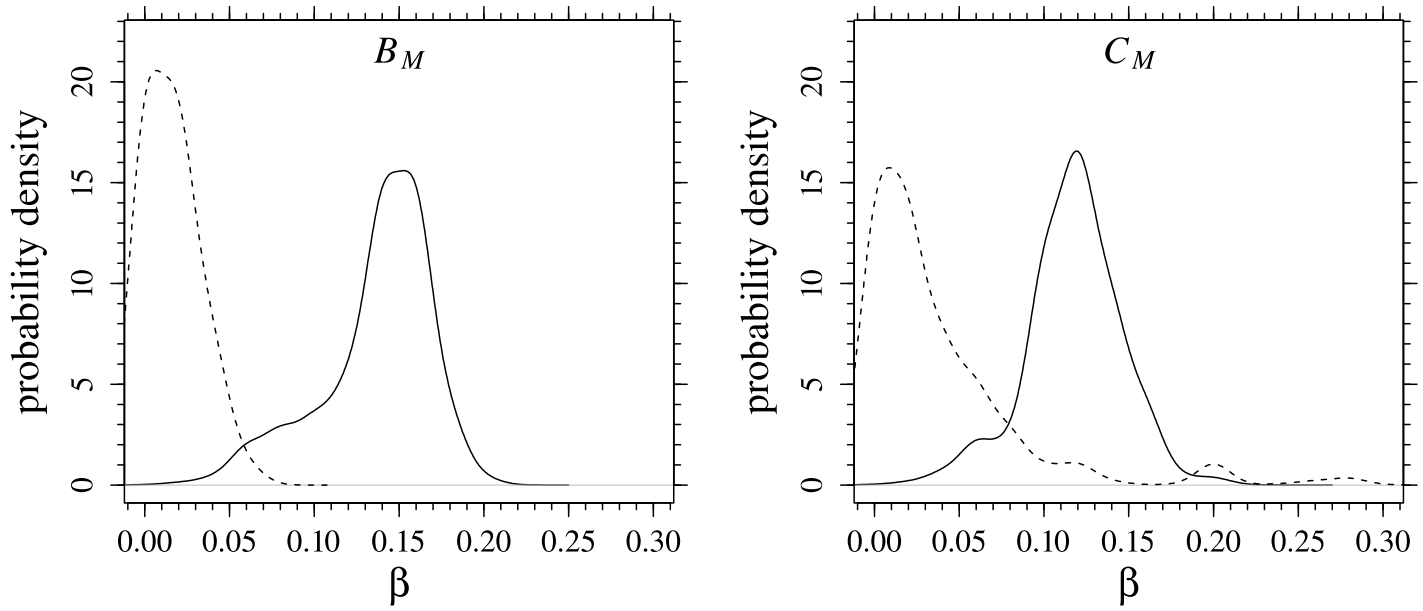

Marginalized density of probability for the recovered β parameter for the two different evolutionary scenarios. The solid line corresponds to models sampled from the grid at β = 0.16, while the dashed one to models sampled at β = 0.0.

The relevance of the uncertainty on the β recovery is clearly related to the purpose of the fit, while it impacts in a relevant way on every single system fit, it allows a global approach

The analysis of detached eclipsing double lined binary systems is a powerful method

However..

- A statistically robust recovery of stellar parameters and treatment of the error sources is needed
- Warning against relying on fits which allow too much free parameters which could mask the effects of any given unknown source

- Asteroseismic data will provide further important constraints, even if very few binary systems have solar-like oscillations detected in both components, to…

…determine convective core extension, distinguish between Red Giant Branch and clump stars, estimate surface He abundance, etc… (see e.g. Bouchy & Carrier 2002; Bedding et al. 2004; Kjeldsen et al. 2005, Fletcher et al. 2006; Bazot et al. 2007, Mosser et al. 2011, Bedding et al. 2011, Metcalfe et al. 2012, 2015; Miglio et al. 2014, Davies et al. 2015, Appourchaux et al. 2012, 2015, Bazot et al. 2016 etc..)

BACKUP

(Claret & Torres 2017)

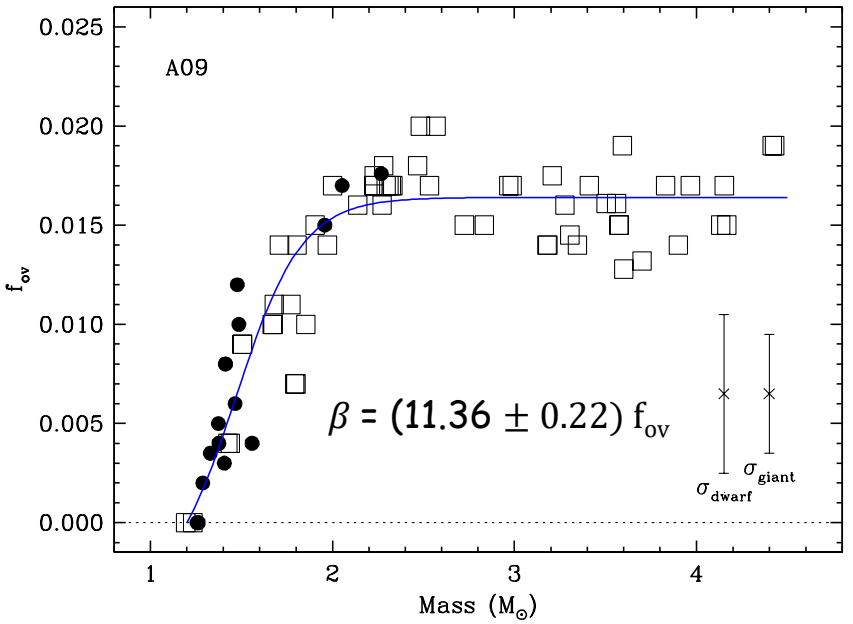

Figure 2. Inferred f_{ov} values from MESA models using the A09 mixture (Table 2) as a function of stellar mass. Filled circles represent the stars in the present sample (including YZ Cas and TZ For), and open squares are values taken for the 29 dwarf and giant DLEBs from Table 3 of Claret & Torres (2017), determined in the same way with the same element mixture and helium content. Typical error bars for dwarfs and giants are indicated on the lower right.

$\Delta M \leq 1\%$, $\Delta R \leq$ few %

$M_1/M_2 \leq 1.05$

spectroscopic abundances

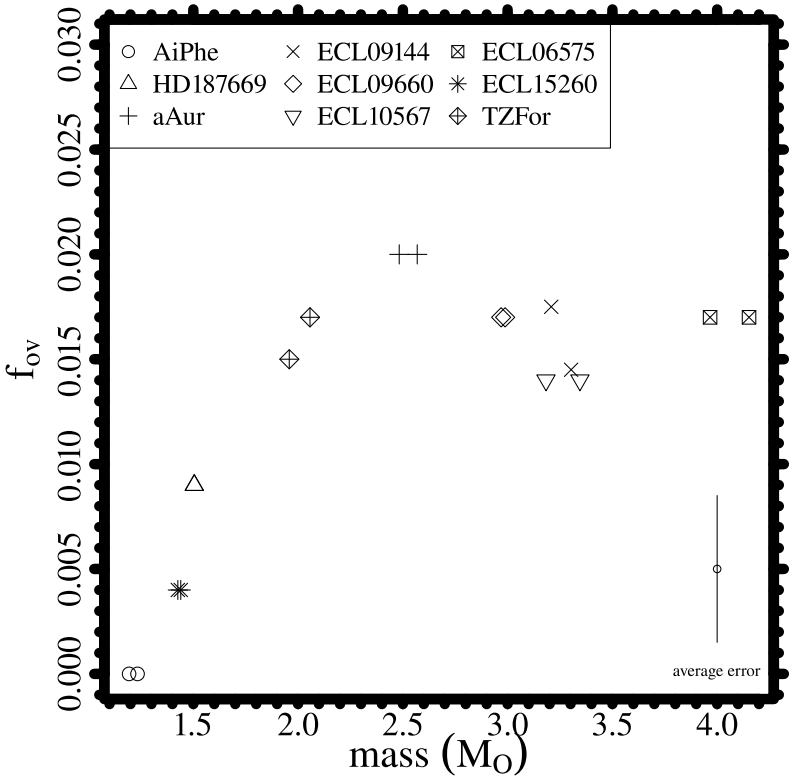

Mass loss up to the RGB tip

- **Mass loss in RGB is difficult to measure** (see e.g. Mc Donald & van Loon 2007, 2012, Meszoras et al. 2009, Groenewegen 2014….)
- **Recent constraints give for the parameter of the Reimers mass loss formulation*** (Reimers 1975) : $\eta = 0.5 \pm 0.1$ (Mc Donald & Zijlstra2015), $0.1 < \eta < 0.3$ (Miglio et al. 2012)

Analysis of the effects of different assumptions about mass loss on the recovery of **single star** characteristics:
(see e.g. Casagrande et al. 2014, 2016, 2017 Valle et al. 2017, etc..)

- **Significant impact of mass loss indetermination for red clump stars and very little effect for RGB stars except in the phases after the RGB bump in which the uncertainty on the age estimate can reach values comparable to the random errors**
- **Mass loss effects vanish for stars with mass M $\geq$ 1.5 $M_{\odot}$**

➡ impact of RGB mass loss on age determination for binary systems ➡ ?

* $\dot{M} = \eta \times 4 \times 10^{-13} \times \frac{LR}{M} \quad (M_{\odot}\ \mathrm{yr}^{-1}),$

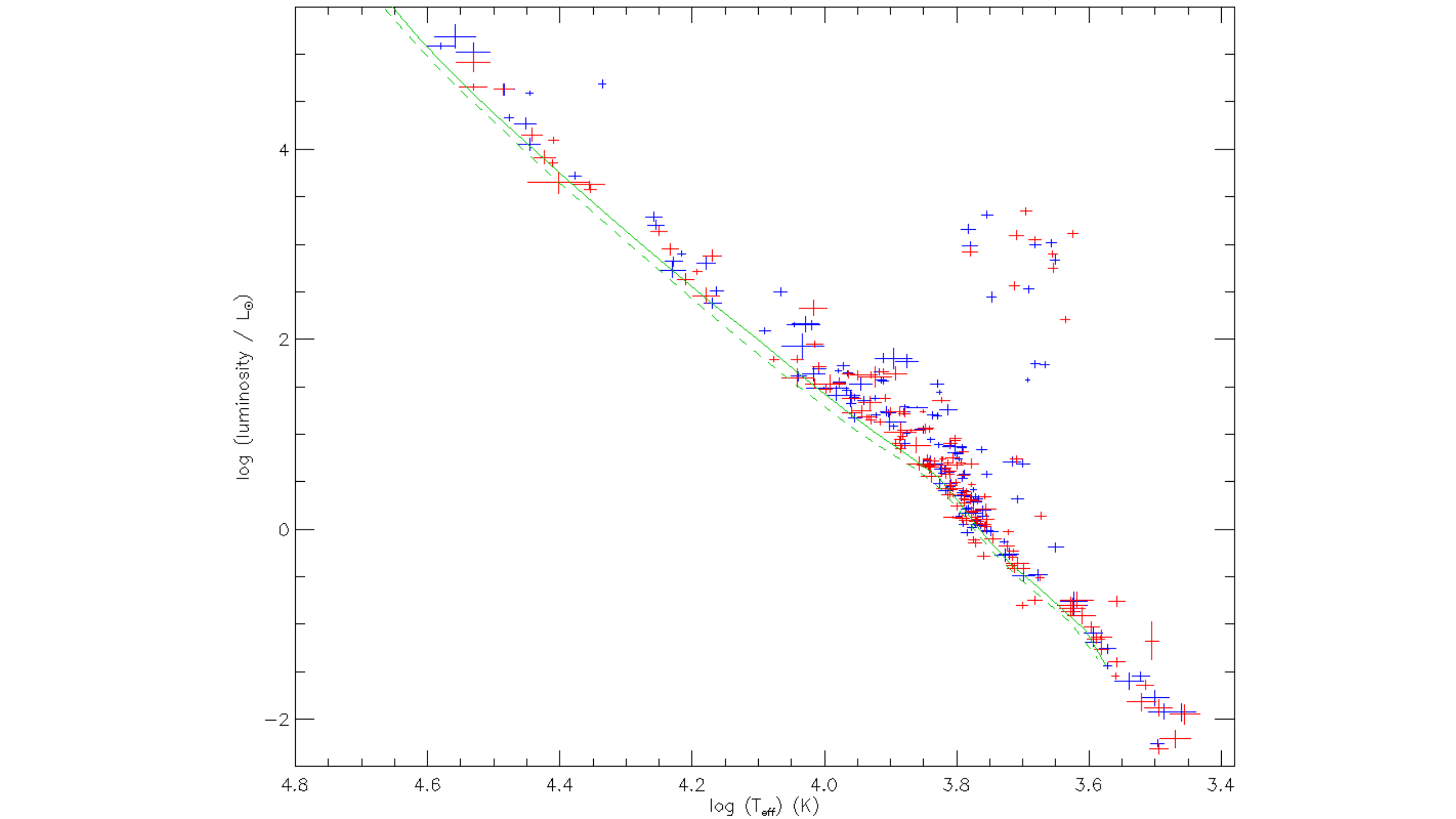
log (luminosity / L⊙)
4
2
0
−2
4.8
4.6
4.4
4.2
4.0
3.8
3.6
3.4
log (T_eff) (K)

Code:	EOS	Radiative Opacity	Boundary Conditions	Convection	Y, Z	overshooting	diffusion
Pisa models	OPAL06 SCVH95	OPAL F05 (AS09)	non-grey, $\tau_{bc} = 10$ BT-Settl AHF11 CK03 ($T_{eff} \geq 10^4$K)	MLT α_{ML}=2.00	Y=0.274, Z= 0.013	β_{ov} = 0.25	Thoul et al. (1994)
BASTI	FreeEOS	OPAL F05 (C11)	Vernazza et al. (1981) ($M > 0.45\ M_{\odot}$) BT-Settl AHF11 (VLM), $\tau_{bc} = 100$	MLT α_{ML}=2.00	Y=0.264, Z= 0.01258	β_{ov} = 0.20	No
BHAC15	SCVH95	OPAL AF94 (AS09+C11)	non-grey, $\tau_{bc} = 100$ BT-Settl AHF12	MLT α_{ML}=1.6	Y=0.280, Z= 0.015	No	No
MIST	OPAL06 SCVH95	OPAL F05 (AS09)	non-grey, $\tau_{bc} = 100$ ATLAS12	MLT α_{ML}=1.82	Y=0.270, Z= 0.014	diffusive	Thoul et al. (1994)
PARSEC	FreeEOS	OPAL M09 (C11)	non-grey, $\tau_{bc} = 2/3$ BT-Settl AHF11	MLT α_{ML}=1.7	Y=0.274, Z= 0.013	$\beta_{ov} \approx 0.25$	Thoul et al. (1994)

Observed quantities for the two stars: $q^{S_{1,2}} \equiv \{T_{\mathrm{eff},S_{1,2}}, [\mathrm{Fe/H}]_{S_{1,2}}, M_{S_{1,2}}, R_{S_{1,2}}\}$

Nominal uncertainty in the observed quantities: $\sigma^{1,2} = \{\sigma(T_{\mathrm{eff},S_{1,2}}), \sigma([\mathrm{Fe/H}]_{S_{1,2}}), \sigma(M_{S_{1,2}}), \sigma(R_{S_{1,2}})\}$

For each point j on the estimation grid of stellar models, we define: $q^j \equiv \{T_{\mathrm{eff},j}, [\mathrm{Fe/H}]_j, M_j, R_j\}$

Likelihood function: $L^{1,2}{}_j = \left(\prod_{i=1}^{4} \frac{1}{\sqrt{2\pi\sigma_i^{1,2}}}\right) \times \exp\left(-\frac{X^2_{1,2}}{2}\right)$, where: $X^2_{1,2} = \sum_{i=1}^{4} \left(\frac{q_i^{S_{1,2}} - q_i^j}{\sigma_i}\right)^2$

The single-star likelihood functions are independently evaluated for the two stars for each grid point within 3σ of all the variables from $S_{1,2}$; the joint likelihood for the system is computed as the product of the single-star likelihood functions.

Coevality is explicitly assumed computing the joint likelihood function only for the couples of models in the two 3σ boxes with ages within 10 Myr. Let $\mathcal{L}_{max}$ be the maximum value obtained in this step.

The joint-star estimated age is obtained by averaging the corresponding quantity of all the couples of models with likelihood greater than 0.95 × $\mathcal{L}_{max}$

Observed quantities for the two stars: $q^{S_{1,2}} \equiv \{T_{\mathrm{eff},S_{1,2}}, [\mathrm{Fe/H}]_{S_{1,2}}, M_{S_{1,2}}, R_{S_{1,2}}\}$

Nominal uncertainty in the observed quantities: $\sigma^{1,2} = \{\sigma(T_{\mathrm{eff},S_{1,2}}), \sigma([\mathrm{Fe/H}]_{S_{1,2}}), \sigma(M_{S_{1,2}}), \sigma(R_{S_{1,2}})\}$

For each point j on the estimation grid of stellar models, we define: $q^j \equiv \{T_{\mathrm{eff},j}, [\mathrm{Fe/H}]_j, M_j, R_j\}$

Likelihood function: $L^{1,2}{}_j = \left(\prod_{i=1}^{4} \frac{1}{\sqrt{2\pi\sigma_i^{1,2}}}\right) \times \exp\left(-\frac{\chi^2_{1,2}}{2}\right)$, where: $\chi^2_{1,2} = \sum_{i=1}^{4} \left(\frac{q_i^{S_{1,2}} - q_i^j}{\sigma_i}\right)^2$

The single-star likelihood functions are independently evaluated for the two stars for each grid point within 3σ of all the variables from $S_{1,2}$;

Let $L^{1,2}{}_{max}$ be the two maximum values obtained in this step

The single-star ages are estimated by averaging the corresponding quantity of all the models with likelihood greater than $0.95 \times L^{1,2}{}_{max}$

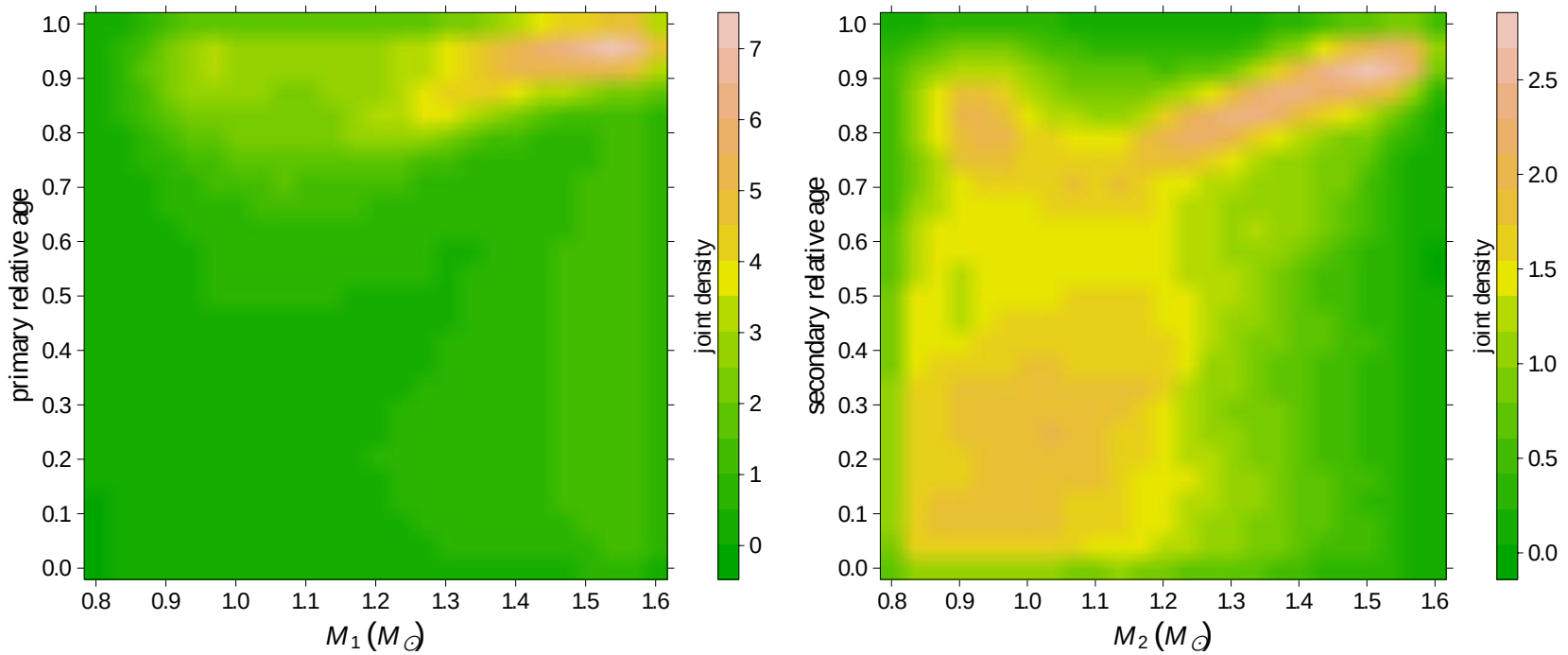

Fig. A.1. *Left*: joint density of mass and relative ages in the sample of primary stars. The colours correspond to the different densities of probability. *Right*: same as the left panel for secondary stars. The colour scales of the two panels are different.

The sample of primary stars is biased towards high masses and high relative ages since these models have higher intrinsic luminosity. The distribution of secondary stars is more diffuse, since several young low-mass models are present in the sample

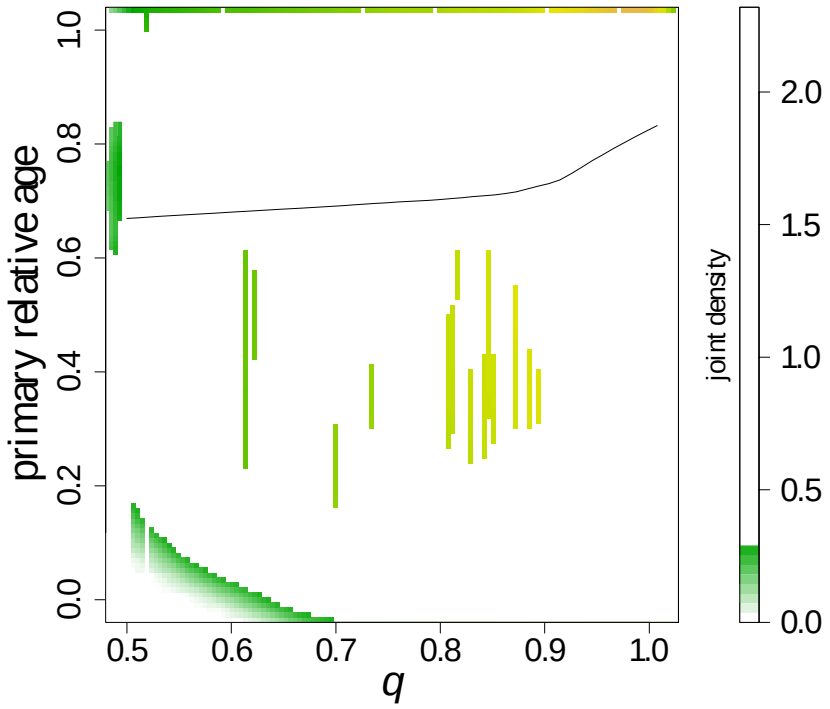

Fig. A.2. Joint density of mass ratio q and primary relative age in the sample of binary stars. The solid line displays the LOESS-smoothed trend of relative age versus mass ratio q.

For binary systems with near equal masses, the sampling returns more evolved stars. This bias comes from later evolutionary phases needing more points to adequately follow the rapid evolution

Observational errors are sampled from a multivariate normal distribution assuming correlation of $\rho = 0.95$ between the two effective temperatures, $\rho = 0.95$ between the two metallicities, $\rho = 0.8$ between the two masses, and zero between the two radii.

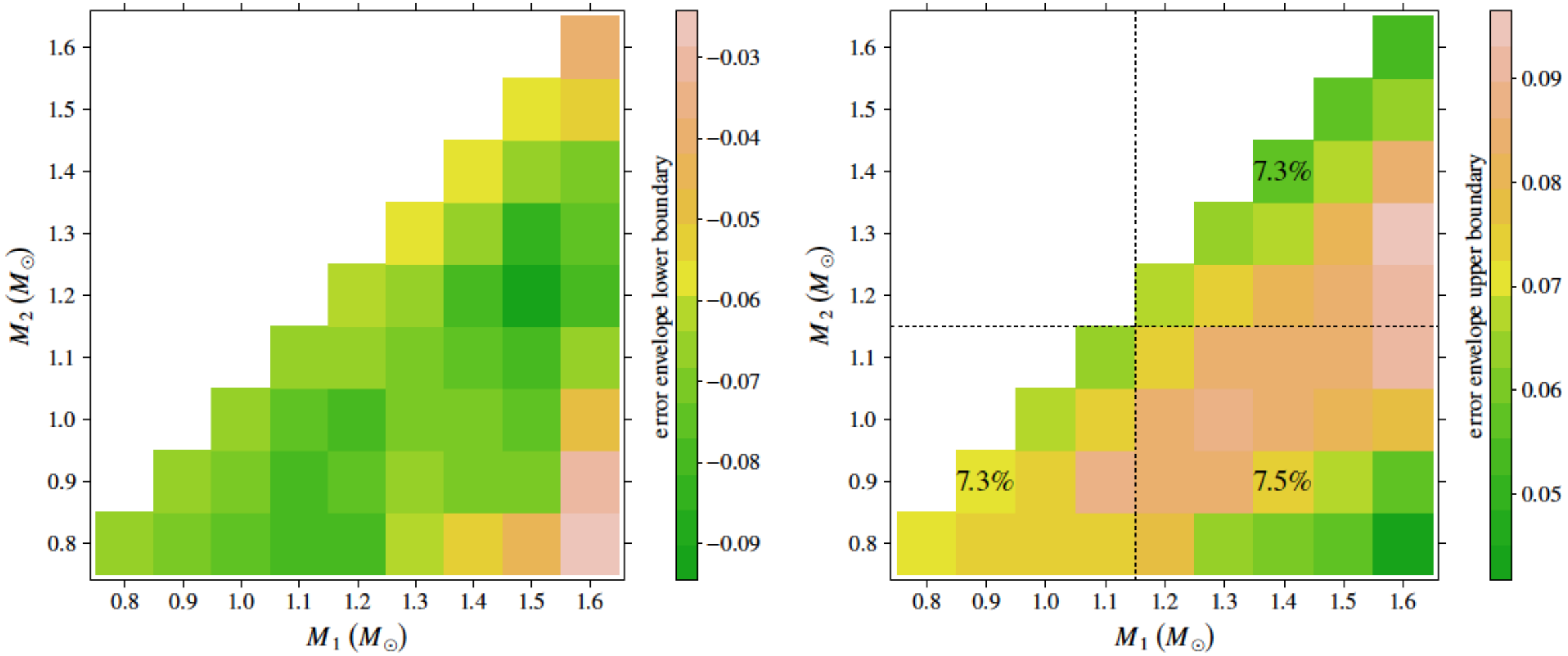

Fig. 3. *Upper row*: left lower boundary of the 1σ 2D relative error envelope for joint likelihood estimates as a function of the mass of the binary system stars. The percentages on the plot refer to mean values in different ranges of mass (see text). *Right*: same as the left panel, but for the upper boundary of the 2D relative error envelope. *Lower row*: left ratio of lower boundary of the 1σ 2D relative error envelope due to different

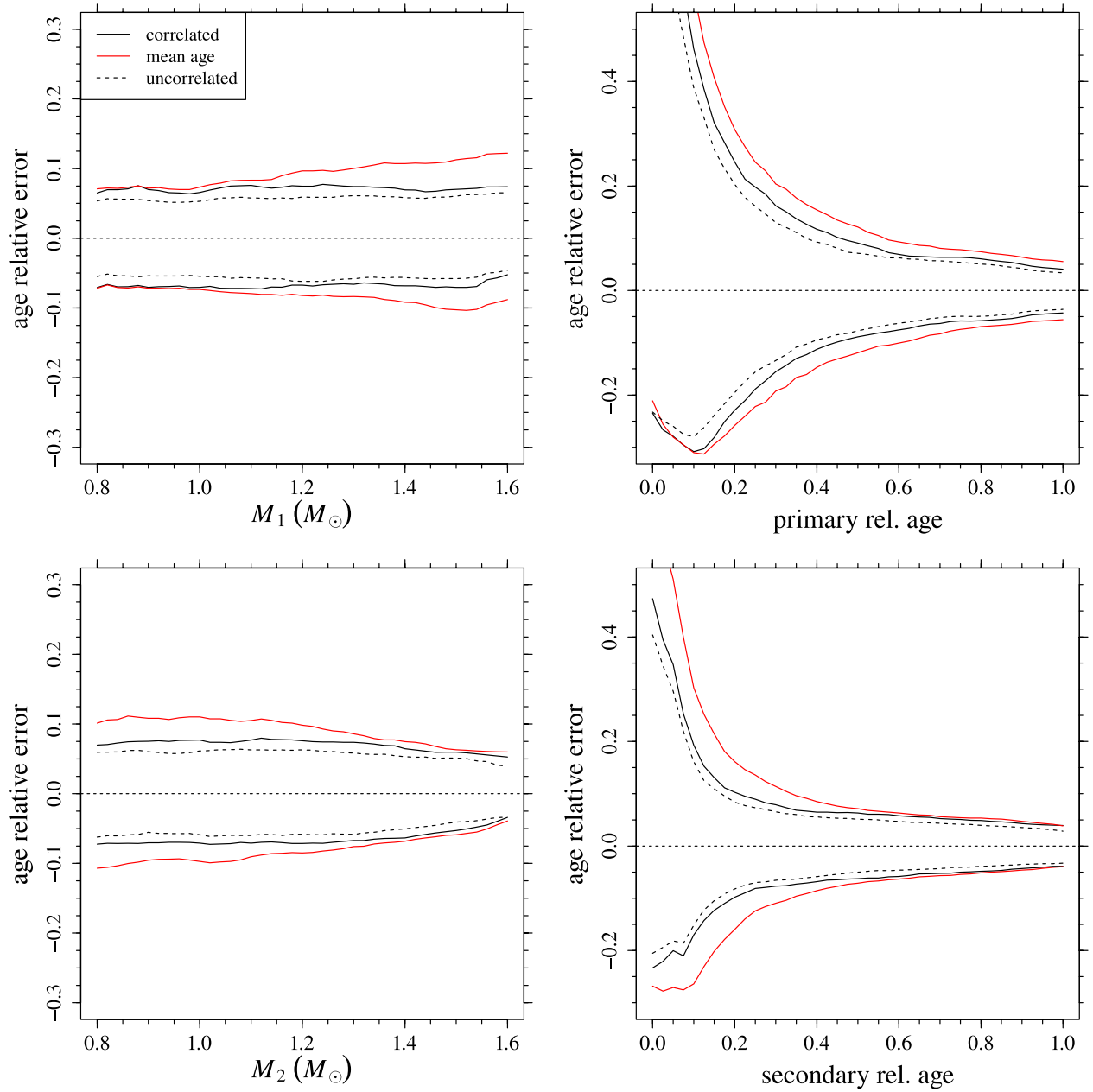

Fig. 2. *Upper row*: 1σ envelope of the age relative error in dependence on the mass of the primary star (*left panel*), and on its relative age (*right panel*). The solid black line corresponds to accounting for correlations in covariance matrix (see text) and assumes that the stars are coeval; the red solid line assumes the same covariance matrix without assumption of coeval stars in the recovery (see Sect. 2); the dashed line assumes coeval stars and a diagonal covariance matrix. *Lower row*: same as the upper row, but for the secondary star.

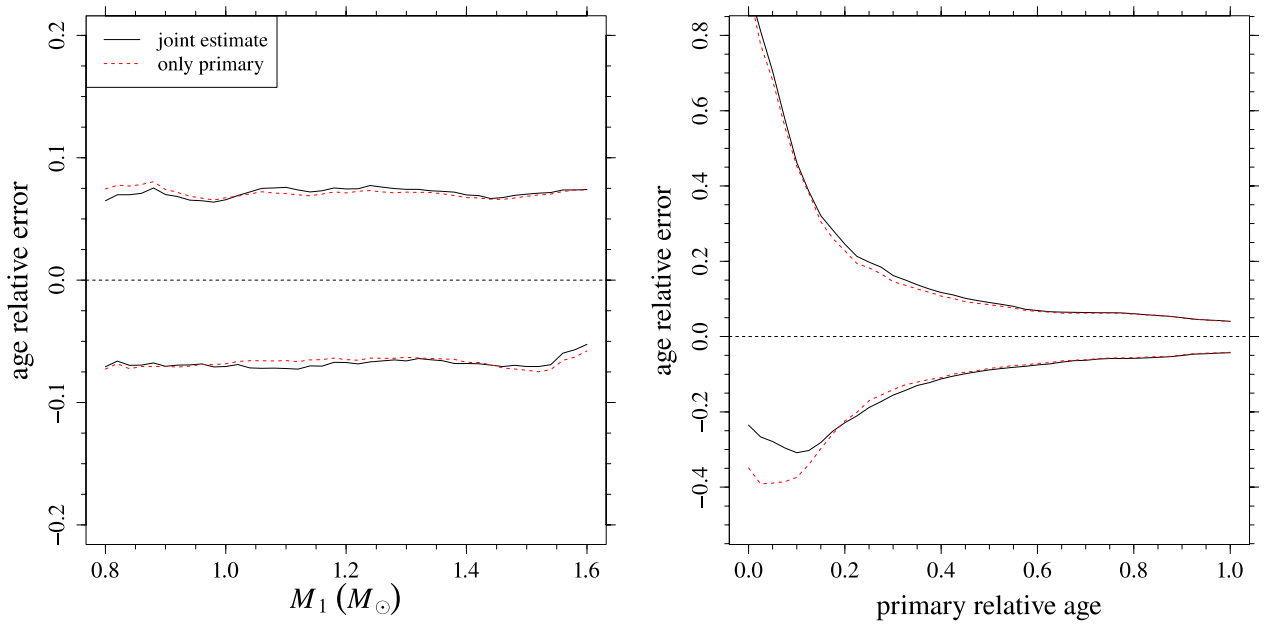

Fig. 4. *Left*: 1σ envelope of the age-relative error in dependence on the mass of the primary star (solid line), compared with the same quantity computed only with the data of the primary star (dashed line). *Right*: same as the left panel, but as a function of relative age of the primary star.

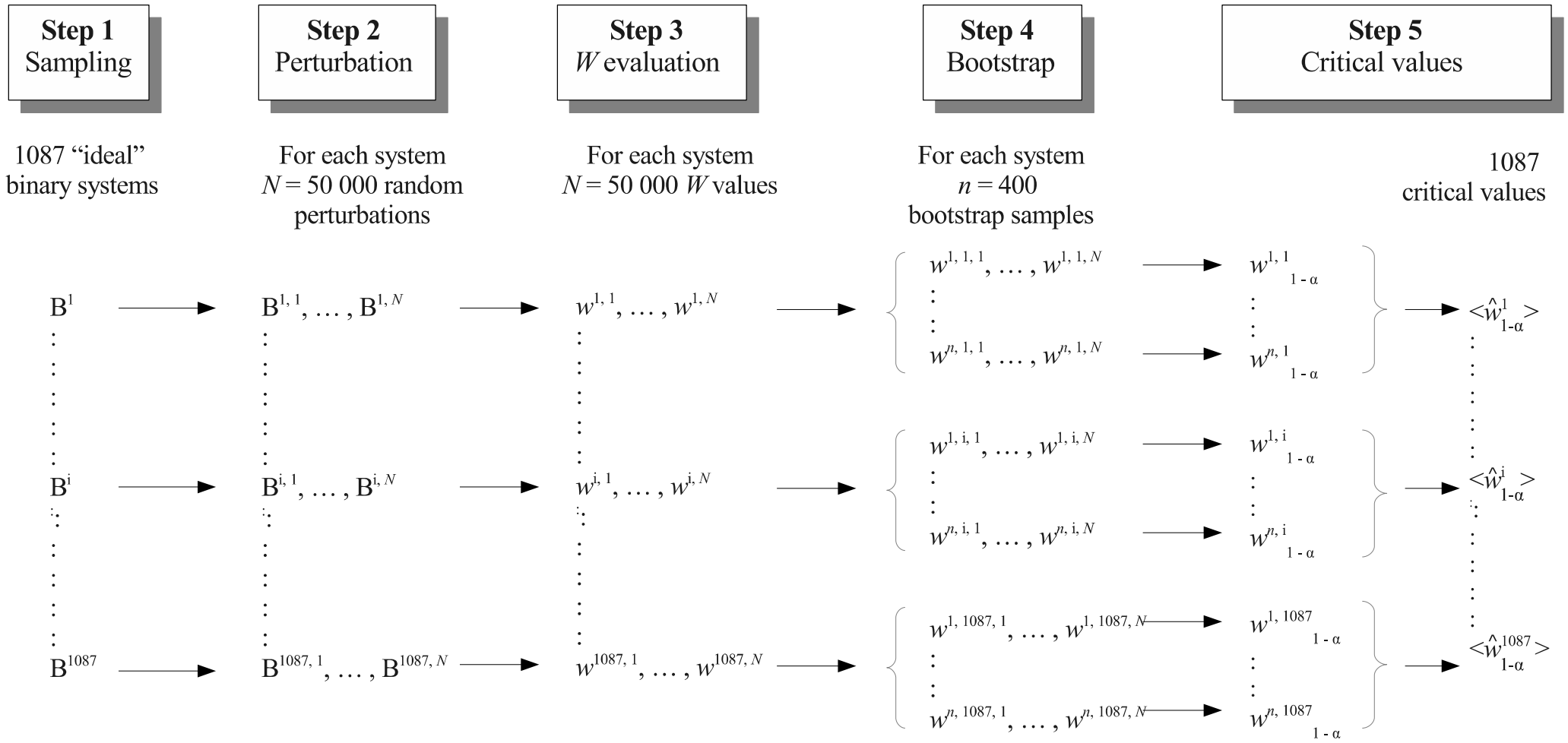
Step 1
Sampling
Step 2
Perturbation
Step 3
W evaluation
Step 4
Bootstrap
Step 5
Critical values
1087 "ideal" binary systems
For each system N = 50 000 random perturbations
For each system N = 50 000 W values
For each system n = 400 bootstrap samples
1087 critical values
B1
Bi
B1087
B1, 1, … , B1, N
Bi, 1, … , Bi, N
B1087, 1, … , B1087, N
w1, 1, … , w1, N
wi, 1, … , wi, N
w1087, 1, … , w1087, N
w1, 1, 1, … , w1, 1, N
wn, 1, 1, … , wn, 1, N
w1, 1 1 - α
wn, 1 1 - α
w1, i, 1, … , w1, i, N
wn, i, 1, … , wn, i, N
w1, i 1 - α
wn, i 1 - α
w1, 1087, 1, … , w1, 1087, N
wn, 1087, 1, … , wn, 1087, N
w1, 1087 1 - α
wn, 1087 1 - α
<ŵ1 1-α>
<ŵi 1-α>
<ŵ1087 1-α>

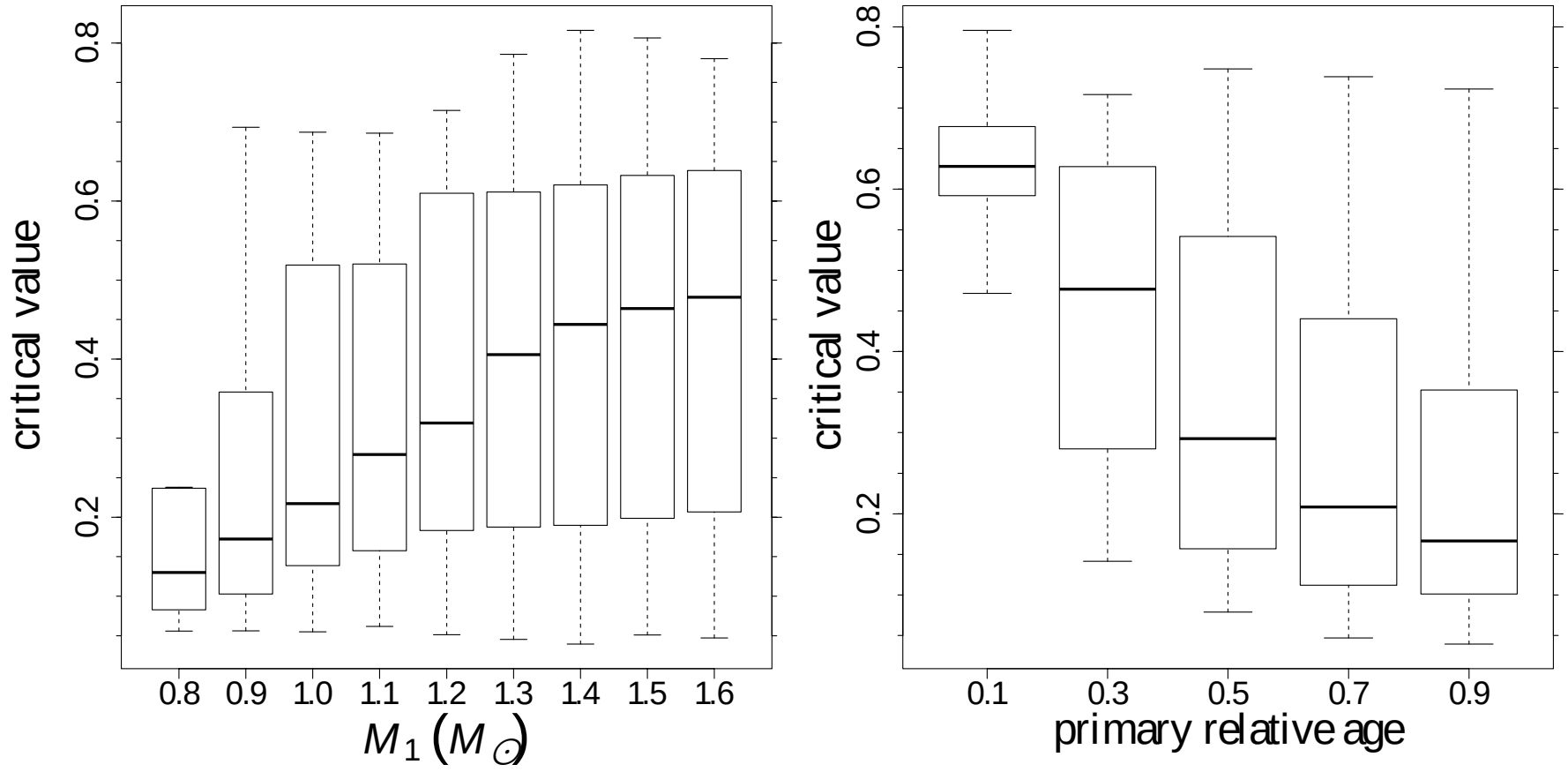

Fig. 3. *Left*: boxplot of the $W_{0.95}$ quantile estimates as a function of the mass of the primary star. *Right*: same as the left panel, but for the dependence on the relative age of the primary star.

Appendix A: Tables of critical values

Table A.1. Critical values $W_{0.95}$ in dependence on masses of the stars M_1 and M_2 (both in solar units), and on their initial metallicity [Fe/H].

M_1	[Fe/H]	M_2								
		0.8	0.9	1.0	1.1	1.2	1.3	1.4	1.5	1.6
0.80	–0.55	0.591								
0.90	–0.55	0.643	0.561							
1.00	–0.55	0.625	0.595	0.517						
1.10	–0.55	0.617	0.603	0.581	0.536					
1.20	–0.55	0.683	0.692	0.641	0.620	0.545				
1.30	–0.55		0.786	0.741	0.667	0.611	0.588			
1.40	–0.55		0.816	0.763	0.663	0.617	0.594	0.579		
1.50	–0.55			0.792	0.695	0.601	0.594	0.587	0.568	
1.60	–0.55				0.692	0.564	0.554	0.582	0.605	0.472
0.80	–0.25	0.598								
0.90	–0.25	0.662	0.585							
1.00	–0.25	0.661	0.629	0.572						
1.10	–0.25	0.629	0.606	0.603	0.534					
1.20	–0.25	0.623	0.619	0.613	0.603	0.507				
1.30	–0.25		0.726	0.699	0.688	0.614	0.539			
1.40	–0.25			0.779	0.734	0.682	0.593	0.574		
1.50	–0.25			0.796	0.740	0.676	0.592	0.574	0.562	
1.60	–0.25				0.732	0.650	0.582	0.576	0.601	0.458
0.80	0.00	0.602								
0.90	0.00	0.659	0.603							
1.00	0.00	0.673	0.645	0.598						
1.10	0.00	0.681	0.637	0.628	0.588					
1.20	0.00	0.702	0.648	0.615	0.610	0.541				
1.30	0.00		0.686	0.623	0.628	0.604	0.518			
1.40	0.00			0.730	0.696	0.674	0.618	0.535		
1.50	0.00			0.806	0.767	0.710	0.677	0.571	0.544	
1.60	0.00				0.774	0.688	0.670	0.592	0.594	0.455
0.80	0.25	0.625								
0.90	0.25	0.683	0.618							
1.00	0.25	0.678	0.660	0.620						
1.10	0.25	0.678	0.654	0.648	0.608					
1.20	0.25	0.708	0.658	0.630	0.633	0.584				
1.30	0.25		0.717	0.644	0.632	0.606	0.535			
1.40	0.25			0.688	0.631	0.616	0.577	0.534		
1.50	0.25			0.769	0.713	0.674	0.632	0.595	0.510	
1.60	0.25				0.780	0.729	0.677	0.661	0.586	0.445
0.80	0.55	0.643								
0.90	0.55	0.693	0.644							
1.00	0.55	0.687	0.671	0.630						
1.10	0.55	0.671	0.653	0.659	0.620					
1.20	0.55	0.715	0.653	0.649	0.647	0.604				
1.30	0.55		0.699	0.643	0.633	0.630	0.580			
1.40	0.55		0.731	0.659	0.611	0.630	0.626	0.495		
1.50	0.55			0.708	0.643	0.592	0.601	0.537	0.421	
1.60	0.55			0.748	0.685	0.612	0.610	0.619	0.559	0.281

Notes. Values are computed for primary relative age $r = 0.1$.

Appendix A: Tables of critical values

Table A.1. Critical values $W_{0.95}$ in dependence on masses of the stars M_1 and M_2 (both in solar units), and on their initial metallicity [Fe/H].

M_1	[Fe/H]	M_2								
		0.8	0.9	1.0	1.1	1.2	1.3	1.4	1.5	1.6
0.80	–0.55	0.591								
0.90	–0.55	0.643	0.561							
1.00	–0.55	0.625	0.595	0.517						
1.10	–0.55	0.617	0.603	0.581	0.536					
1.20	–0.55	0.683	0.692	0.641	0.620	0.545				
1.30	–0.55		0.786	0.741	0.667	0.611	0.588			
1.40	–0.55		0.816	0.763	0.663	0.617	0.594	0.579		
1.50	–0.55			0.792	0.695	0.601	0.594	0.587	0.568	
1.60	–0.55				0.692	0.564	0.554	0.582	0.605	0.472
0.80	–0.25	0.598								
0.90	–0.25	0.662	0.585							
1.00	–0.25	0.661	0.629	0.572						
1.10	–0.25	0.629	0.606	0.603	0.534					
1.20	–0.25	0.623	0.619	0.613	0.603	0.507				
1.30	–0.25		0.726	0.699	0.688	0.614	0.539			
1.40	–0.25			0.779	0.734	0.682	0.593	0.574		
1.50	–0.25			0.796	0.740	0.676	0.592	0.574	0.562	
1.60	–0.25				0.732	0.650	0.582	0.576	0.601	0.458
0.80	0.00	0.602								
0.90	0.00	0.659	0.603							
1.00	0.00	0.673	0.645	0.598						
1.10	0.00	0.681	0.637	0.628	0.588					
1.20	0.00	0.702	0.648	0.615	0.610	0.541				
1.30	0.00		0.686	0.623	0.628	0.604	0.518			
1.40	0.00			0.730	0.696	0.674	0.618	0.535		
1.50	0.00			0.806	0.767	0.710	0.677	0.571	0.544	
1.60	0.00				0.774	0.688	0.670	0.592	0.594	0.455
0.80	0.25	0.625								
0.90	0.25	0.683	0.618							
1.00	0.25	0.678	0.660	0.620						
1.10	0.25	0.678	0.654	0.648	0.608					
1.20	0.25	0.708	0.658	0.630	0.633	0.584				
1.30	0.25		0.717	0.644	0.632	0.606	0.535			
1.40	0.25			0.688	0.631	0.616	0.577	0.534		
1.50	0.25			0.769	0.713	0.674	0.632	0.595	0.510	
1.60	0.25				0.780	0.729	0.677	0.661	0.586	0.445
0.80	0.55	0.643								
0.90	0.55	0.693	0.644							
1.00	0.55	0.687	0.671	0.630						
1.10	0.55	0.671	0.653	0.659	0.620					
1.20	0.55	0.715	0.653	0.649	0.647	0.604				
1.30	0.55		0.699	0.643	0.633	0.630	0.580			
1.40	0.55		0.731	0.659	0.611	0.630	0.626	0.495		
1.50	0.55			0.708	0.643	0.592	0.601	0.537	0.421	
1.60	0.55			0.748	0.685	0.612	0.610	0.619	0.559	0.281

Notes. Values are computed for primary relative age $r = 0.1$.

Table A.3. As in Table A.1, but for a primary relative age $r = 0.5$.

M_1	[Fe/H]	M_2								
		0.8	0.9	1.0	1.1	1.2	1.3	1.4	1.5	1.6
0.80	–0.55	0.129								
0.90	–0.55	0.201	0.132							
1.00	–0.55	0.318	0.195	0.126						
1.10	–0.55	0.474	0.288	0.180	0.117					
1.20	–0.55	0.618	0.416	0.275	0.165	0.103				
1.30	–0.55	0.678	0.536	0.364	0.235	0.143	0.101			
1.40	–0.55	0.608	0.619	0.455	0.315	0.193	0.143	0.113		
1.50	–0.55	0.526	0.653	0.558	0.418	0.285	0.202	0.146	0.117	
1.60	–0.55	0.457	0.613	0.611	0.498	0.404	0.349	0.236	0.162	0.090
0.80	–0.25	0.129								
0.90	–0.25	0.208	0.138							
1.00	–0.25	0.337	0.196	0.132						
1.10	–0.25	0.496	0.308	0.196	0.129					
1.20	–0.25	0.647	0.455	0.299	0.183	0.112				
1.30	–0.25	0.698	0.599	0.427	0.274	0.156	0.098			
1.40	–0.25	0.629	0.661	0.551	0.377	0.221	0.144	0.110		
1.50	–0.25	0.541	0.676	0.652	0.459	0.280	0.192	0.148	0.113	
1.60	–0.25	0.477	0.643	0.690	0.553	0.366	0.288	0.222	0.158	0.092
0.80	0.00	0.130								
0.90	0.00	0.212	0.140							
1.00	0.00	0.329	0.201	0.138						
1.10	0.00	0.490	0.303	0.195	0.136					
1.20	0.00	0.627	0.452	0.300	0.197	0.132				
1.30	0.00	0.676	0.610	0.442	0.286	0.179	0.108			
1.40	0.00	0.597	0.700	0.594	0.419	0.257	0.157	0.099		
1.50	0.00	0.529	0.675	0.687	0.548	0.363	0.223	0.131	0.104	
1.60	0.00	0.483	0.638	0.725	0.638	0.457	0.296	0.189	0.149	0.087
0.80	0.25	0.132								
0.90	0.25	0.203	0.139							
1.00	0.25	0.314	0.197	0.141						
1.10	0.25	0.499	0.289	0.194	0.139					
1.20	0.25	0.649	0.436	0.293	0.191	0.134				
1.30	0.25	0.699	0.608	0.450	0.288	0.186	0.122			
1.40	0.25	0.630	0.701	0.615	0.418	0.256	0.161	0.109		
1.50	0.25	0.545	0.671	0.698	0.574	0.364	0.220	0.148	0.104	
1.60	0.25	0.481	0.636	0.729	0.671	0.498	0.325	0.222	0.151	0.079
0.80	0.55	0.134								
0.90	0.55	0.210	0.144							
1.00	0.55	0.308	0.202	0.141						
1.10	0.55	0.469	0.295	0.194	0.148					
1.20	0.55	0.663	0.441	0.278	0.191	0.147				
1.30	0.55	0.709	0.636	0.406	0.273	0.187	0.136			
1.40	0.55	0.640	0.737	0.598	0.396	0.271	0.186	0.127		
1.50	0.55	0.567	0.696	0.696	0.542	0.348	0.240	0.156	0.112	
1.60	0.55	0.494	0.652	0.748	0.639	0.459	0.323	0.201	0.167	0.082

Table A.4. As in Table A.1, but for a primary relative age $r = 0.7$.

M_1	[Fe/H]	M_2								
		0.8	0.9	1.0	1.1	1.2	1.3	1.4	1.5	1.6
1.40	–0.55	0.688	0.503	0.348	0.219	0.135	0.082	0.063		
1.50	–0.55	0.641	0.616	0.431	0.294	0.199	0.144	0.083	0.064	
1.60	–0.55	0.581	0.666	0.498	0.394	0.283	0.220	0.177	0.112	0.050
0.80	–0.25	0.086								
0.90	–0.25	0.142	0.098							
1.00	–0.25	0.225	0.141	0.090						
1.10	–0.25	0.357	0.228	0.149	0.086					
1.20	–0.25	0.507	0.323	0.208	0.124	0.088				
1.30	–0.25	0.639	0.458	0.308	0.186	0.104	0.065			
1.40	–0.25	0.713	0.577	0.415	0.264	0.150	0.084	0.064		
1.50	–0.25	0.658	0.660	0.518	0.343	0.200	0.132	0.092	0.065	
1.60	–0.25	0.599	0.719	0.606	0.424	0.266	0.201	0.162	0.114	0.049
0.80	0.00	0.083								
0.90	0.00	0.142	0.099							
1.00	0.00	0.227	0.139	0.093						
1.10	0.00	0.351	0.219	0.137	0.087					
1.20	0.00	0.506	0.329	0.220	0.138	0.096				
1.30	0.00	0.636	0.464	0.311	0.197	0.125	0.076			
1.40	0.00	0.692	0.606	0.440	0.291	0.177	0.100	0.070		
1.50	0.00	0.625	0.670	0.572	0.399	0.250	0.150	0.079	0.064	
1.60	0.00	0.566	0.722	0.646	0.492	0.331	0.208	0.134	0.094	0.047
0.80	0.25	0.084								
0.90	0.25	0.139	0.093							
1.00	0.25	0.217	0.138	0.092						
1.10	0.25	0.345	0.208	0.136	0.090					
1.20	0.25	0.526	0.305	0.213	0.135	0.087				
1.30	0.25	0.660	0.440	0.301	0.199	0.127	0.086			
1.40	0.25	0.713	0.608	0.444	0.283	0.181	0.111	0.083		
1.50	0.25	0.654	0.678	0.595	0.397	0.250	0.155	0.093	0.076	
1.60	0.25	0.595	0.718	0.671	0.509	0.346	0.233	0.155	0.102	0.057
0.80	0.55	0.083								
0.90	0.55	0.140	0.093							
1.00	0.55	0.217	0.139	0.091						
1.10	0.55	0.330	0.218	0.139	0.095					
1.20	0.55	0.492	0.313	0.205	0.138	0.098				
1.30	0.55	0.675	0.451	0.289	0.199	0.137	0.098			
1.40	0.55	0.716	0.629	0.402	0.275	0.188	0.127	0.104		
1.50	0.55	0.662	0.728	0.539	0.361	0.249	0.163	0.112	0.096	
1.60	0.55	0.611	0.739	0.651	0.480	0.336	0.241	0.154	0.116	0.069

Table A.5. As in Table A.1, but for a primary relative age $r = 0.9$.

M_1	[Fe/H]	M_2								
		0.8	0.9	1.0	1.1	1.2	1.3	1.4	1.5	1.6
0.80	–0.55	0.057								
0.90	–0.55	0.097	0.056							
1.00	–0.55	0.164	0.110	0.055						
1.10	–0.55	0.254	0.166	0.094	0.064					
1.20	–0.55	0.381	0.241	0.148	0.081	0.051				
1.30	–0.55	0.511	0.328	0.209	0.117	0.069	0.047			
1.40	–0.55	0.620	0.418	0.279	0.170	0.108	0.115	0.039		
1.50	–0.55	0.703	0.513	0.352	0.225	0.155	0.095	0.071	0.051	
1.60	–0.55	0.668	0.596	0.436	0.321	0.240	0.195	0.143	0.127	0.079
0.80	–0.25	0.057								
0.90	–0.25	0.105	0.062							
1.00	–0.25	0.171	0.111	0.060						
1.10	–0.25	0.266	0.182	0.117	0.068					
1.20	–0.25	0.403	0.253	0.161	0.101	0.066				
1.30	–0.25	0.539	0.365	0.241	0.144	0.086	0.045			
1.40	–0.25	0.664	0.472	0.326	0.205	0.123	0.070	0.045		
1.50	–0.25	0.721	0.595	0.425	0.280	0.182	0.139	0.132	0.113	
1.60	–0.25	0.695	0.669	0.515	0.362	0.240	0.207	0.179	0.162	0.093
0.80	0.00	0.056								
0.90	0.00	0.103	0.063							
1.00	0.00	0.175	0.109	0.067						
1.10	0.00	0.271	0.175	0.108	0.062					
1.20	0.00	0.399	0.258	0.170	0.105	0.075				
1.30	0.00	0.547	0.367	0.244	0.155	0.098	0.056			
1.40	0.00	0.654	0.497	0.343	0.228	0.143	0.092	0.065		
1.50	0.00	0.694	0.621	0.461	0.308	0.216	0.148	0.136	0.112	
1.60	0.00	0.656	0.681	0.556	0.409	0.294	0.205	0.164	0.157	0.100
0.80	0.25	0.056								
0.90	0.25	0.101	0.063							
1.00	0.25	0.166	0.104	0.063						
1.10	0.25	0.263	0.167	0.104	0.064					
1.20	0.25	0.407	0.242	0.164	0.098	0.063				
1.30	0.25	0.567	0.346	0.246	0.158	0.091	0.055			
1.40	0.25	0.668	0.468	0.335	0.227	0.154	0.119	0.090		
1.50	0.25	0.717	0.621	0.455	0.296	0.197	0.137	0.114	0.093	
1.60	0.25	0.681	0.676	0.567	0.393	0.264	0.201	0.141	0.128	0.101
0.80	0.55	0.058								
0.90	0.55	0.103	0.060							
1.00	0.55	0.163	0.104	0.062						
1.10	0.55	0.251	0.169	0.105	0.064					
1.20	0.55	0.376	0.248	0.158	0.101	0.065				
1.30	0.55	0.535	0.353	0.238	0.160	0.104	0.058			
1.40	0.55	0.685	0.491	0.319	0.222	0.159	0.116	0.081		
1.50	0.55	0.723	0.633	0.411	0.286	0.201	0.137	0.105	0.080	
1.60	0.55	0.688	0.700	0.516	0.370	0.272	0.191	0.143	0.119	0.060

Table 3. SCEPtER bias on the recovered age due to the change in the stellar code input.

	Mass ($M_\odot$)								
	0.8	0.9	1.0	1.1	1.2	1.3	1.4	1.5	1.6
Overshooting β = 0.2									
p^{p}_{50}			0.0	–0.7	–3.6	–6.2	–5.7	–6.1	–4.9
p^{s}_{50}	–0.2	–0.2	–1.0	–3.0	–4.7	–6.6	–6.8	–6.6	–6.1
Overshooting β = 0.4									
p^{p}_{50}			0.0	–3.3	–10.3	–10.7	–10.2	–10.7	–10.5
p^{s}_{50}	–0.8	–1.6	–4.0	–8.2	–11.9	–10.9	–11.2	–11.2	–9.4
$\Delta Y/\Delta Z$ = 1									
p^{p}_{50}	–6.4	–6.8	–9.7	–10.1	–10.7	–10.0	–9.8	–9.2	–7.8
p^{s}_{50}	–7.9	–8.3	–10.0	–10.2	–9.9	–9.7	–9.2	–8.1	–6.8
$\Delta Y/\Delta Z$ = 3									
p^{p}_{50}	6.9	10.1	10.5	11.4	11.4	10.5	10.1	9.7	10.2
p^{s}_{50}	9.4	10.5	11.6	10.6	10.5	10.4	9.7	8.7	8.6
No microscopic diffusion									
p^{p}_{50}	8.0	6.2	5.1	4.0	3.8	3.3	2.8	2.6	2.9
p^{s}_{50}	6.4	4.9	3.9	3.4	3.3	3.1	2.6	2.0	1.7

Notes. Median age relative errors (p^{p}_{50} and p^{s}_{50}) are reported as a function of the mass of the primary and secondary star. Values are expressed as percent.

Table 4. SCEPtER bias on the recovered age due to the change in the stellar code input.

	Mass ratio q										
Input	0.50	0.55	0.60	0.65	0.70	0.75	0.80	0.85	0.90	0.95	1.00
β = 0.2	–3.7	–3.6	–3.7	–3.8	–3.9	–3.8	–3.5	–3.2	–2.6	–3.4	–3.4
β = 0.4	–8.2	–9.2	–9.7	–9.8	–9.5	–9.0	–8.1	–7.3	–6.1	–5.0	–4.6
$\Delta Y/\Delta Z$ = 1	–7.6	–8.0	–9.0	–9.3	–9.7	–9.8	–9.9	–9.8	–8.9	–9.1	–8.9
$\Delta Y/\Delta Z$ = 3	10.0	10.5	11.2	11.3	11.1	11.3	11.3	11.2	10.2	9.9	9.7
No diffusion	4.0	3.8	3.4	3.3	3.4	3.7	3.9	4.1	3.8	3.4	3.2

Notes. Median age relative errors are reported as a function of the mass ratio of the binary system. Values are expressed as percent.

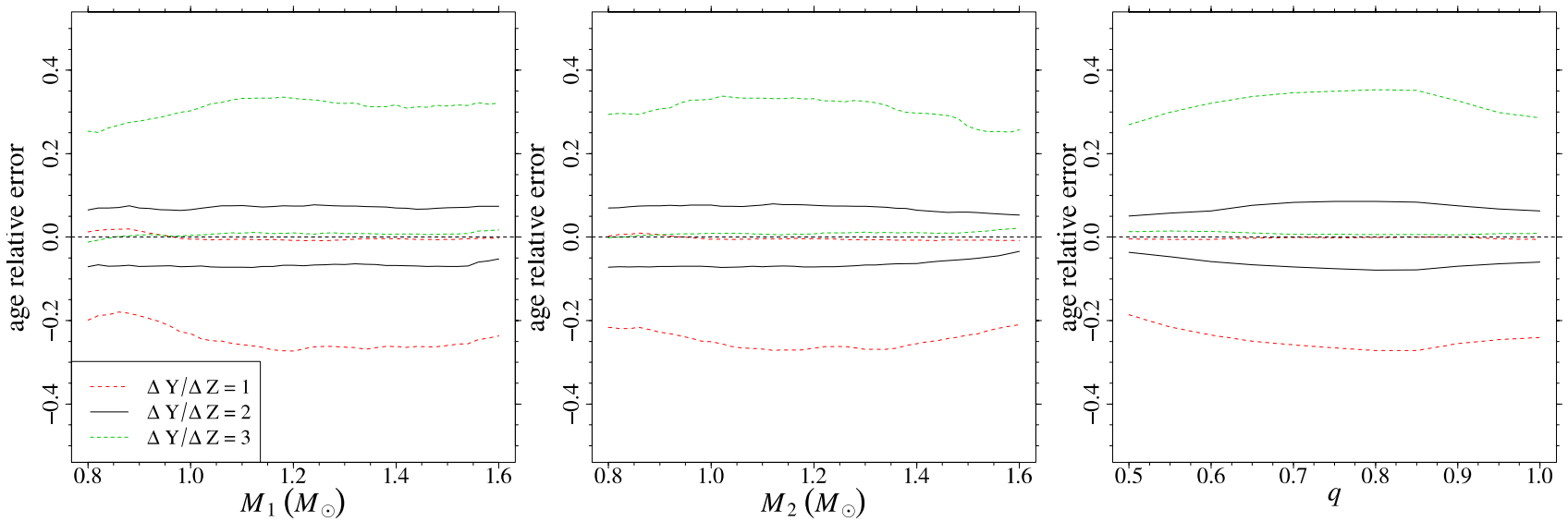

Fig. 7. *Left*: standard 1σ envelope of the binary system age relative error in dependence on the mass of the primary star (solid black), compared with the same quantity obtained by sampling from the grid with a different initial helium abundance computed assuming $\Delta Y/\Delta Z = 1$ (dashed red) and $\Delta Y/\Delta Z = 3$ (dot dashed green). *Middle*: same as the left panel, but in dependence on the mass of the secondary star. *Right*: same as the *left panel*, but in dependence on the system mass ratio q.

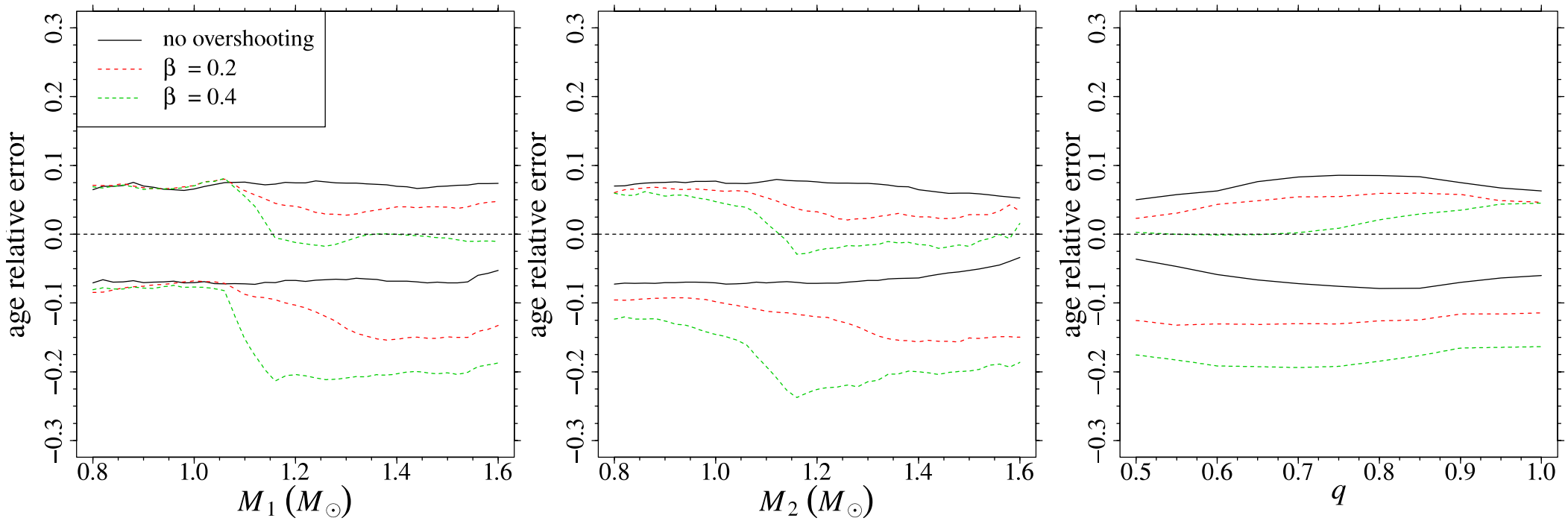

Fig. 5. *Left*: standard 1σ envelope of the binary system age relative error in dependence on the mass of the primary star (solid black), compared with the same quantity obtained by sampling from grids with different core -overshooting efficiency $\beta = 0.2$ (dashed red) and $\beta = 0.4$ (dot dashed green). *Middle*: same as the left panel, but in dependence on the mass of the secondary star. *Right*: same as the left panel, but in dependence on the system mass ratio q.

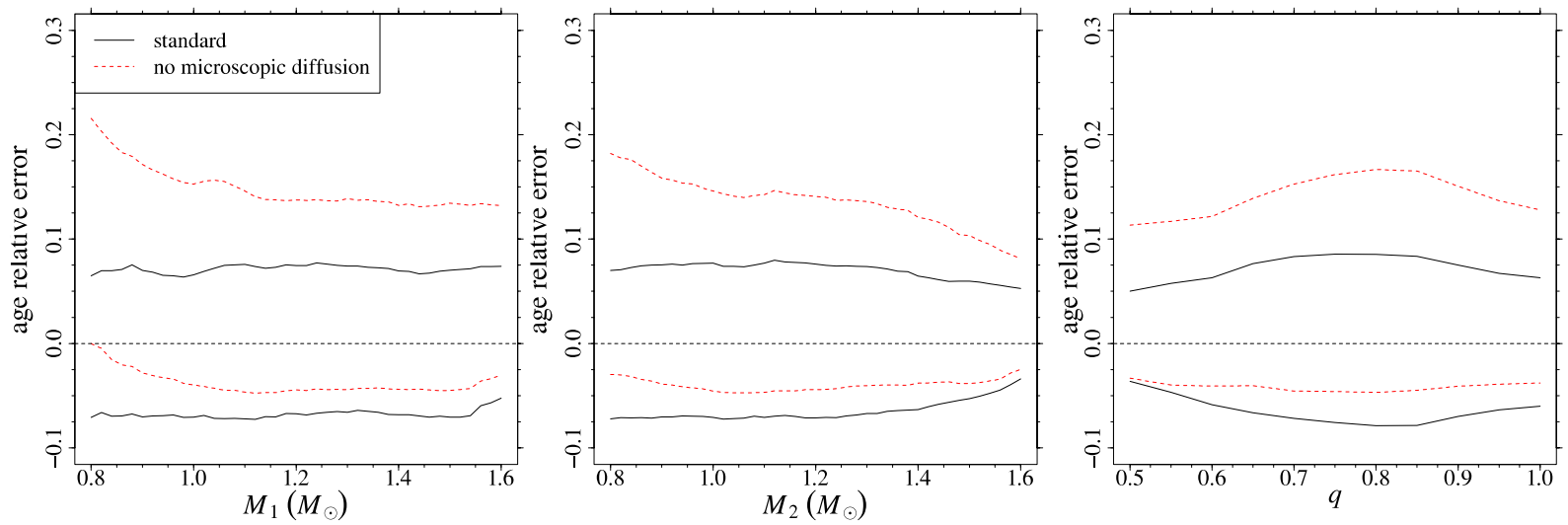

Fig. 9. *Left*: standard 1σ envelope of the binary-system age-relative error in dependence on the mass of the primary star (solid black), compared with the same quantity obtained by sampling from the standard grid and reconstruction on a grid of stellar models computed without microscopic diffusion (dashed red). *Middle*: same as the left panel, but in dependence on the mass of the secondary star. *Right*: same as the left panel, but in dependence on the system's mass ratio q.

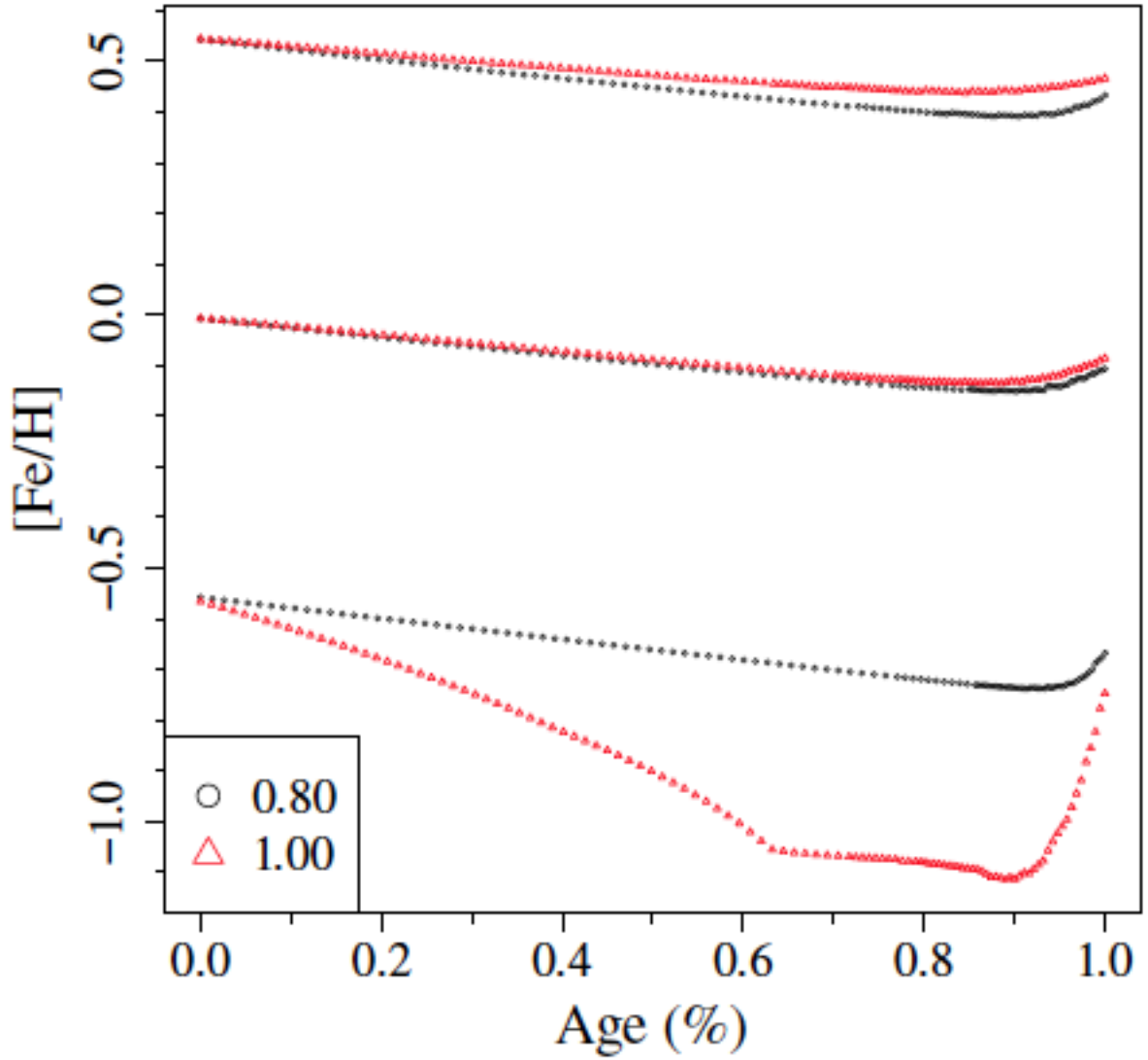

Fig. 12. Evolution of surface [Fe/H] for two different masses $M = 0.80$ and 1.00 $M_{\odot}$ (identified by the black circle and red triangle, respectively) and initial [Fe/H] = −0.55, 0.00, and 0.55.

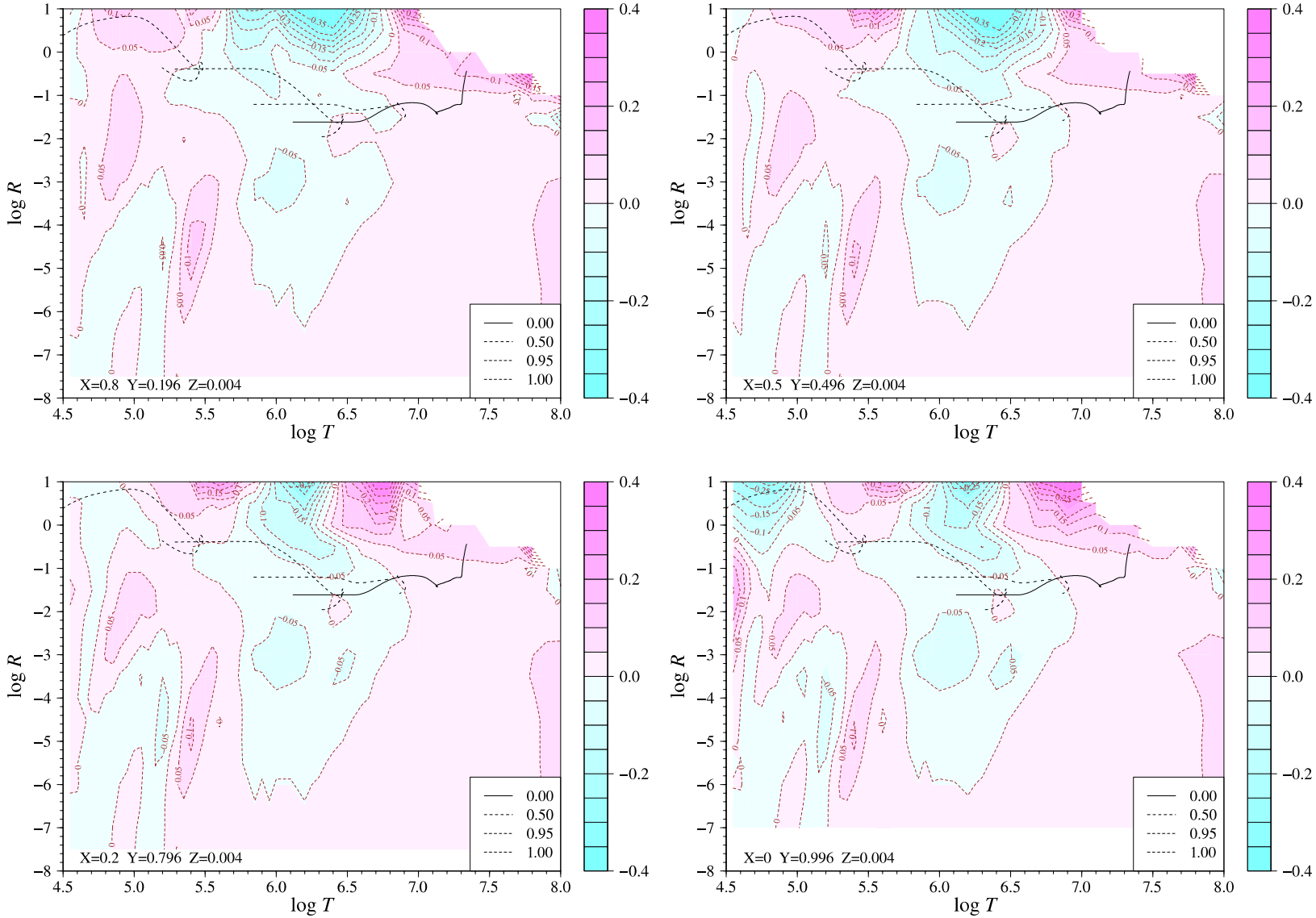

Fig. 1. Contour plots of the difference between OPAL and OP calculations for different hydrogen abundance X and metallicity $Z = 0.004$. The temperature T is in K, while R is in g cm^{-3} K^{-3}. The colored scale marks the values of the relative difference $(k_{\rm r}^{\rm OPAL} - k_{\rm r}^{\rm OP})/k_{\rm r}^{\rm OPAL}$. Solid line: evolutionary path of the stellar center; dashed line: evolutionary path of the 0.50 mass fraction of the structure; dotted line: path of the 0.95 mass fraction of the structure; dot-dashed line: path of the 0.99974 mass fraction of the structure, labeled as 1.00.

Blancard et al. 2012

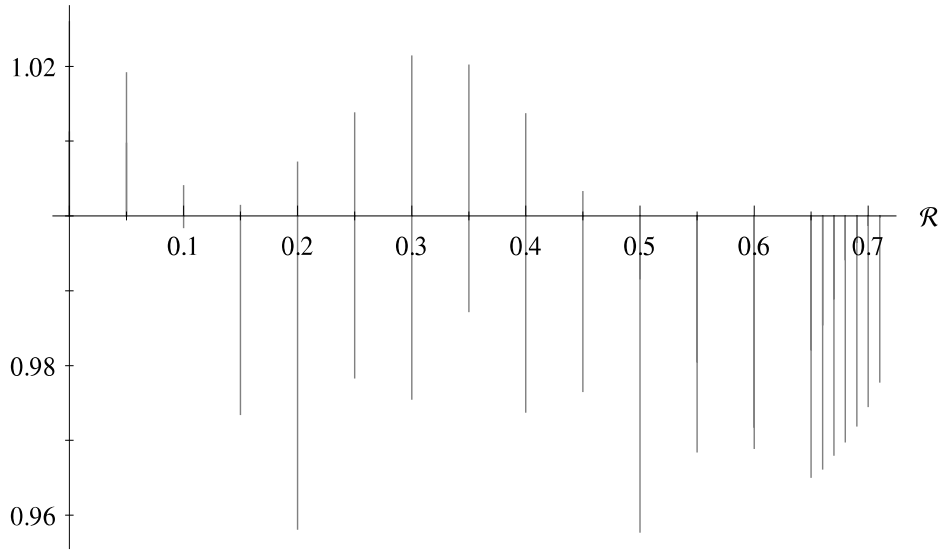

Figure 1. Comparison of Rosseland mean opacities for a solar mixture from initial Grevesse and Sauval composition (see the text). Variation of $\kappa_{\rm R}^{\rm OPAS}/\kappa_{\rm R}^{\rm OP}$ (blue circle) and $\kappa_{\rm R}^{\rm OPAL}/\kappa_{\rm R}^{\rm OP}$ (red circle) ratios as a function of the reduced solar radius.

Mondet at al. 2015

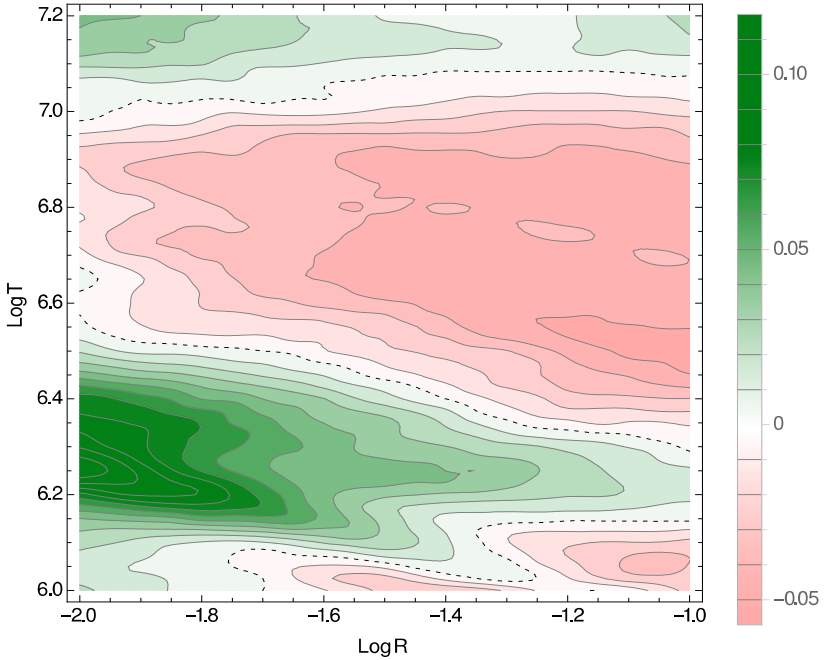

Figure 5. Comparison of OPAS Rosseland opacities to OPAL values expressed as $\kappa_{\rm R}^{\rm OPAS}/\kappa_{\rm R}^{\rm OPAL} - 1$ (AGS'09 composition, $X = 0.35$, $Z = 0.02$).

OP vs OPAL

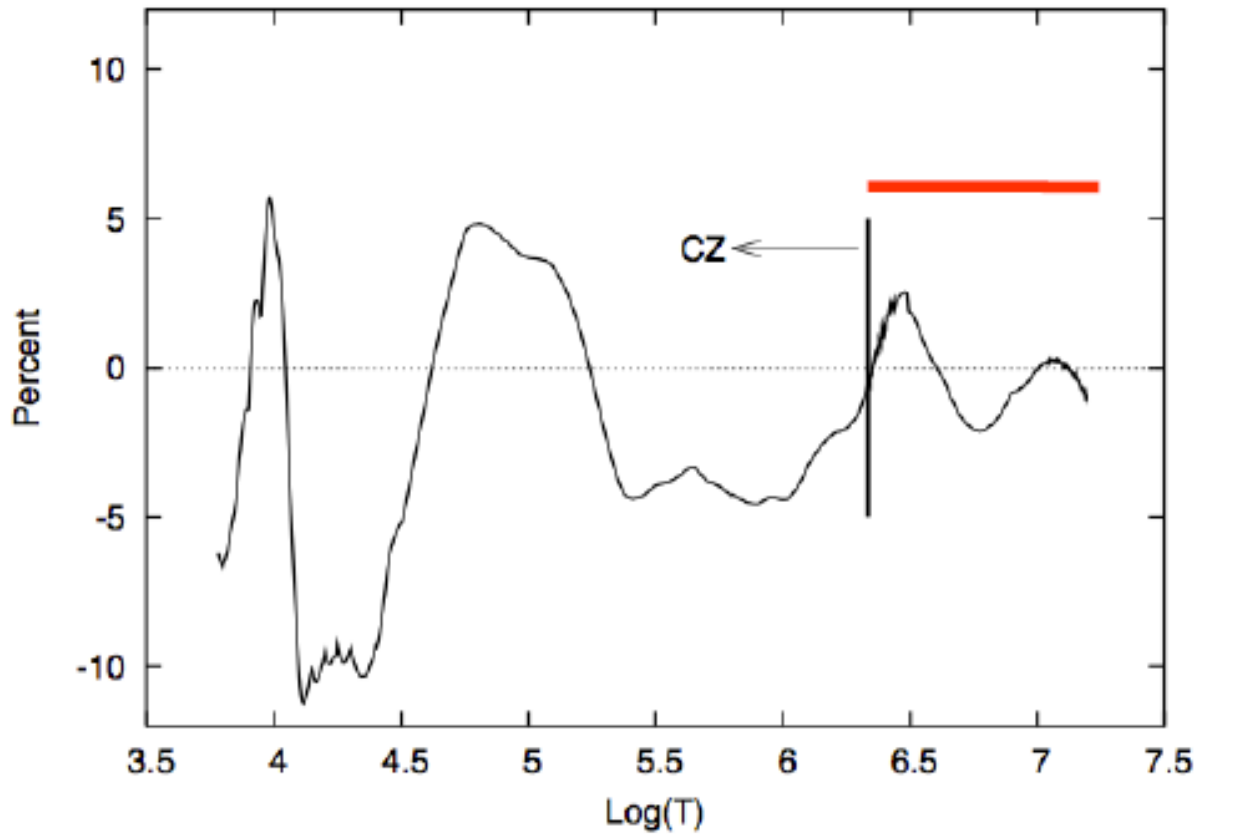

Badnell et al. 2005

α enhanced isochrones

* **Salaris et al. 1993, showed that α enhanced models can be reproduced by the solar scaled ones with the same total metallicity provided that the ratio of the high (C,N,O,Ne) over the low (Mg, Si, S, Ca, Fe) ionization potential elements is preserved.**

* **This is no more valid for old clusters with Z≥0.01 (Weiss et al. 1995, Salaris & Weiss 1998) while in low age (< 1 Gyr) clusters the discrepancy is reduced (Salasnich et al. 2000)**

- **If the abundance of only one α element is varied solar scaled models cannot be used (see e.g. oxygen enhanced isochrones by Bergbusch & Vandenberg 1992 and references therein)**

* **The effect of the α enhancement on bolometric corrections is negligible (Cassisi et al. 2004)**

Is microscopic diffusion fully efficient in stars?

Element diffusion in stars (Aller & Chapman, 1960) **includes different processes:**
- **gravitational settling**
- **thermal diffusion**
- **diffusion driven by composition gradients**
- **radiative acceleration** (Michaud, 1970)

Sometimes a turbulent diffusion term (Schatzman 1969) **is included**

In the Sun:

- Theoretical error on the gravitational settling rate is estimated to be about 15% (Thoul et al. 1994) .....however:

- Thermal diffusion contributes about 40% to the diffusion velocity below the convective zone (Turcotte et al. 1998) and its uncertainty is estimated up to 30% → contribution to the uncertainty on velocity of about 12% (Montalbán et al. 2006)

- The assumption of fully ionized stellar matter leads to an underestimate of the diffusion velocities by 20% for Fe and by 9% for O (Turcotte et al. 1998)

- One should take into account the intermediate-coupling regime for the plasma (see e.g. Chaboyer et al. 1992) moreover the adoption of Burgers' equ.s seems to lead to an uncertainty of about 10% (Roussel-Dupré 1982, see also discussions in Schlattl 2002, Schlattl & Salaris 2003, Thoul & Montalban 2007)

- The degree of diffusion depends on the detailed model structure

- Extra-mixing? Turbulences?

Element settling

If radiative acceleration is neglected He and metals settle out the surface convection zone on the main sequence and they are dredged back when the convection zone deepens on the giant branch

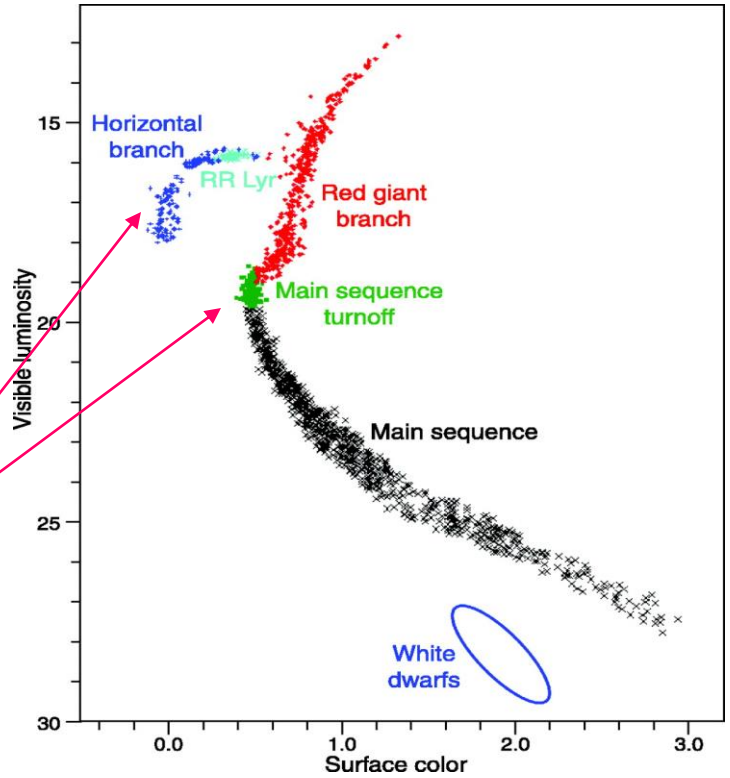

The radiative acceleration role in old clusters:

Radiative acceleration is calculated to be significantly efficient for the external abundance of metals in MS, low metallicity ([Fe/H] < -2.3) not too old ($M_{TO} > 0.7\ M_{\odot}$) cluster stars with Te>5900 K

High efficiency for TO and hot HB stars

Thus, in some cases, not only metal settling is reduced but overabundances of some elements with respect of the original composition are present

[Fe/H] surface abundance predictions

- **If one neglects radiative acceleration and do not include extra-mixings one expect a reduction of 0.2 ÷ 0.3 dex in [Fe/H] due to gravitational settling** (see e.g. Chaboyer et al. 2001, Ramirez & Cohen 2003)

- **If radiative acceleration (and extra-mixing at the bottom of the convective envelope) are included not only the Fe settling at the TO can be reduced but an overabundance up to a factor 10 is predicted for the lowest metallicity clusters**

(see e.g. Richard et al. 2002)

Theoretical predictions for Fe and some other element can be reconciled in some cases with observations taking into account radiative acceleration, a given amount of turbulent diffusion, the uncertainty in the estimated effective temperature and the observational errors

(see e.g. Richard et al. 2001)

Influence of diffusion on isochrones

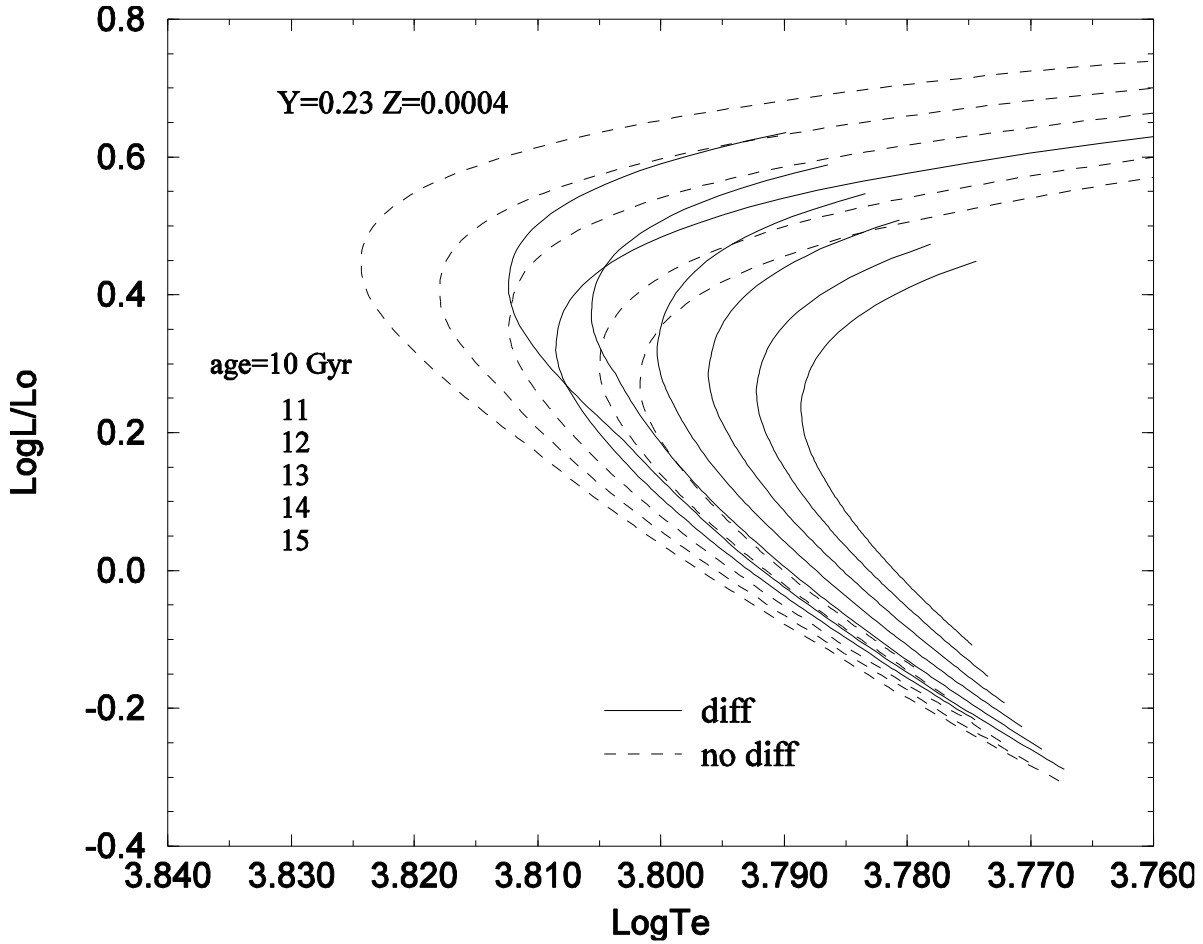

(Castellani et al. 1997, see also Proffitt & Michaud 1991, Proffitt & Vandenberg 1991, Straniero et al. 1997 and many others)

External convection efficiency

- **Theoretical calculations are generally performed by adopting the mixing length formalism** (see e.g. Canuto & Mazzitelli 1991, Ventura et al. 1998, Mazzitelli et al. 1999, and references therein for different formalisms)

- **The mixing length value is usually calibrated by requiring the agreement with the observed stellar colors as a function of the adopted atmospheric models.**

- **A mixing length (star temperature) change also arises in a small change of the bolometric correction**

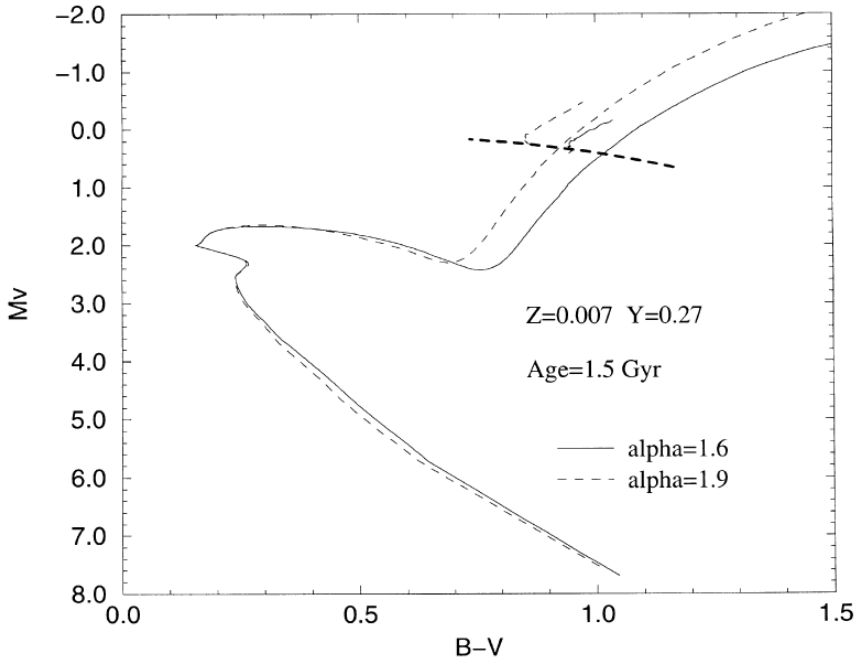

(Castellani, Degl'Innocenti, Marconi 1999)

However if reasonable values are adopted the influence on the stellar cluster age determination by isochrone fitting is small (see e.g. Chaboyer 1995)

*** Theoretical calculations are also influenced by the ways adopted to decrease the core overshooting efficiency with the stellar mass**

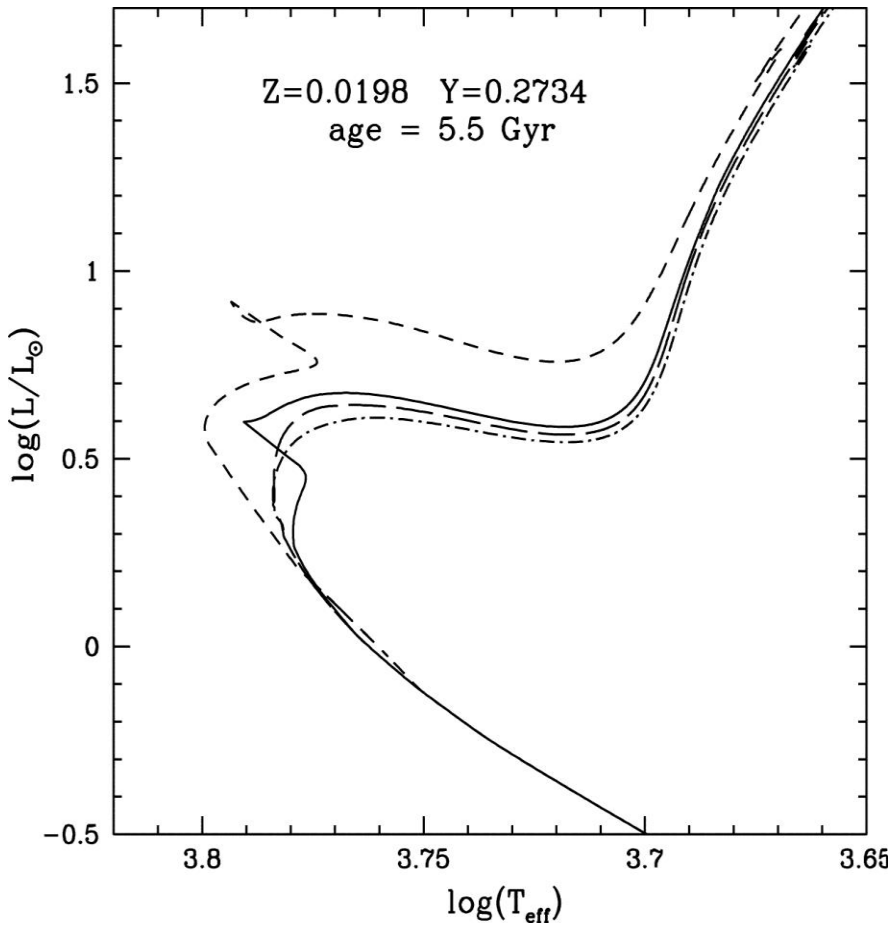

(Pietrinferni et al. 2004)

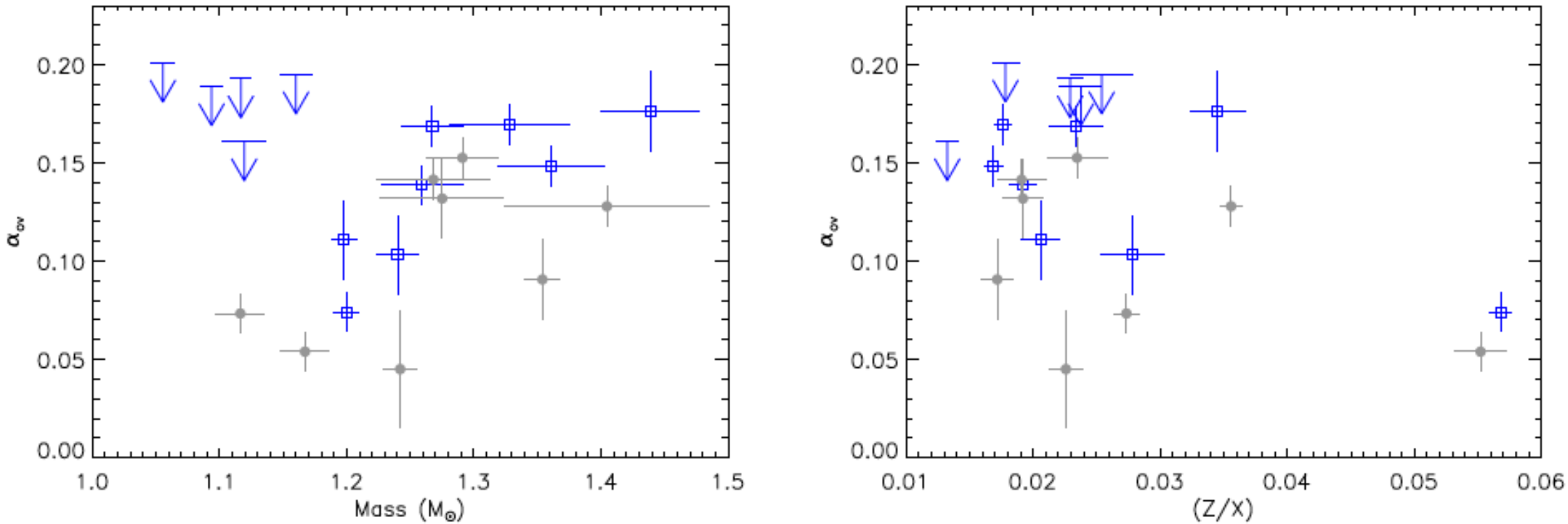

Fig. 13. Amount of core overshooting found for the stars of the sample that have a convective core as a function of the fitted stellar mass (*left*) and as a function of the fitted initial metallicity (*right*). Blue squares indicate models computed without microscopic diffusion and gray circles, models where microscopic diffusion is included following Burgers (1969). The vertical arrows indicate upper limits of α_{ov} (see Sect. 5.1.2).

Deheuvels et al. 2016

Stancliffe et al. 2015

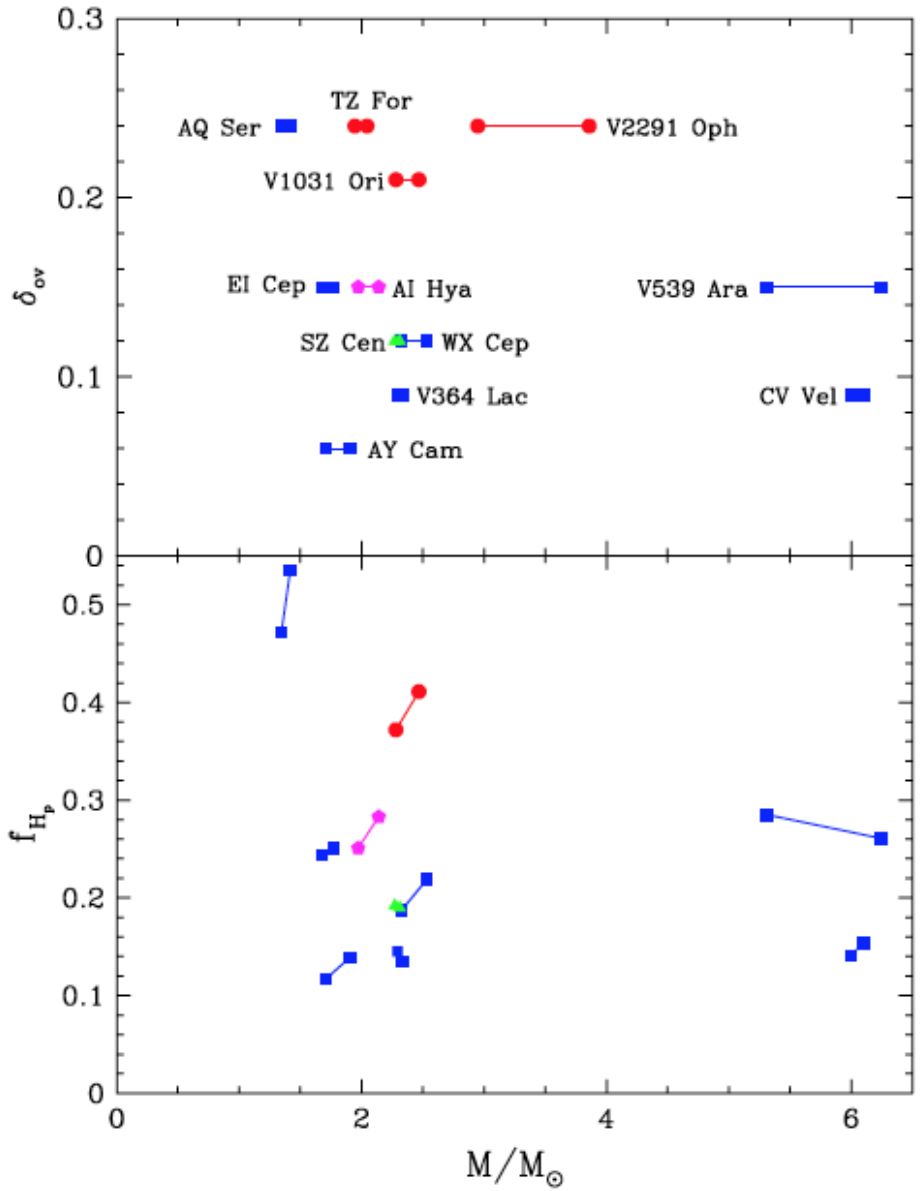

Fig. 8. Extent of overshooting as a function of mass. *Upper panel*: overshooting in terms of δ_{ov}, while *lower panel*: same quantity in terms of a fraction of the pressure scale height. Symbols denote the best fit metallicity for the systems: $Z = 0.01$ (triangles), $Z = 0.02$ (squares), $Z = 0.03$ (circles) and $Z = 0.04$ (pentagons).

Table B.1. Binaries systems in our sample.

Name	Mass ($M_\odot$)	Radius ($R_\odot$)	$T_{\rm eff}$ (K)	[Fe/H]	Source
SMC-108.1-14904	4.416 ± 0.041	46.95 ± 0.53	5675 ± 105	−0.80 ± 0.15	1
	4.429 ± 0.037	64.05 ± 0.50	4955 ± 90		
OGLE-LMC-ECL-CEP-0227	4.165 ± 0.032	34.92 ± 0.34	6050 ± 160		2
	4.134 ± 0.037	44.85 ± 0.29	5120 ± 130		
OGLE-LMC-ECL-06575	4.152 ± 0.030	39.79 ± 1.35	4903 ± 72	−0.45 ± 0.10	3
	3.966 ± 0.032	49.35 ± 1.45	4681 ± 77		
OGLE-LMC-ECL-CEP-2532	3.90 ± 0.10	28.95 ± 1.4	6345 ± 150		4
	3.83 ± 0.10	37.7 ± 1.7	4800 ± 220		
LMC-562.05-9009	3.70 ± 0.03	28.6 ± 0.2	6030 ± 150:		5
	3.60 ± 0.03	26.6 ± 0.2	6030 ± 150:		
χ^2 Hya	3.605 ± 0.078	4.390 ± 0.039	11750 ± 190		6
	2.632 ± 0.049	2.159 ± 0.030	11100 ± 230		
OGLE-LMC-ECL-26122	3.593 ± 0.055	32.71 ± 0.51	4989 ± 80	−0.15 ± 0.10	3
	3.411 ± 0.047	22.99 ± 0.48	4995 ± 81		
OGLE-LMC-ECL-01866	3.574 ± 0.038	46.96 ± 0.61	4541 ± 85	−0.70 ± 0.10	3*
	3.575 ± 0.028	28.20 ± 1.06	5327 ± 72		
OGLE-SMC-113.3-4007	3.561 ± 0.025	48.4 ± 0.7	4813 ± 100		7*
	3.504 ± 0.028	45.8 ± 0.7	4800 ± 100		
OGLE-LMC-ECL-10567	3.345 ± 0.040	25.6 ± 1.6	5067 ± 73	−0.81 ± 0.20	3
	3.183 ± 0.038	36.0 ± 2.0	4704 ± 80		
OGLE-LMC-ECL-09144	3.303 ± 0.028	26.18 ± 0.31	5288 ± 81	−0.23 ± 0.10	3
	3.208 ± 0.026	18.64 ± 0.30	5470 ± 96		
OGLE-051019.64-685812.3	3.278 ± 0.032	26.05 ± 0.29	5300 ± 100		6
	3.179 ± 0.029	19.76 ± 0.34	5450 ± 100		
OGLE-LMC-ECL-09660	2.988 ± 0.018	43.87 ± 1.14	4677 ± 75	−0.44 ± 0.10	3*
	2.969 ± 0.020	23.75 ± 0.66	5352 ± 70		
SMC-101.8-14077	2.835 ± 0.055	23.86 ± 0.31	5170 ± 90	−1.01 ± 0.15	1*
	2.725 ± 0.034	17.90 ± 0.50	5580 ± 95		
α Aur	2.5687 ± 0.0074	11.98 ± 0.57	4970 ± 50	−0.04 ± 0.06	8
	2.4828 ± 0.0067	8.83 ± 0.33	5730 ± 60		
WX Cep	2.533 ± 0.050	3.996 ± 0.030	8150 ± 250		6
	2.324 ± 0.045	2.712 ± 0.023	8900 ± 250		
V1031 Ori	2.468 ± 0.018	4.323 ± 0.034	7850 ± 500		6
	2.281 ± 0.016	2.978 ± 0.064	8400 ± 500		
V364 Lac	2.333 ± 0.014	3.309 ± 0.021	8250 ± 150		6
	2.295 ± 0.024	2.986 ± 0.020	8500 ± 150		
SZ Cen	2.311 ± 0.026	4.556 ± 0.032	8100 ± 300		6
	2.272 ± 0.021	3.626 ± 0.026	8380 ± 300		
YZ Cas	2.263 ± 0.012	2.525 ± 0.011	9520 ± 120	+0.01 ± 0.11	9
	1.325 ± 0.007	1.331 ± 0.006	6880 ± 240		
OGLE-LMC-ECL-25658	2.230 ± 0.019	27.57 ± 0.24	4721 ± 75	−0.63 ± 0.10	10*
	2.229 ± 0.019	21.41 ± 0.15	4860 ± 70		
V885 Cyg	2.228 ± 0.026	3.387 ± 0.026	8150 ± 150		6
	2.000 ± 0.029	2.346 ± 0.017	8375 ± 150		
AI Hya	2.140 ± 0.038	3.916 ± 0.031	6700 ± 60		6
	1.973 ± 0.036	2.767 ± 0.019	7100 ± 65		
VV Crv	1.978 ± 0.010	3.375 ± 0.010	6500 ± 200		11

Notes. The first line for each system corresponds to the primary, and the next to the secondary. Sources flagged with an asterisk indicate cases where we have swapped the primary/secondary identification relative to the original publication (see text). Temperatures for LMC-562.05-9009 are listed as uncertain in the original source. The [Fe/H] value adopted here for OGLE-LMC-ECL-25658 is the average of the individual estimates reported.

References. 1 – Graczyk et al. (2014); 2 – Pilecki et al. (2013); 3 – Pietrzyński et al. (2013); 4 – Pilecki et al. (2015); 5 – Gieren et al. (2015); 6 – Torres et al. (2010); 7 – Graczyk et al. (2012); 8 – Torres et al. (2015); 9 – Pavlovski et al. (2014); 10 – Elgueta et al. (2016); 11 – Fekel et al. (2013); 12 – Sandberg Lacy & Fekel (2011); 13 – Hełminiak et al. (2015).

Claret & Torres 2016

Table B.1. continued.

Name	Mass ($M_\odot$)	Radius ($R_\odot$)	$T_{\rm eff}$ (K)	[Fe/H]	Source
	1.513 ± 0.008	1.650 ± 0.008	6638 ± 200		
AY Cam	1.905 ± 0.040	2.772 ± 0.020	7250 ± 100		6
	1.709 ± 0.036	2.026 ± 0.017	7395 ± 100		
HY Vir	1.838 ± 0.009	2.806 ± 0.008	6850 ± 130		12
	1.404 ± 0.006	1.519 ± 0.008	6550 ± 120		
SMC-130.5-04296	1.805 ± 0.027	46.00 ± 0.35	4515 ± 75	−0.88 ± 0.15	1*
	1.854 ± 0.025	25.44 ± 0.25	4912 ± 80		
OGLE-LMC-ECL-03160	1.792 ± 0.027	16.36 ± 1.06	4954 ± 83	−0.48 ± 0.20	3
	1.799 ± 0.028	37.42 ± 0.52	4490 ± 82		
EI Cep	1.7716 ± 0.0066	2.897 ± 0.048	6750 ± 100		6
	1.6801 ± 0.0062	2.330 ± 0.044	6950 ± 100		
SMC-126.1-00210	1.674 ± 0.037	43.52 ± 1.02	4480 ± 70	−0.86 ± 0.15	1
	1.669 ± 0.039	39.00 ± 0.98	4510 ± 70		
HD 187669	1.505 ± 0.004	22.62 ± 0.50	4330 ± 70	−0.25 ± 0.10	13*
	1.504 ± 0.004	11.33 ± 0.28	4650 ± 80		
OGLE-LMC-ECL-15260	1.440 ± 0.024	23.51 ± 0.69	4706 ± 87	−0.47 ± 0.15	3
	1.426 ± 0.022	42.17 ± 0.33	4320 ± 81		
AI Phe	1.2336 ± 0.0045	2.932 ± 0.048	5010 ± 120	−0.14 ± 0.10	6
	1.1934 ± 0.0041	1.818 ± 0.024	6310 ± 150		

Table 1
Binaries systems in our sample.

Name	Mass ($M_\odot$)	Radius ($R_\odot$)	$T_{\rm eff}$ (K)	[Fe/H]	Source
YZ Cas	2.263 ± 0.012	2.525 ± 0.011	9520 ± 120	+0.01 ± 0.11	1
	1.325 ± 0.007	1.331 ± 0.006	6880 ± 240		
TZ For	2.057 ± 0.001	8.34 ± 0.12	4930 ± 100	+0.01 ± 0.04	2,3,4
	1.958 ± 0.001	3.97 ± 0.09	6650 ± 200		
V442 Cyg	1.560 ± 0.024	2.073 ± 0.034	6900 ± 100		4,5
	1.407 ± 0.023	1.663 ± 0.033	6800 ± 100		
GX Gem	1.488 ± 0.011	2.326 ± 0.012	6195 ± 100	−0.12 ± 0.10	4,6
	1.467 ± 0.010	2.236 ± 0.012	6165 ± 100		
BW Aqr	1.479 ± 0.019	2.062 ± 0.044	6350 ± 100	−0.07 ± 0.11	4,7,8
	1.377 ± 0.021	1.786 ± 0.043	6450 ± 100		
AQ Ser	1.417 ± 0.021	2.451 ± 0.027	6340 ± 100		9
	1.346 ± 0.024	2.281 ± 0.014	6430 ± 100		
BF Dra	1.414 ± 0.003	2.086 ± 0.012	6360 ± 150	−0.03 ± 0.15	10
	1.375 ± 0.003	1.922 ± 0.012	6400 ± 150		
BK Peg	1.414 ± 0.007	1.988 ± 0.008	6265 ± 85	−0.12 ± 0.07	8
	1.257 ± 0.005	1.474 ± 0.017	6320 ± 90		
CO And	1.2892 ± 0.0073	1.727 ± 0.021	6140 ± 130	+0.01 ± 0.15	11
	1.2643 ± 0.0073	1.694 ± 0.017	6170 ± 130		

Note. — The first line for each system corresponds to the more evolved star. In some cases we list Torres et al. (2010) as an additional source, as the original determinations were slightly revised in that work through the use of updated physical constants. The [Fe/H] value for YZ Cas is that of the secondary; the primary is an Am star. The [Fe/H] value for TZ For is the weighted average for the primary and secondary, and the radii have been updated for this work as described in the text. Sources are: (1) Pavlovski et al. (2014); (2) Andersen et al. (1991); (3) Gallenne et al. (2016); (4) Torres et al. (2010); (5) Lacy & Frueh (1987); (6) Lacy et al. (2008); (7) Clausen (1991); (8) Clausen et al. (2010); (9) Torres et al. (2014); (10) Lacy et al. (2012); (11) Lacy et al. (2010).

Claret & Torres 2018

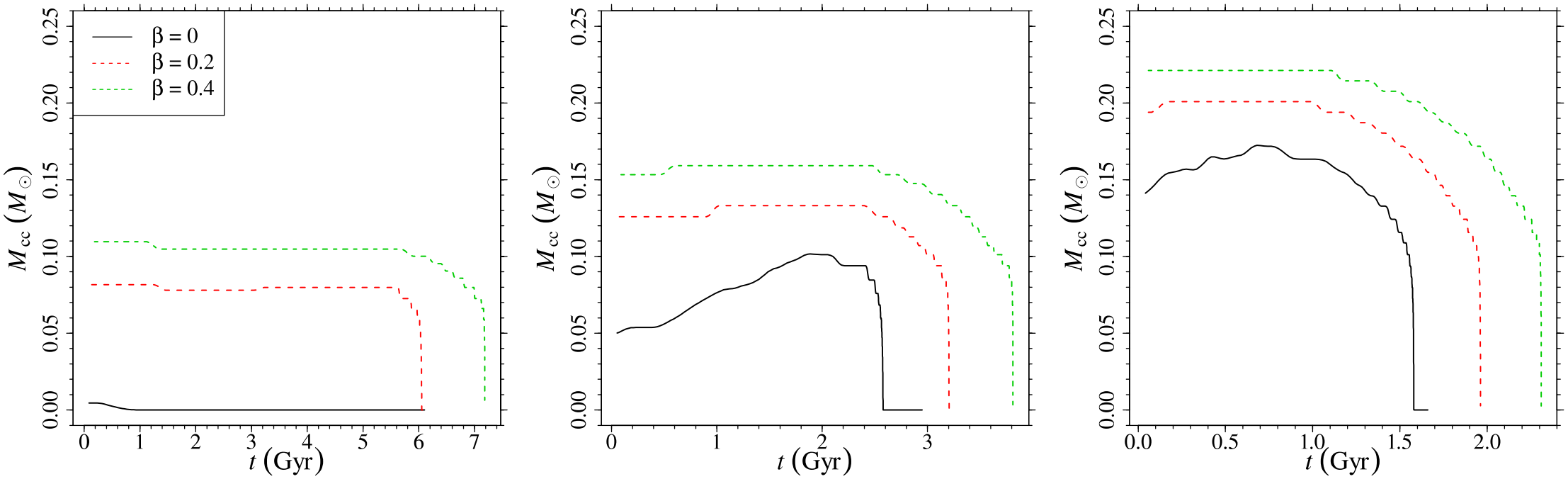

Fig. 1. *Left*: extension of the convective core (in $M_\odot$), from ZAMS to central hydrogen exhaustion, for three different values of the overshooting parameter $\beta = 0.0$, 0.2, and 0.4 for a model of $M = 1.12\ M_\odot$ at initial [Fe/H] = 0.0. *Middle*: same as in the *left panel*, but for $M = 1.36\ M_\odot$. *Right*: same as in the *left panel*, but for $M = 1.60\ M_\odot$.

Table 1. Median (q_{50}) and 1σ random envelope (q_{16}, q_{84}) of the estimated core overshooting parameter, as a function of the mass of the primary star, of its relative age r, and of the mass ratio of the system q.

	Primary star mass ($M_\odot$)										
	1.1	1.2	1.3	1.4	1.5	1.6					
q_{16}	0.13	0.10	0.10	0.10	0.07	0.07					
q_{50}	0.21	0.20	0.20	0.20	0.20	0.20					
q_{84}	0.30	0.28	0.30	0.30	0.30	0.32					
	Primary star relative age r										
	0.0	0.1	0.2	0.3	0.4	0.5	0.6	0.7	0.8	0.9	1.0
q_{16}	0.03	0.04	0.05	0.04	0.04	0.04	0.04	0.03	0.03	0.10	0.17
q_{50}	0.15	0.15	0.16	0.16	0.16	0.17	0.20	0.17	0.12	0.19	0.20
q_{84}	0.34	0.33	0.31	0.33	0.33	0.35	0.35	0.35	0.33	0.28	0.28
	Mass ratio q										
	0.65	0.70	0.75	0.80	0.85	0.90	0.95	1.0			
q_{16}	0.07	0.07	0.06	0.06	0.06	0.06	0.10	0.11			
q_{50}	0.20	0.20	0.20	0.20	0.20	0.20	0.20	0.20			
q_{84}	0.35	0.33	0.32	0.31	0.31	0.30	0.30	0.30			

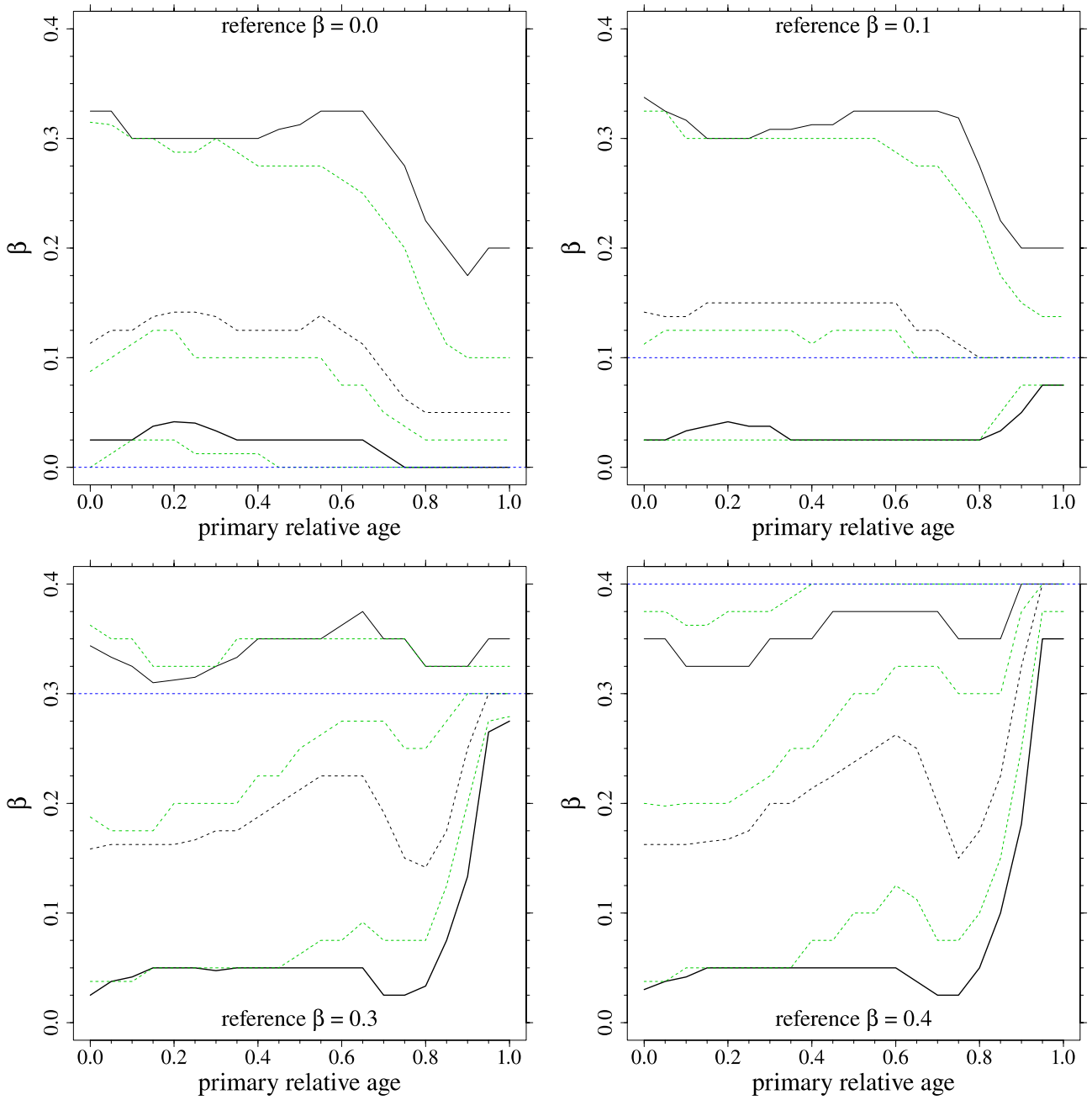

Fig. 3. Same as in the *right panel* of Fig. 2, but sampling from the grid with different β values reported in the labels. The green dot-dashed lines refer to the scenario in which the nominal errors on the observables are halved.

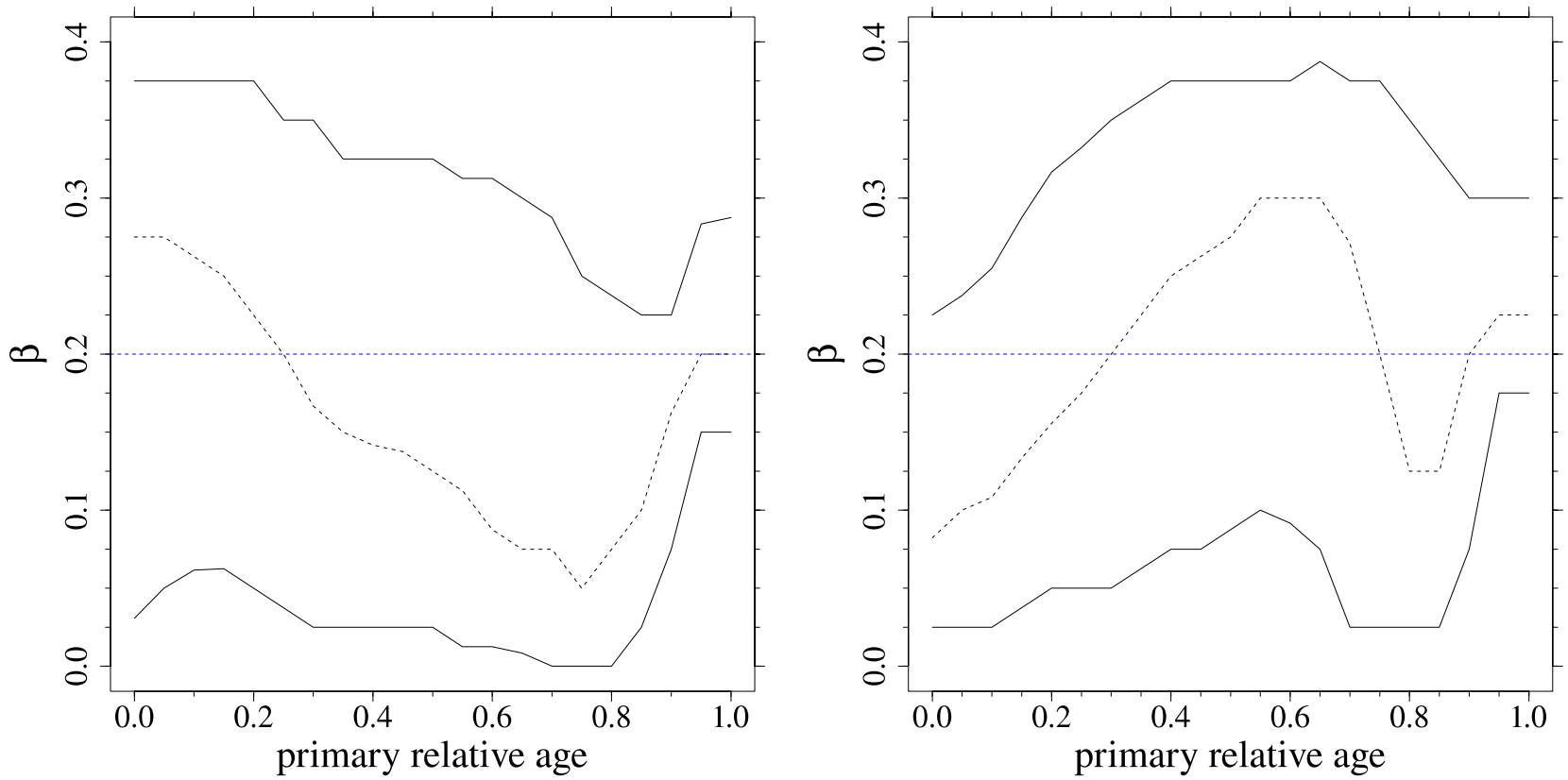

Fig. 5. *Left*: as in the right panel of Fig. 2, but sampling from a grid with $\Delta Y/\Delta Z = 1$. *Right*: same as in the *left panel*, but sampling from a grid with $\Delta Y/\Delta Z = 3$. In both cases the reconstruction was performed with the standard grid with $\Delta Y/\Delta Z = 2$.

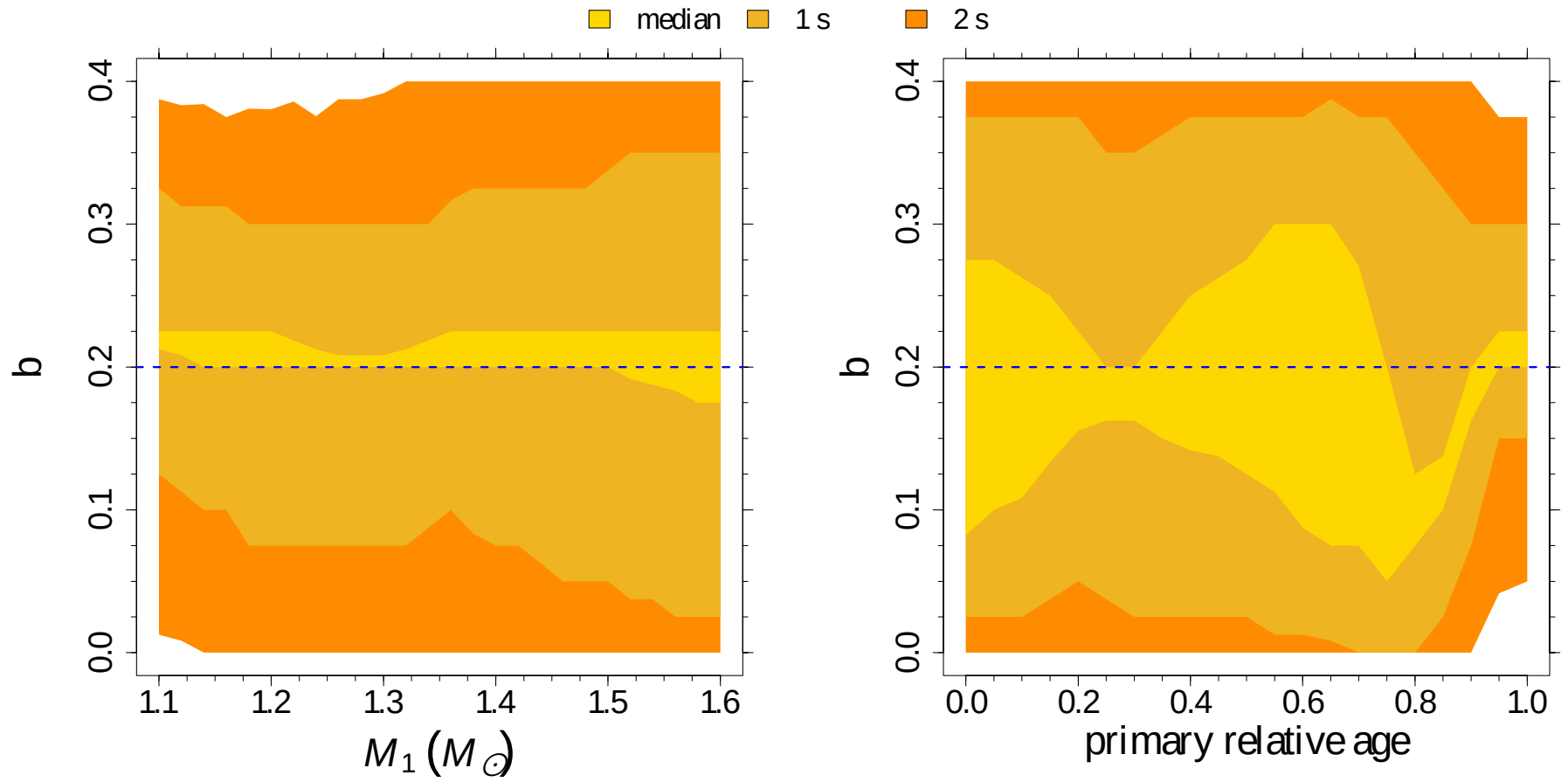

Fig. 6. *Left*: overall uncertainty (statistical and systematic) that is due to the considered variations in $\Delta Y/\Delta Z$, in dependence on the mass of the primary star. The lighter region shows the uncertainty on the median of the estimated β caused by ignoring the correct initial helium value. The intermediate colour regions show the overall error up to 1σ that is due to the cumulated contribution of observational errors and systematic bias as a result of the unknown initial helium value. The darker regions correspond to cumulated errors up to 2σ. *Right*: same as in the *left panel*, but in dependence on the relative age of the primary star.

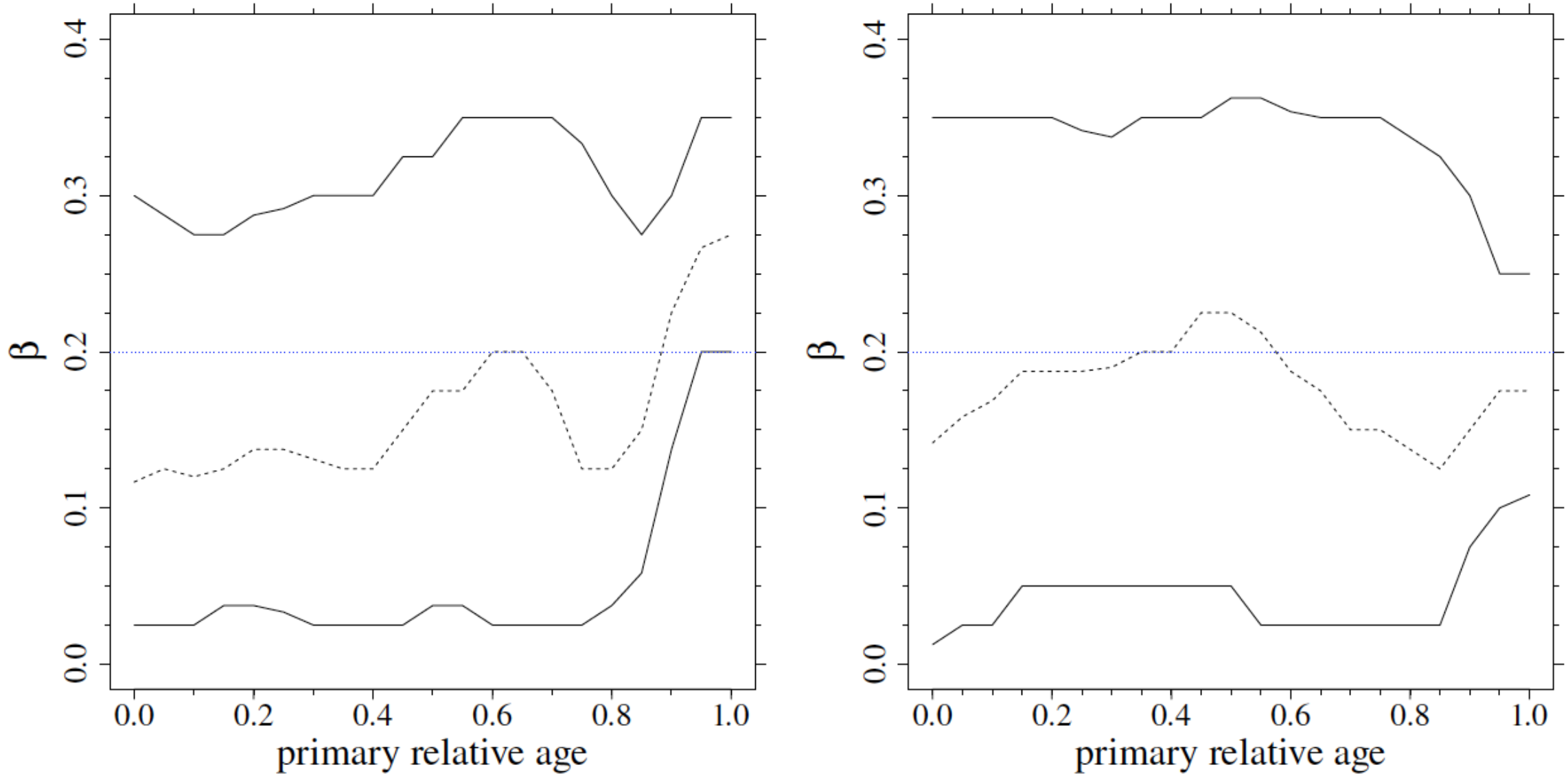

Fig. 7. *Left*: as in the right panel of Fig. 2, but sampling from a grid with $\alpha_{\rm ml} = 1.50$. *Right*: same as in the *left panel*, but sampling from a grid with $\alpha_{\rm ml} = 1.98$. In both cases the reconstruction was performed with the standard grid with $\alpha_{\rm ml} = 1.74$.

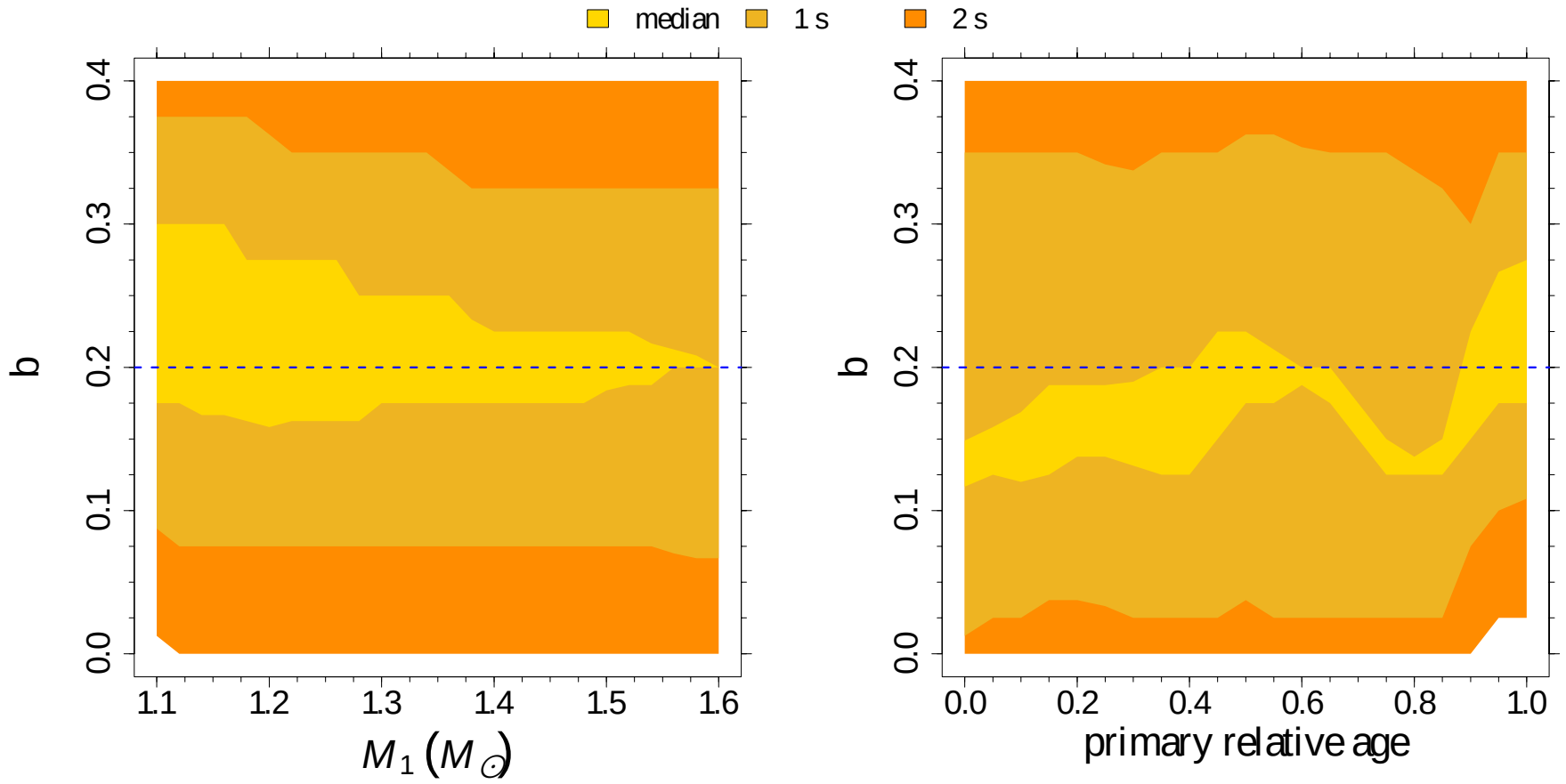

Fig. 8. *Left*: overall uncertainty (statistical and systematic) that is due to the considered variations in α_{ml}, in dependence on the mass of the primary star. The lighter region shows the uncertainty on the median of the estimated β that is a result of ignoring the correct mixing-length value. The intermediate colour regions show the overall error up to 1σ caused by the cumulated contribution of observational errors and systematic bias that is due to the unknown mixing-length value. The darker regions correspond to errors up to 2σ. *Right*: same as in the *left panel*, but in dependence on the relative age of the primary star.

diffusion

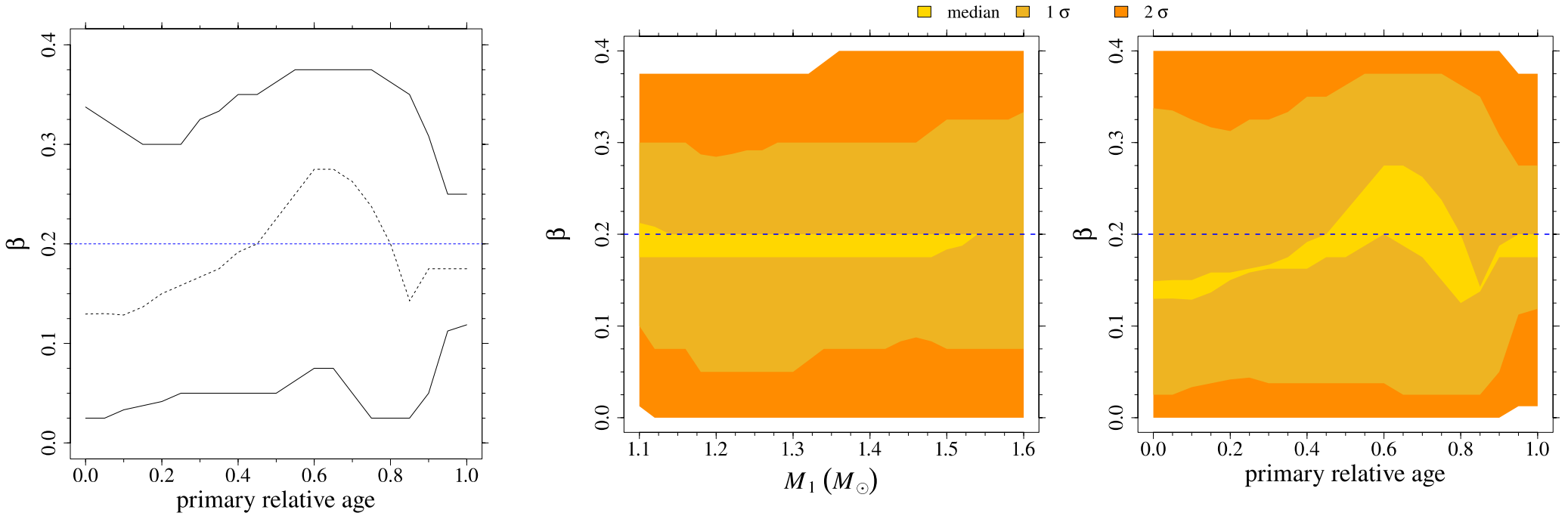
β
0.0
0.1
0.2
0.3
0.4
0.0
0.2
0.4
0.6
0.8
1.0
primary relative age
median
1 σ
2 σ
β
1.1
1.2
1.3
1.4
1.5
1.6
$M_1\ (M_\odot)$
β
primary relative age

Table 2. Overall uncertainty, statistical (1σ and 2σ) and systematic (q^{l}_{50}, q^{u}_{50}) as a result of the considered variations in $\Delta Y/\Delta Z$, $\alpha_{\rm ml}$, and microscopic diffusion efficiency as a function of the mass of the primary star.

	Primary star mass ($M_{\odot}$)					
	1.1	1.2	1.3	1.4	1.5	1.6
Unknown initial helium content						
$q_{0.025}$	0.01	0.00	0.00	0.00	0.00	0.00
$q_{0.16}$	0.12	0.07	0.07	0.07	0.05	0.03
q^{l}_{50}	0.21	0.20	0.20	0.20	0.20	0.17
q^{u}_{50}	0.23	0.22	0.21	0.23	0.23	0.23
$q_{0.84}$	0.32	0.30	0.30	0.33	0.34	0.35
$q_{0.975}$	0.39	0.38	0.39	0.40	0.40	0.40
Unknown mixing-length						
$q_{0.025}$	0.01	0.00	0.00	0.00	0.00	0.00
$q_{0.16}$	0.09	0.07	0.07	0.07	0.07	0.07
q^{l}_{50}	0.17	0.16	0.17	0.17	0.18	0.20
q^{u}_{50}	0.30	0.28	0.25	0.23	0.23	0.20
$q_{0.84}$	0.38	0.36	0.35	0.33	0.33	0.33
$q_{0.975}$	0.40	0.40	0.40	0.40	0.40	0.40
Unknown element diffusion efficiency						
$q_{0.025}$	0.01	0.00	0.00	0.00	0.00	0.00
$q_{0.16}$	0.10	0.05	0.05	0.07	0.07	0.07
q^{l}_{50}	0.17	0.17	0.17	0.17	0.18	0.20
q^{u}_{50}	0.21	0.20	0.20	0.20	0.20	0.20
$q_{0.84}$	0.30	0.28	0.30	0.30	0.32	0.33
$q_{0.975}$	0.38	0.38	0.38	0.40	0.40	0.40

Table 3. Same as

Table 3
Revised Physical Parameters of Capella

Parameter	Primary	Secondary
Mass ($M_\odot$)	2.5687 ± 0.0074	2.4828 ± 0.0067
$q \equiv M_B/M_A$	0.96653 ± 0.00062	
a (10^6 km)	111.11 ± 0.10	
a (AU)	0.74272 ± 0.00069	
π_{orb} (mas)	75.994 ± 0.089	
Distance (pc)	13.159 ± 0.015	
Radius ($R_\odot$)	11.98 ± 0.57	8.83 ± 0.33
log g (cgs)	2.691 ± 0.041	2.941 ± 0.032
T_{eff} (K)	4970 ± 50	5730 ± 60
Luminosity ($L_\odot$)[a]	78.7 ± 4.2	72.7 ± 3.6
BC_V (mag)	−0.304 ± 0.055	−0.089 ± 0.051
M_V (mag)	0.296 ± 0.016	0.167 ± 0.015
$v \sin i$ (km s^{-1})[b]	4.1 ± 0.4	35.0 ± 0.5
P_{rot} (days)[c]	104 ± 3	8.5 ± 0.2
Age (Myr)[d]	590–650	
[Fe/H]	−0.04 ± 0.06	
A(Li)	1.08 ± 0.11	3.28 ± 0.13
$^{12}C/^{13}C$ [e]	27 ± 4	...
C/N [c]	0.57 ± 0.06	3.30 ± 0.16

Notes.
[a] Computed from V, π_{orb}, and BC_V from Flower (1996), adopting $M^\odot_{bol} = 4.732$ (see T09 and Torres 2010).
[b] Average of 5 measurements from the literature for the primary and 10 for the secondary that account for macroturbulence, including our own (see text).
[c] Measured values adopted from T09.
[d] Age range from the MESA and Granada models (see the text).
[e] Measurement by Tomkin et al. (1976).

Table 1. Observational constraints for the TZ Fornacis binary system from Gallenne et al. (2016), but with stellar radii from Andersen (1991).

	Primary	Secondary
M ($M_\odot$)	2.057 ± 0.001	1.958 ± 0.001
R ($R_\odot$)	8.32 ± 0.12	3.96 ± 0.09
$T_{\rm eff}$ (K)	4930 ± 30	6650 ± 200
[Fe/H]	0.02 ± 0.05	−0.05 ± 0.1

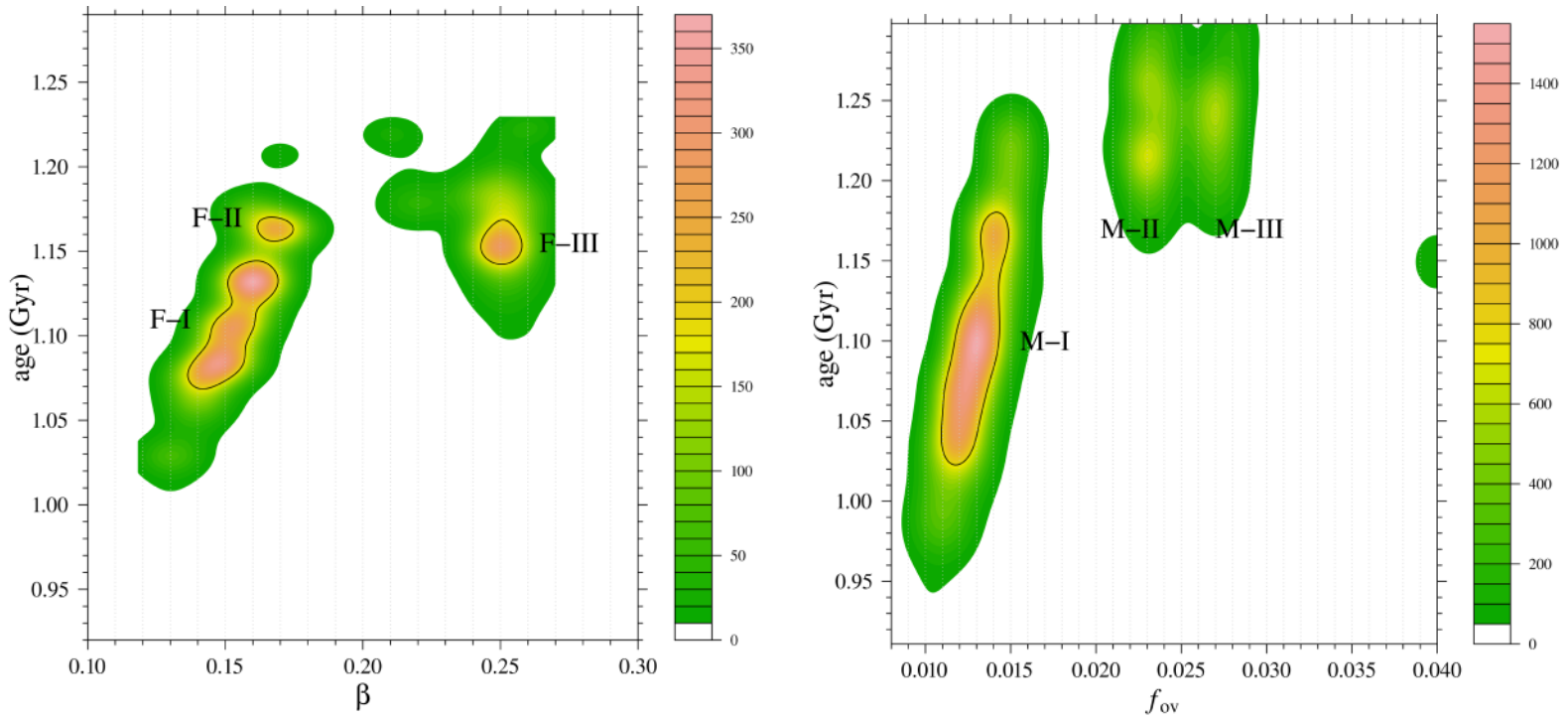

Fig. 1. *Left*: joint two-dimensional density of probability for the estimated overshooting parameter β and the age of the binary system. The estimates were obtained by relying on FRANEC stellar models. The solid black line corresponds to points for which the density is half of the maximum value. *Right*: same as in the *left panel*, but for estimates from the MESA grid.

Table 2. Multiple solutions for the TZ Fornacis binary system from the FRANEC grid of stellar models.

	F-I			F-II			F-I, II			F-III		
	q_{16}	q_{50}	q_{84}	q_{16}	q_{50}	q_{84}	q_{16}	q_{50}	q_{84}	q_{16}	q_{50}	q_{84}
Y	0.261	0.262	0.263	0.263	0.264	0.264	0.261	0.262	0.263	0.262	0.263	0.264
Z	0.012	0.013	0.014	0.015	0.015	0.016	0.013	0.013	0.015	0.014	0.015	0.016
β	0.140	0.151	0.160	0.160	0.170	0.170	0.141	0.155	0.163	0.240	0.250	0.255
age (Gyr)	1.07	1.10	1.13	1.16	1.16	1.17	1.08	1.11	1.16	1.14	1.16	1.19
M_{cc} ($M_\odot$)	–	–	–	–	–	–	–	–	–	0.169	0.171	0.174
Fit parameters												
$T_{eff,1}$ (K)		4952			4917			4947			4914	
$T_{eff,2}$ (K)		6896*			6788			6875*			6701	
R_1 ($R_\odot$)		8.39			8.43			8.39			8.61*	
R_2 ($R_\odot$)		4.03			4.04			4.03			3.71**	
χ^2		2.93			3.65			2.54			14.38	
p		0.23			0.16			0.28			0.001	

Notes. F-I, F-II, F-I, II and F-III identify the different islands of solutions (see text). q_{50} represents the median of the considered stellar quantities in the different solution islands, while q_{16} and q_{84} corresponds to the 16th and 84th quantiles. For some solutions, the distributions are skewed and q_{16} or q_{84} coincide with the median q_{50}. One asterisk marks the quantities, which differ by more than 1σ from the corresponding observational constraints; two asterisks indicate a difference larger than 2σ. For each solution, the goodness-of-fit χ^2 and the test p value are reported.

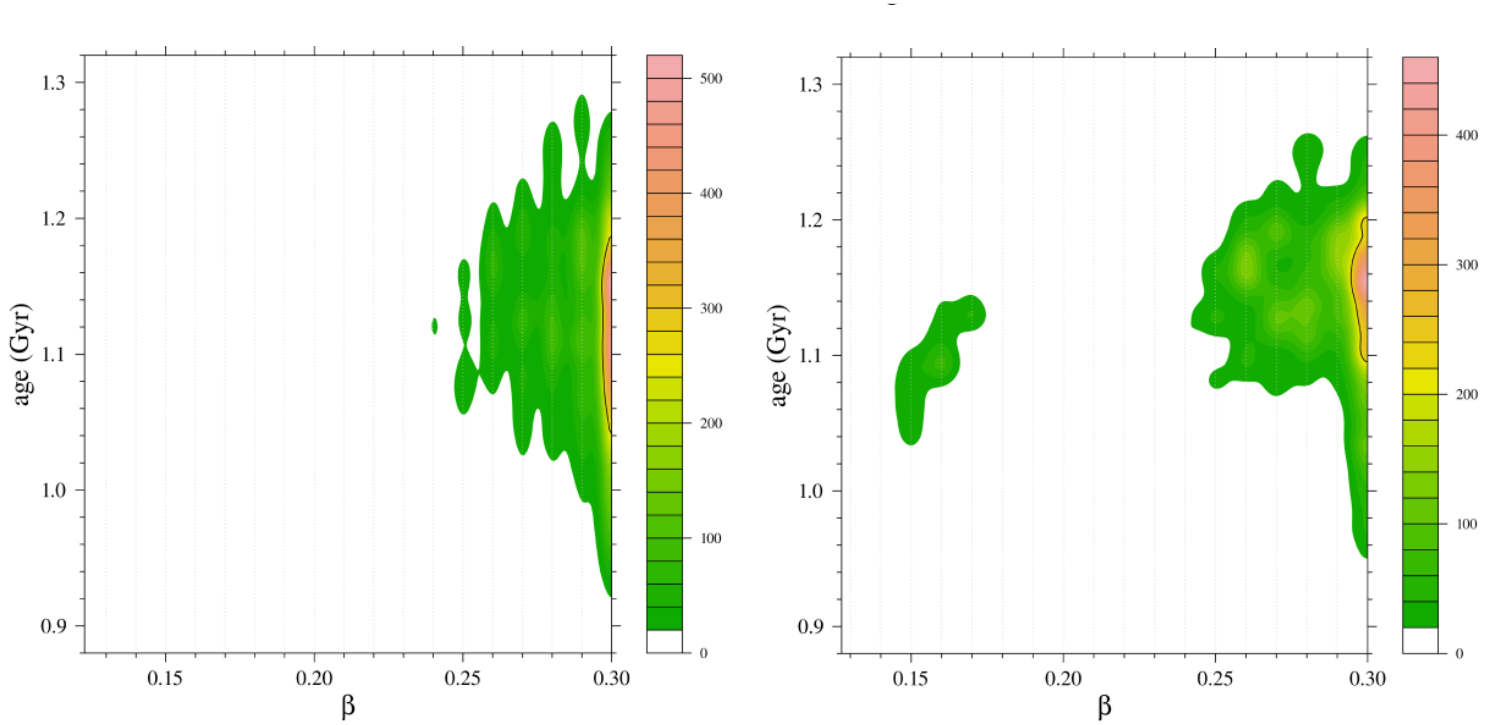

Fig. 4. *Left*: as in Fig. 1, but for estimates obtained while assuming errors of 1.5% and 3% on the primary and secondary star masses. A multi-mass grid of stellar models was adopted for the recovery (see text). *Right*: as in the *left panel*, but assuming errors of 1% on both stellar masses.

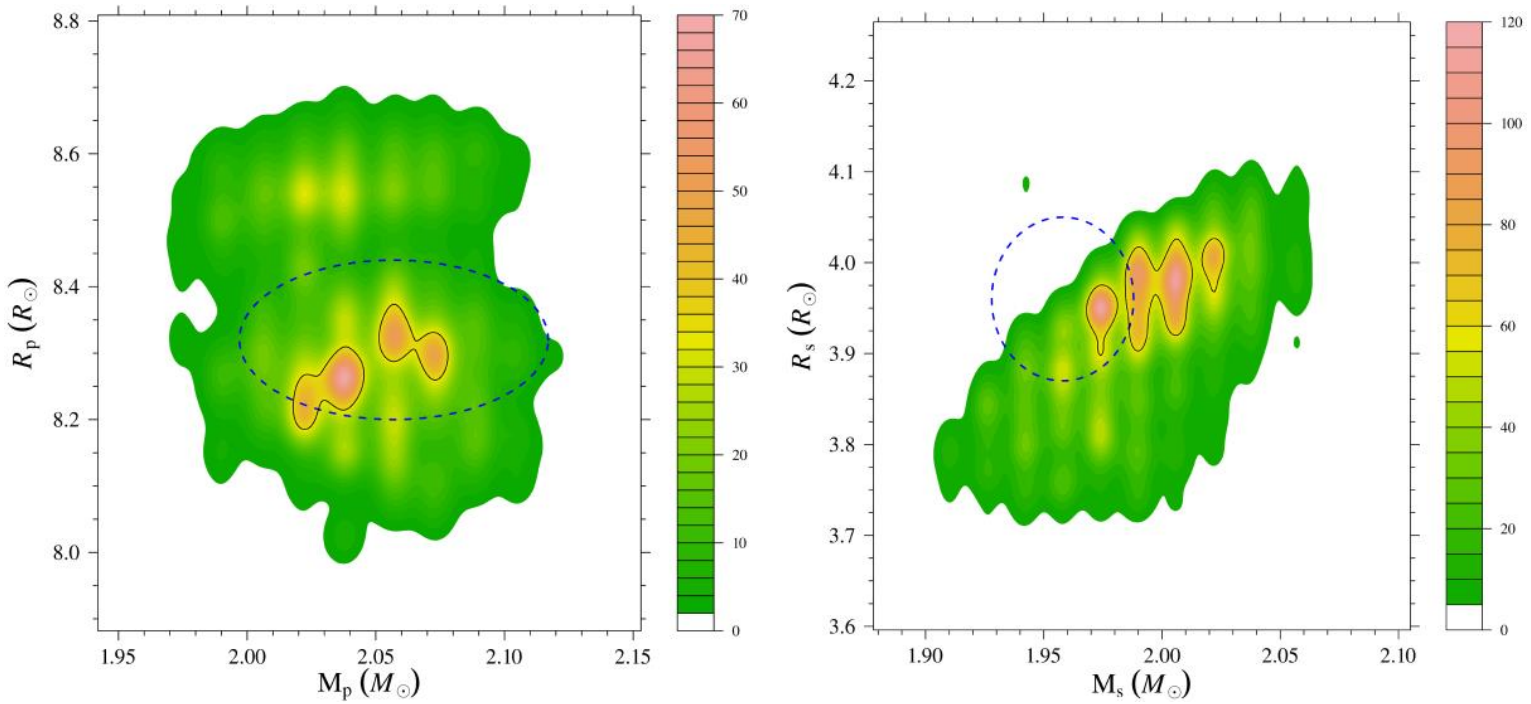

Fig. 5. *Left*: 2D density of probability for the best-fit mass and radius for the primary star. The blue-dashed ellipse marks the 1σ uncertainty on the observational values. The results were obtained relying on a multi-mass grid, with errors on the stellar masses from Andersen (1991) (see text). *Right*: same as in the *left panel*, but for the secondary star.

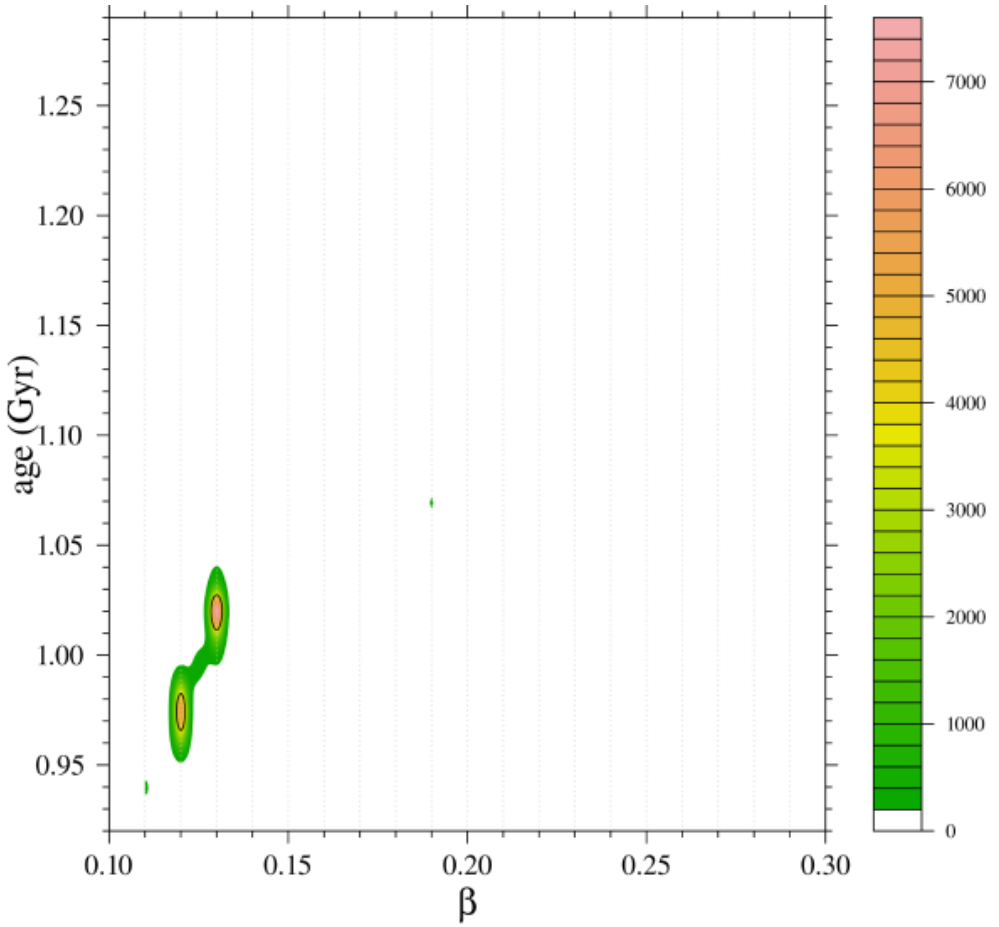

Fig. 6. Same as in Fig. 1 for FRANEC grid, but for estimates obtained by keeping fixed the helium-to-metal enrichment ratio $\Delta Y/\Delta Z = 2$.

Table 5. Solutions obtained whilst relaxing the common overshooting efficiencies hypothesis from FRANEC grids of stellar models.

	OV-I			OV-II		
	q_{16}	q_{50}	q_{84}	q_{16}	q_{50}	q_{84}
Y	0.261	0.263	0.269	0.262	0.263	0.264
Z	0.012	0.013	0.015	0.013	0.015	0.016
β_1	0.140	0.151	0.160	0.160	0.180	0.200
β_2	0.030	0.058	0.080	0.260	0.270	0.270
age (Gyr)	0.96	1.02	1.06	1.15	1.18	1.20
$M_{\rm cc}$ ($M_\odot$)	–	–	–	0.169	0.171	0.173
$T_{\rm eff,1}$ (K)		4937			4922	
$T_{\rm eff,2}$ (K)		6779			6667	
R_1 ($R_\odot$)		8.27			8.57**	
R_2 ($R_\odot$)		4.04			3.78**	
χ^2		1.42			8.96	
p		0.23			0.003	

Table 4. Multi-mass and fixed initial helium solutions from FRANEC grids of stellar models.

	MM-A			MM-B			$\Delta Y/\Delta Z = 2$		
	q_{16}	q_{50}	q_{84}	q_{16}	q_{50}	q_{84}	q_{16}	q_{50}	q_{84}
Y	0.262	0.263	0.271	0.262	0.263	0.266	0.272	0.275	0.277
Z	0.013	0.014	0.015	0.013	0.014	0.016	0.012	0.013	0.014
β	0.270	0.300	0.300	0.270	0.297	0.300	0.120	0.130	0.130
age (Gyr)	1.04	1.12	1.19	1.09	1.15	1.19	0.97	1.01	1.02
M_{cc} ($M_\odot$)	0.169	0.174	0.180	0.169	0.172	0.175	–	–	–
χ^2		3.34			2.74			8.08	
p		0.50			0.60			0.04	

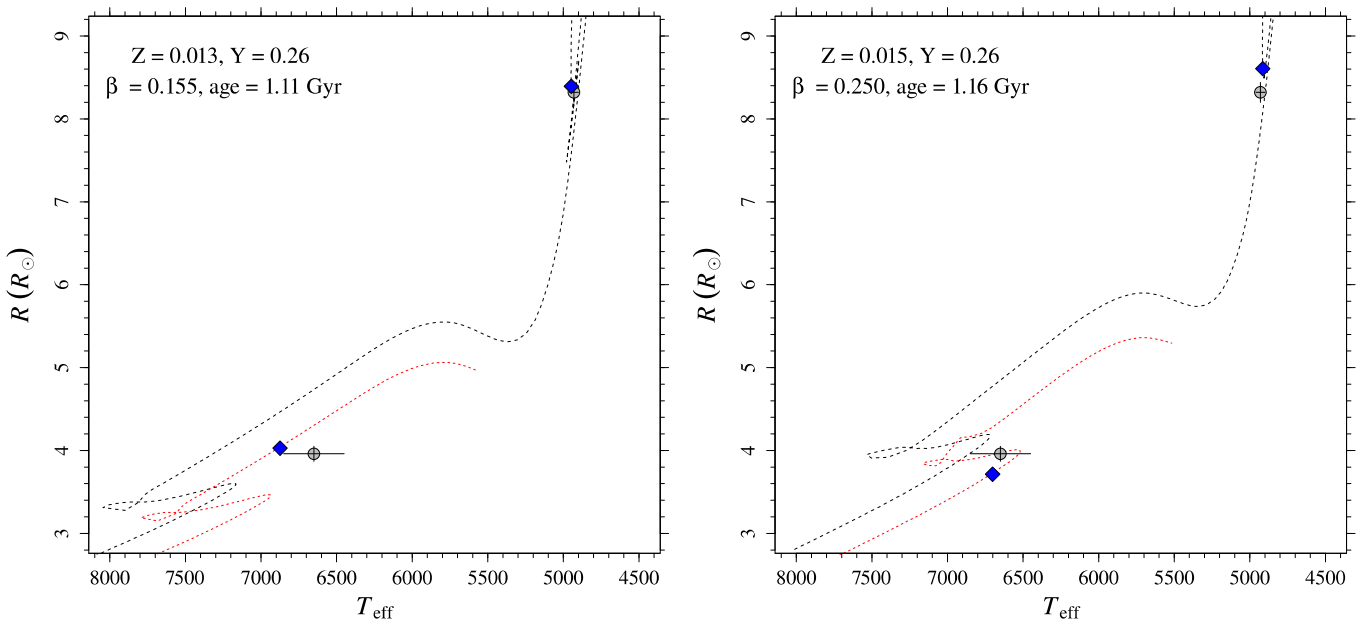

Fig. 2. *Top row*: comparison between the observational values of effective temperature and radius of the two stars (grey circle) and the evolutionary track for the best solutions found in the analysis of the FRANEC models. The blue diamonds mark the best fit theoretical positions for primary and secondary stars. The error bars correspond to 1σ errors. Initial metallicity and helium abundance, overshooting efficiency β, and age of the system for the four solutions are displayed in the panels. *Left panel*: shows the solution F-I,II, while *right panel* shows solution F-III (see Table 2).

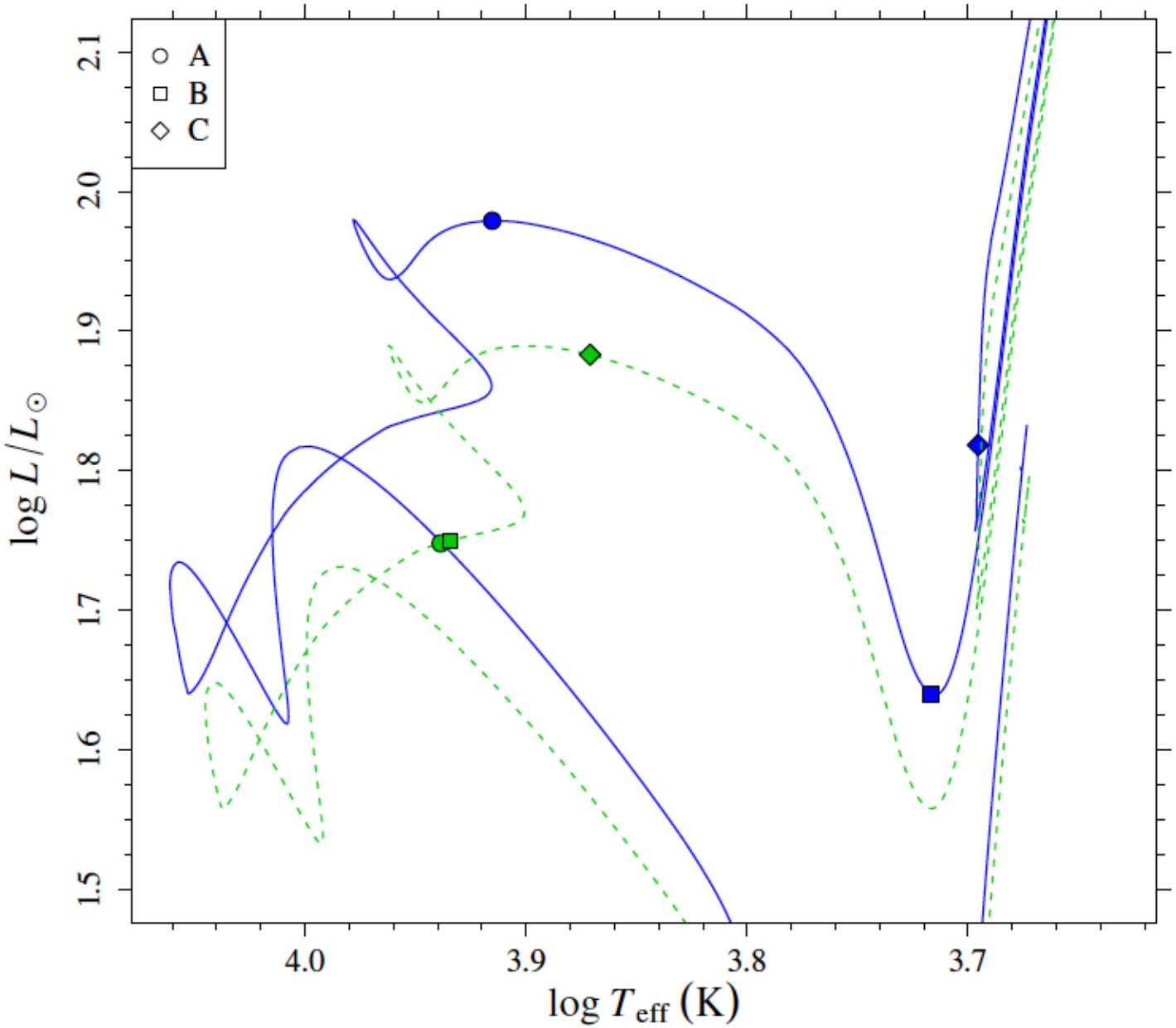

Fig. 1. HR diagram for the reference primary $M_1 = 2.50\ M_\odot$ (blue solid line) and secondary $M_2 = 2.38\ M_\odot$ (green dashed line) stars. The three studied scenarios are identified by circles (*A*), squares (*B*), and diamonds (*C*). The parameters adopted for the stellar evolution are: $M_1 = 2.50\ M_\odot$, $M_2 = 2.38\ M_\odot$, $Z = 0.0134$, $Y = 0.275$, $\beta = 0.16$.

Table 1. Estimated stellar parameters from Monte Carlo simulations for the standard (A, B, C) and the more precise scenarios (A_M, B_M and C_M) described in the text.

Scenario	Reference age (Gyr)	Age (Gyr)	Bias (%)	β	Y	Age (Gyr)		β	
						σ	σ_g	σ	σ_g
A	0.557	$0.535^{+0.034}_{-0.032}$	-3.9	$0.13^{+0.11}_{-0.05}$	$0.281^{+0.016}_{-0.018}$	0.029	0.018	0.063	0.037
B	0.563	$0.541^{+0.027}_{-0.028}$	-3.8	$0.13^{+0.03}_{-0.05}$	$0.277^{+0.018}_{-0.015}$	0.023	0.015	0.034	0.021
C	0.639	$0.585^{+0.032}_{-0.043}$	-8.5	$0.12^{+0.02}_{-0.08}$	$0.283^{+0.012}_{-0.013}$	0.034	0.021	0.040	0.027
A_M	0.557	0.538±0.027	-3.4	$0.14^{+0.04}_{-0.06}$	$0.275^{+0.020}_{-0.012}$	0.024	0.012	0.042	0.021
B_M	0.563	$0.544^{+0.042}_{-0.025}$	-3.3	$0.14^{+0.02}_{-0.04}$	$0.278^{+0.017}_{-0.015}$	0.024	0.012	0.029	0.014
C_M	0.639	$0.592^{+0.016}_{-0.022}$	-7.3	0.12±0.02	$0.285^{+0.010}_{-0.019}$	0.024	0.010	0.026	0.010

Notes. The columns contain: the label of the system to be analysed; the reference age of the system; the estimated age with its 1σ error; the relative bias in the estimated age; the estimated overshooting parameter β with its 1σ error; the estimated initial helium abundance with its 1σ error; the two error components of σ and σ_g for the age; the two error components of σ and σ_g for the overshooting (see Sect. 3.2). The reference values of overshooting parameter and initial helium abundance are $\beta = 0.16$ and $Y = 0.275$.

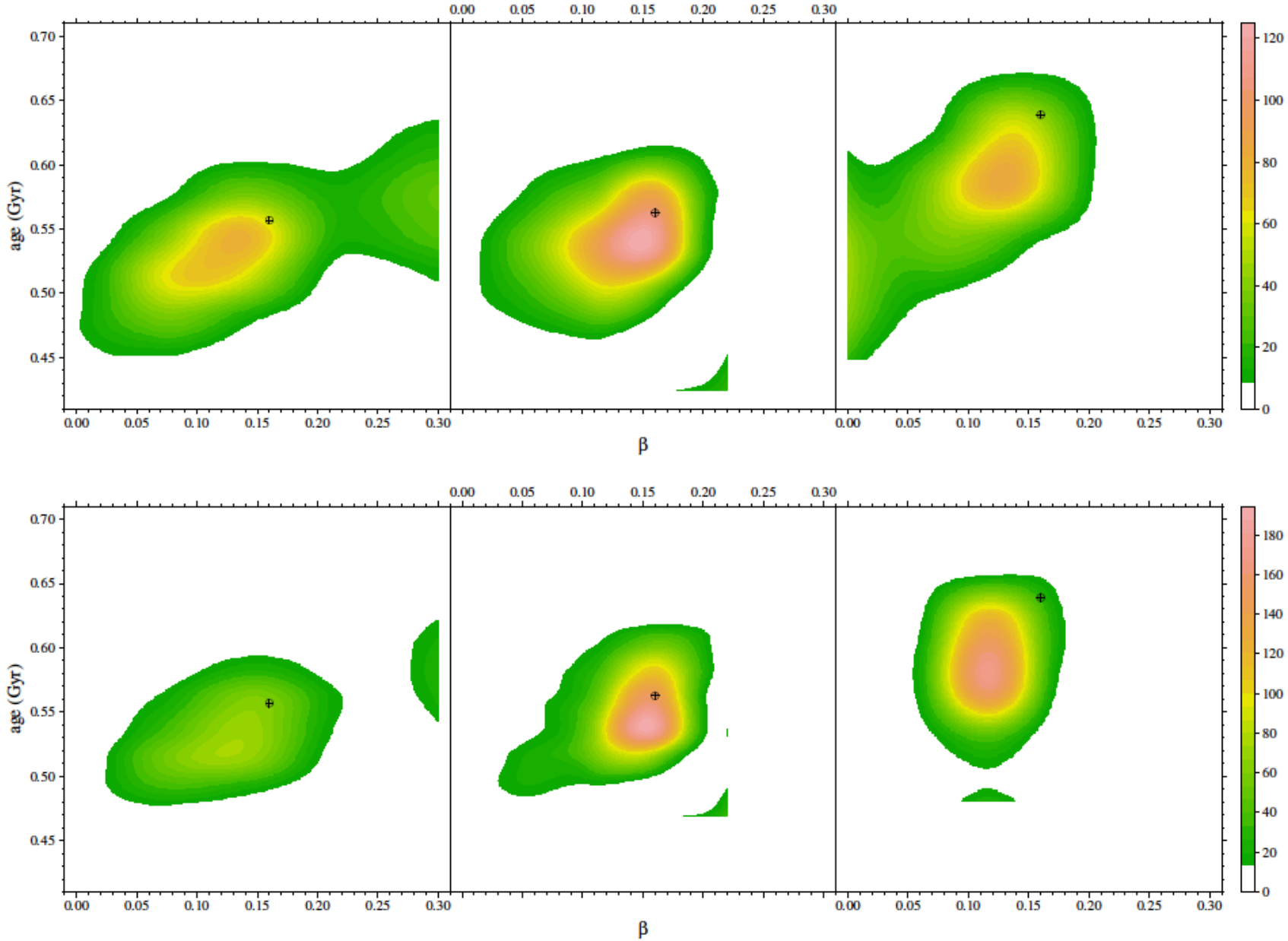

Fig. 2. *Top row*: *left* Bi-dimensional probability density in the β vs. age plane, marginalized with respect to initial helium and metallicity for scenario *A*. *Middle*: As in the *left* panel but for scenario *B*. *Right*: As in the *left* panel but for scenario *C*. *Bottom row*: As in the *top row* but for scenarios A_M, B_M, and C_M. The crosses mark the reference β and age values for all six cases. The little island of non-null density in the middle panel of the top row, and those in the middle and right panels of the bottom row, are numerical artefacts.

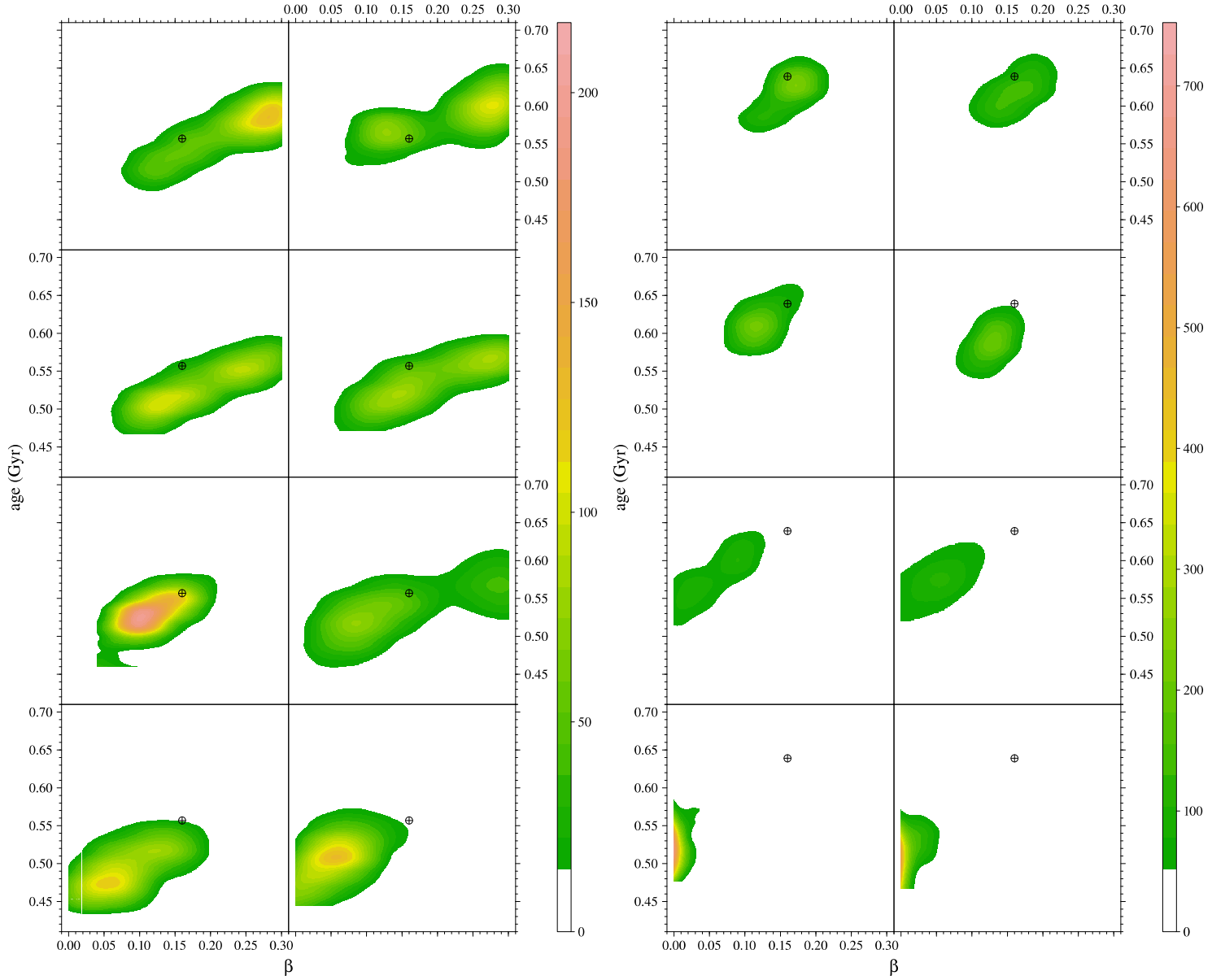

Fig. 5. *Left* panel, *top* row: Two realisations of the bi-dimensional density of probability in the age vs. β plane for two artificial systems under scenario A, with median estimated $\beta = 0.26$. *Second row*: As in the *top row* but for median estimated $\beta = 0.18$. *Third row*: As in the *top row* but for median estimated $\beta = 0.12$. *Bottom row*: As in the *top row* but for median estimated $\beta = 0.06$. The shown probability densities correspond to eight artificially perturbed systems. *Right* panel: As in the left panel for scenario C; from top to bottom the estimated β are 0.16, 0.12, 0.06, 0.0. The crosses indicate the position of the reference β and age values.

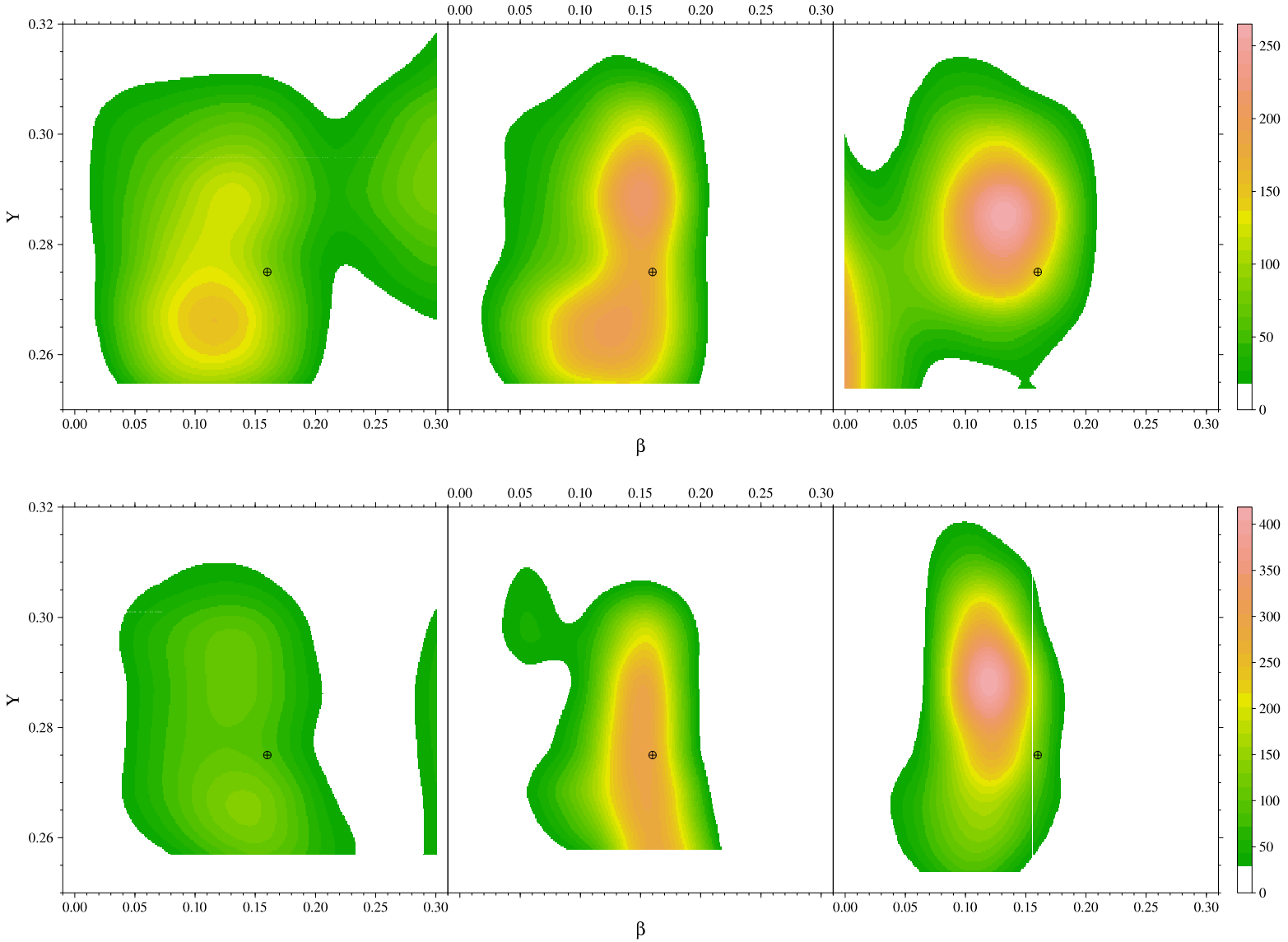

Fig. 3. *Top row*: *left* Bi-dimensional density of probability in the β vs. initial helium abundance plane, marginalized with respect to age and metallicity for scenario *A*. *Middle*: As in the *left* panel but for scenario *B*. *Right*: As in the *left* panel but for scenario *C*. *Bottom row*: As in the *top row*, but for scenarios A_M, B_M, and C_M. The crosses mark the position of the reference β and age for all six cases.

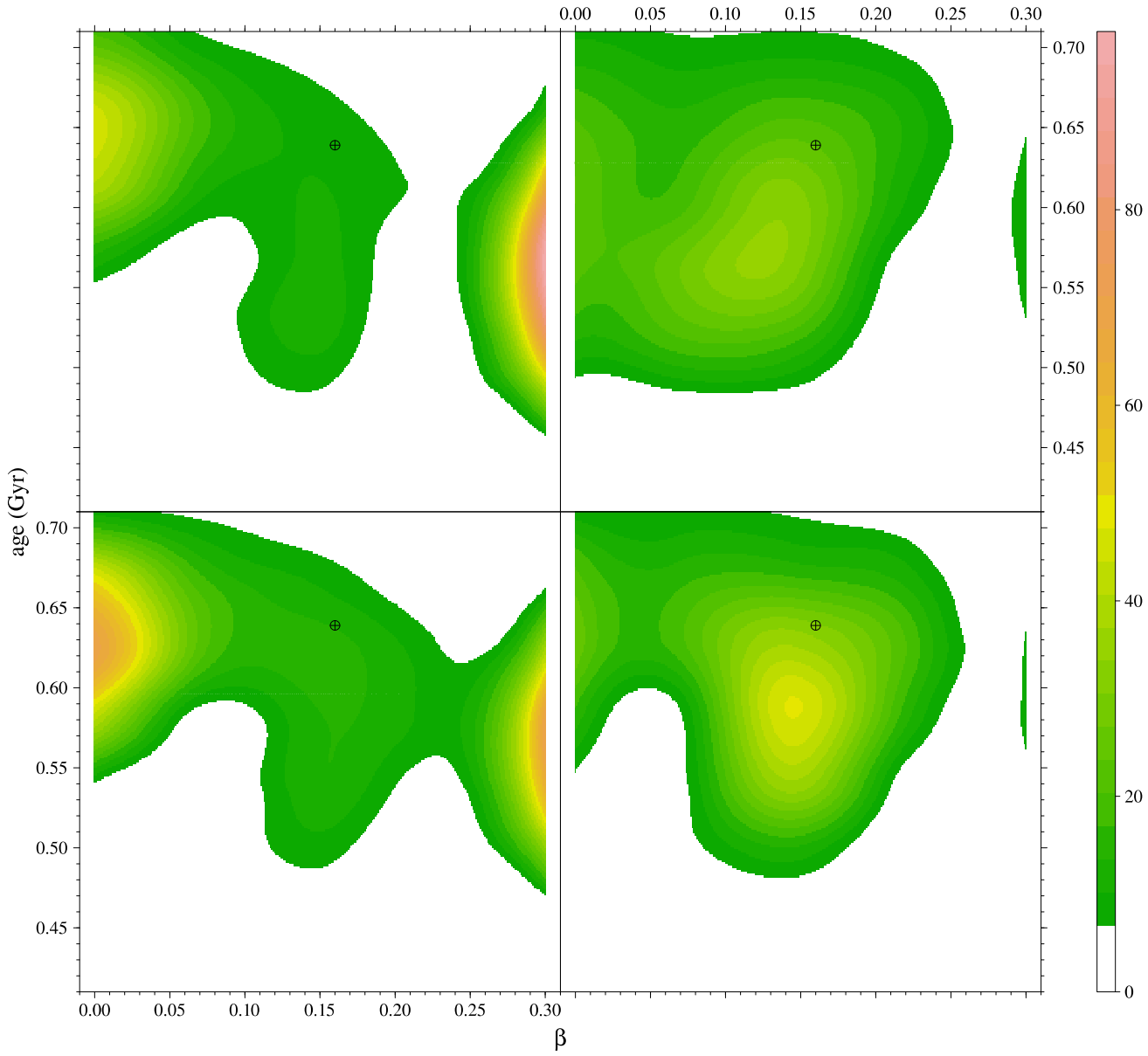

Fig. 6. *Top* row, *left* panel: Bi-dimensional density of probability in the age vs. β plane for scenario *C*, adopting a shift in effective temperature of artificial observations of +150 K. *Right*: Same as in the *left* panel, but for a shift of −150 K. *Bottom* row: Same as in the *top* row, but adopting an error on masses of 0.1%.

Table 2. As in Table 1, but for target binary systems sampled at $\beta = 0.0$.

Scenario	Reference age (Gyr)	Age (Gyr)	Bias (%)	β	Y	Age (Gyr)		β	
						σ	σ_g	σ	σ_g
B	0.501	$0.506^{+0.028}_{-0.023}$	1.0	$0.01^{+0.02}_{-0.01}$	$0.272^{+0.022}_{-0.011}$	0.020	0.013	0.014	0.007
C	0.564	$0.567^{+0.029}_{0.025}$	0.6	$0.02^{+0.08}_{-0.02}$	$0.275^{+0.011}_{-0.012}$	0.024	0.015	0.068	0.035
B_M	0.501	$0.508^{+0.026}_{0.029}$	1.3	0.02 ± 0.02	$0.275^{+0.016}_{-0.012}$	0.021	0.012	0.015	0.005
C_M	0.564	$0.576^{+0.041}_{0.033}$	2.2	$0.02^{+0.04}_{-0.02}$	$0.275^{+0.004}_{-0.011}$	0.028	0.019	0.046	0.017

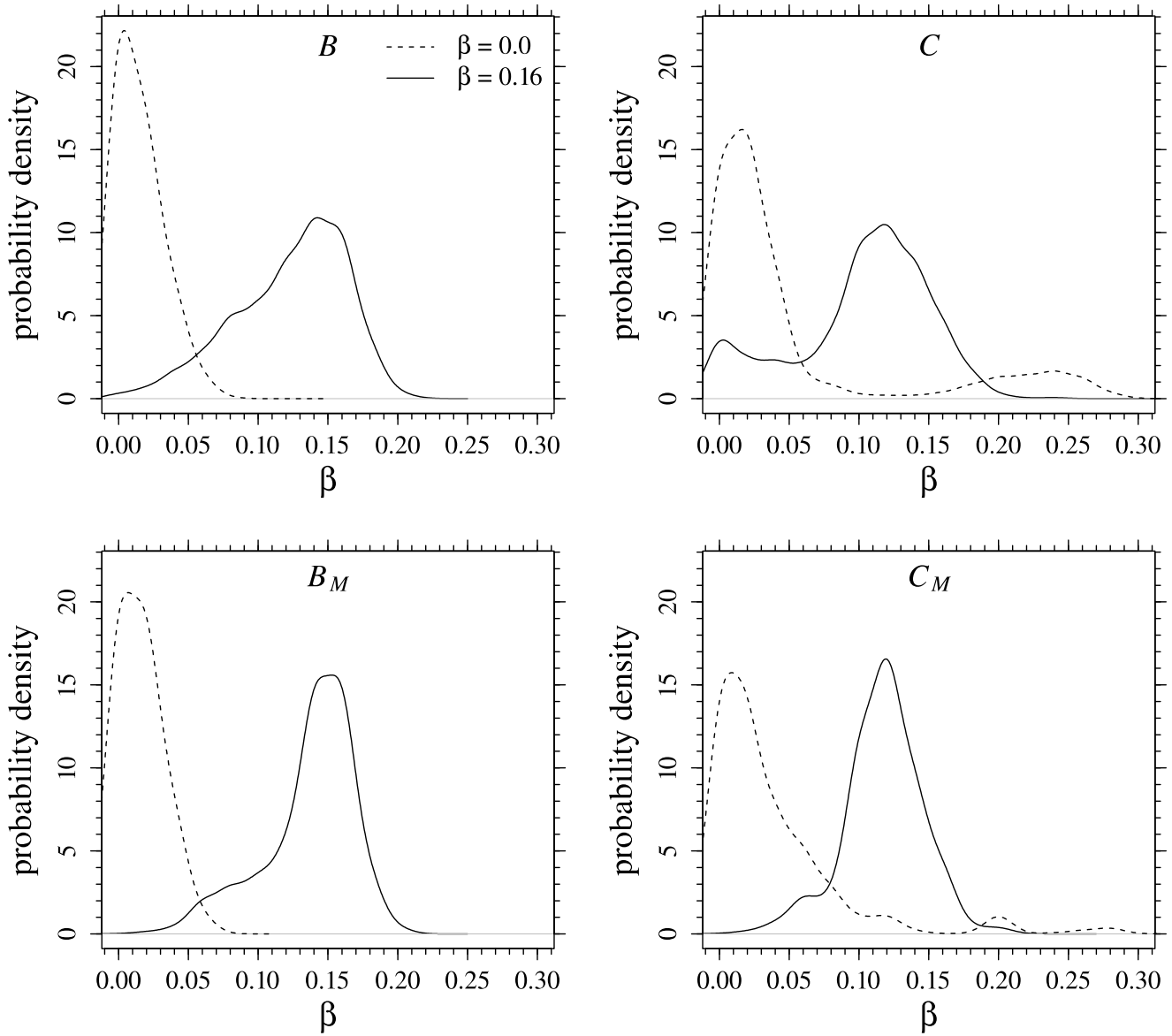

Fig. 7. *Top* row, *left* panel: Marginalized density of probability for the recovered β parameter under scenario B. The solid line corresponds to models sampled from the grid at $\beta = 0.16$, while the dashed one to models sampled at $\beta = 0.0$. *Right* panel: As in the *left* panel, but under scenario C. *Bottom* row: same as in the *top* row, but for precise mass scenarios B_M and C_M.

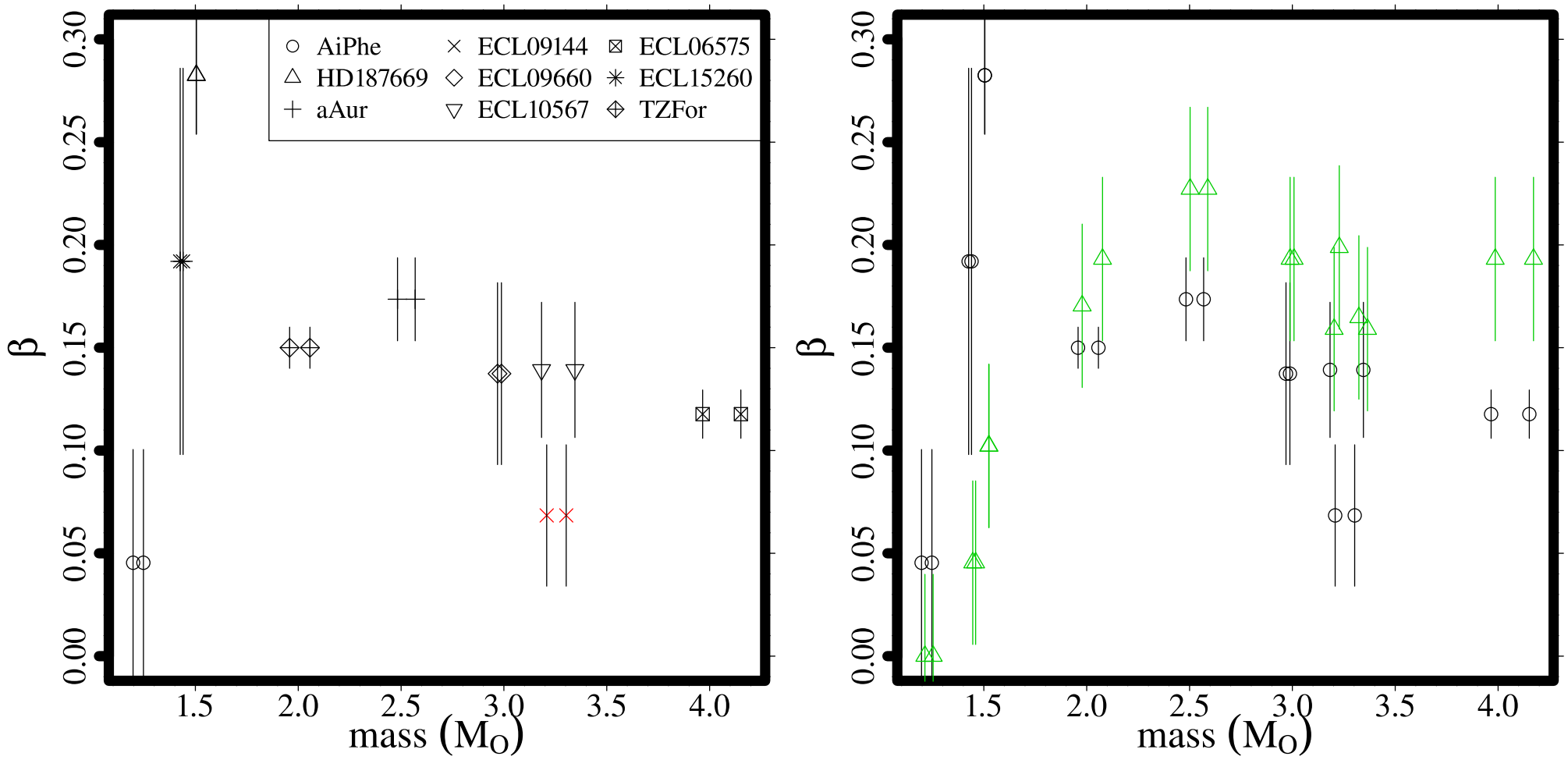
AiPhe
HD187669
aAur
ECL09144
ECL09660
ECL10567
ECL06575
ECL15260
TZFor
β
mass (M$_O$)
0.00
0.05
0.10
0.15
0.20
0.25
0.30
1.5
2.0
2.5
3.0
3.5
4.0

Observational test: binary systems

In agreement with previous results:

For standard models masses tend to underestimated, however

(Gennaro, Prada Moroni, Tognelli 2010)

in the case of double line eclipsing binary systems the agreement is quite good (maximum relative differences ~15% - 20% and in some cases differences as small as 5%, but V1174 Ori)

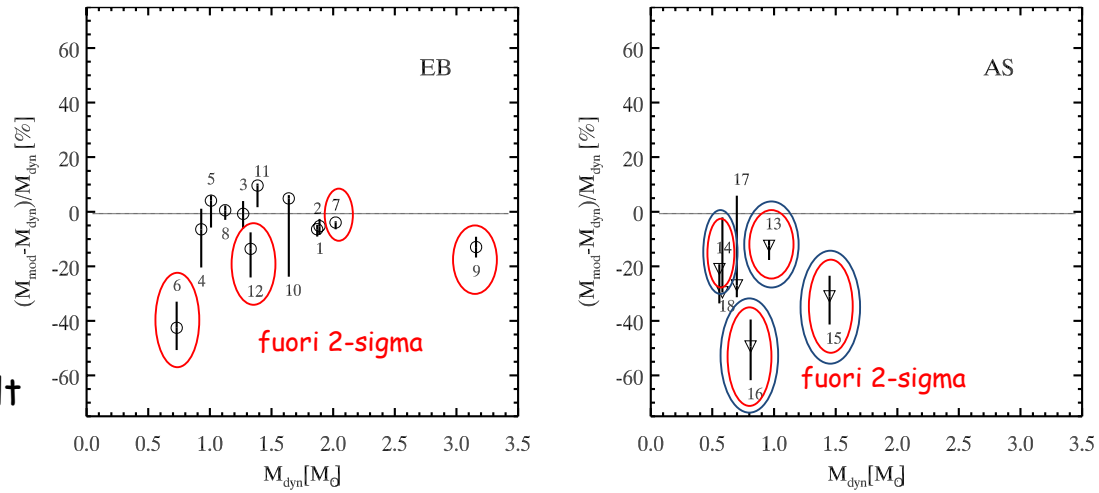

Regarding the age the situation is slightly worse (30% of the systems result not coeval)

Suggestions for the preference for colder models (low external convection efficiency, α=1 ?) in agreement with previous results (see e.g. D'Antona et al. 2000, Simon et al. 2001, Steffen et al. 2001, Baraffe et al. 2002, D'Antona & Montalban 2003, Stassun et al. 2004, Covino et al. 2004, Claret 2006, Alves de Oliveira 2013)

Link (?) with the underestimate of radii in PMS binary systems noticed by several authors (see e.g. Stassun et al. 2006, 2007, Mathieu et al. 2007, Jackson et al. 2009, Torres et al. 2010, Feiden & Chaboyer 2012, Somers & Pinsonneault 2014)